VOLUME 38
NUMBER 3
1999

POLYMER-PLASTICS TECHNOLOGY AND ENGINEERING

SPECIAL ISSUE ON POLYMER AND FIBER RECYCLING

Editor: MUNMAYA K. MISHRA

POLYMER–PLASTICS TECHNOLOGY AND ENGINEERING

June 1999

Aims and Scope. The journal *Polymer–Plastics Technology and Engineering* will provide a forum for the prompt publication of peer-reviewed, English language articles such as state-of-the-art reviews, full research papers, reports, notes/communications, and letters on all aspects of polymer and plastics technology that are industrial, semi-commercial, and/or research oriented. Some examples of the topics covered are specialty polymers (functional polymers, liquid crystalline polymers, conducting polymers, thermally stable polymers, and photoactive polymers), engineering polymers (polymer composites, polymer blends, fiber forming polymers, polymer membranes, pre-ceramics, and reactive processing), biomaterials (bio-polymers, biodegradable polymers, biomedical plastics), applications of polymers (construction plastics materials, electronics and communications, leather and allied areas, surface coatings, packaging, and automobile), and other areas (non-solution based polymerization processes, biodegradable plastics, environmentally friendly polymers, recycling of plastics, advanced materials, polymer plastics degradation and stabilization, natural, synthetic and graft polymers/copolymers, macromolecular metal complexes, catalysts for producing ultra-narrow molecular weight distribution polymers, structure property relations, reactor design and catalyst technology for compositional control of polymers, advanced manufacturing techniques and equipment, plastics processing, testing and characterization, analytical tools for characterizing molecular properties and other timely subjects).

Identification Statement. *Polymer–Plastics Technology and Engineering* is published five times a year in the months of February, April, June, September, and November by Marcel Dekker, Inc., P.O. Box 5005, 185 Cimarron Road, Monticello, NY 12701-5185. Periodicals postage paid at Monticello, NY. POSTMASTER: Send address changes to *Polymer–Plastics Technology and Engineering*, P.O. Box 5005, Monticello, NY 12701-5185.

1999 Subscription Rates for Volume 38 (5 issues)

	Institutional Rate	Individual Professional and Student Rate	International Postage			
			Surface	Airmail		
				Canada	Europe	Asia
Print	$1125	$65	$20	$22.50	$27.50	$35

How to Order. Individual professional and student orders must be prepaid by personal check or may be charged to MasterCard, VISA, or American Express. Please mail payment with your order to: Marcel Dekker Journals, P.O. Box 5017, Monticello, New York 12701-5176. Telephone: 800-228-1160; Fax: 914-796-1772; E-mail: jrnlorders@dekker.com

Printed in the U.S.A.

Print. CODEN: PPTEC7 38(3) i–xii, 401–580 (1999)
ISSN: 0360-2559

POLYMER–PLASTICS TECHNOLOGY AND ENGINEERING

POLYMER–PLASTICS TECHNOLOGY AND ENGINEERING

Library of Congress Catalog Card Number. 74-645000

Online Information. Tables of Contents, Abstracts, Editorial Board listing, and Instructions to Authors regarding manuscript preparation and submission for this publication may be accessed *free of charge* at www.dekker.com/e/p/ppt.

Indexing and Abstracting Services. Articles published in *Polymer–Plastics Technology and Engineering* are selectively indexed or abstracted in:

■ Chemical Abstracts ■ Current Contents/Engineering, Computing, and Technology ■ Engineering Index/COMPENDEX PLUS ■ Fluid Abstracts/ FLUIDEX ■ INSPEC ■ Materials Information ■ Materials Science Citation Index ■ Plastic Rubber Fibers ■ Polymer Contents ■ Rapra Abstracts Database ■ Reaction Citation Index ■ Referativnyi Zhurnal/Russian Academy of Sciences ■ Research Alert ■ Science Citation Index ■ SciSearch/SCI-Expanded ■ World Textile Abstracts ■ WORLD TEXTILES

Manuscript Preparation and Submission. See end of issue.

Contributions to this journal are published free of charge. Effective with Volume 22, Number 2, this journal is printed on acid-free paper.

www.dekker.com

POLYMER AND FIBER RECYCLING

Guest Editor:

SATISH KUMAR
School of Textile and Fiber Engineering
Georgia Institute of Technology
Atlanta, Georgia 30332-0295

This is a special issue of *Polymer–Plastics Technology and Engineering*,
Volume 38, Number 3, 1999.

MARCEL DEKKER, INC. New York • Basel

POLYM.–PLAST. TECHNOL. ENG., 38(3), vii–viii (1999)

CONTRIBUTORS TO THIS ISSUE

J. C. Ammons, Georgia Institute of Technology, Atlanta, Georgia, USA.

G. Bhat, The University of Tennessee, Knoxville, Tennessee, USA.

M. Braun, AlliedSignal Inc., Morristown, New Jersey, USA.

E. J. Daniels, Argonne National Laboratory, Argonne, Illinois, USA.

M. Dever, The University of Tennessee, Knoxville, Tennessee, USA.

W. Ding, Georgia Institute of Technolgy, Atlanta, Georgia, USA.

R. Enick, University of Pittsburgh, Pittsburgh, Pennsylvania, USA.

A. T. Griffith, Auburn University, Auburn, Alabama, USA.

X. Hu, Georgia Institute of Technology, Atlanta, Georgia, USA.

E. Karmana, University of Pittsburgh, Pittsburgh, Pennsylvania, USA.

K. Khait, Northwestern University, Evanston, Illinois, USA.

A. M. Kotliar, Georgia Institute of Technology, Atlanta, Georgia, USA.

S. Kumar, Georgia Institute of Technology, Atlanta, Georgia, USA.

L. L. LeBoeuf, Georgia Institute of Technology, Atlanta, Georgia, USA.

A. B. Levy, AlliedSignal Inc., Morristown, New Jersey, USA.

J. D. Muzzy, Georgia Institute of Technology, Atlanta, Georgia, USA.

V. Narayanan, The University of Tennessee, Knoxville, Tennessee, USA.

D. Newton, Georgia Institute of Technology, Atlanta, Georgia, USA.

Y. Park, Auburn University, Auburn, Alabama, USA.

M. B. Polk, Georgia Institute of Technology, Atlanta, Georgia, USA.

M. J. Realff, Georgia Institute of Technology, Atlanta, Georgia, USA.

C. B. Roberts, Auburn University, Auburn, Alabama, USA.

M. Shah, Georgia Institute of Technology, Atlanta, Georgia, USA.

S. Sifniades, AlliedSignal Inc., Morristown, New Jersey, USA.

S. Simon, University of Pittsburgh, Pittsburgh, Pennsylvania, USA.

R. S. Stein, University of Massachusetts, Amherst, Massachusetts, USA.

J. M. Torkelson, Northwestern University, Evanston, Illinois, USA.

L. Wadsworth, The University of Tennessee, Knoxville, Tennessee, USA.

Y. Wang, Georgia Institute of Technology, Atlanta, Georgia, USA.

C.-Y. Won, Georgia Institute of Technology, Atlanta, Georgia, USA.

Y. Zhang, Georgia Institute of Technology, Atlanta, Georgia, USA.

POLYM.–PLAST. TECHNOL. ENG., 38(3), ix–xi (1999)

PREFACE

RICHARD S. STEIN

University of Massachusetts
Amherst, Massachusetts 01003

The problems associated with the accumulation of polymer solid waste is of great public concern. Landfill space in high-population-density areas of the country is often becoming exhausted, and transportation costs to increasingly more distant areas are becoming prohibitive. Although polymers only amount to about 8% by weight of solid waste, their low density and slow decomposition rates make them a very visible component. There is also concern that polymer use represents a consumption of nonrenewable resources. Discarded polymer objects can be unsightly and also can be damaging to wildlife.

Although reduced use and substitution by other materials are suggested solutions, the performance, convenience, and low cost of synthetic polymers have led to an increasing amount of polymer waste. Recycling is an important means for reducing the fraction of this waste entering landfills and also can lead to the recovery of materials for further use. However, its employment is limited by economic considerations. Polymer manufacturers are unlikely to utilize feedstock of recycle origin if they can use a virgin monomer less expensively.

There are several problems that limit the application of recycling. It is well known that many polymers are immiscible with each other and that the physical properties of immiscible polymer blends are often inferior. There are some products that can be made from such "commingled polymers" such as park benches and marine docks, but the applications are often limited to those where mechanical performance requirements are not high. There is not a large market for such use, so most recycling efforts are directed toward dealing with separated polymers.

Recycling can be categorized as "preconsumer" and "postconsumer." Preconsumer recycling is that carried out by manufacturers using materials arising from their normal production, such as waste from operations (e.g., stamp-

ing and trimming). Such practices have long been employed and are economically attractive. They benefit from manufacturers being able to readily segregate polymers of differing types.

The postconsumer problem is more difficult, and its success usually depends on either devising a scheme for readily identifying and collecting polymers of particular types or employing an economical means for separating mixed polymers. A successful program is that of recycling polyethylene terephthalate (PET) soft drink bottles, where their return is often encouraged by charging deposits to be returned when the used bottles are brought back. "Reverse deposit" machines in supermarkets which identify bottles, grind them up, and return the deposit have facilitated the process. One reason for the success of this program is that the value of PET is greater than that of other polymers such as polyolefins, where recycling is less attractive.

The need is to find sources of recycle feedstock where appreciable amounts of not too greatly mixed polymers can be economically collected and processed. Used carpets have been identified as such a source. It is estimated that in the United States, 7 billion pounds of carpets are shipped each year and these are usually replaced in 5–10 years. The replacement is usually carried out by professionals who could deliver these used carpets to a recycling facility. Most carpets are composed of a nylon facing, a polypropylene backing, and a resin binder. Thus, the separation of these components is a fairly well-defined task. Nylon, like PET, is a high-value-added polymer, so that its recovery is attractive.

The methods described in this collection of articles may be divided into (1) those employing the mixed carpet components, (2) those separating the components by physical processes, and (3) those involving chemical degradation. A good example of method 1 is that of the Northwestern University group who pulverize the mixed component under sufficiently high shear that some chemical degradation occurs. This produces some reaction between components so as to lead to linkage by chemical bonding of fine particles having a high surface area. Although the components do not become miscible, the mixtures have physical properties that are superior to those of normal mixtures so that a greater range of uses may be found. Another approach by a Georgia Tech group uses fibrous carpet waste as a filler for thermoplastic resins (without melting the carpet components) to produce a woodlike material.

Some unique separation techniques employ liquid or supercritical carbon dioxide. The density of liquid CO_2 is such that it can separate the nylon from the polypropylene. It is shown that the CO_2 does not appreciably affect the properties of the components. A different method dissolves the nylon in a formic-acid-based solvent, separates the solution from the other components, and then uses the supercritical CO_2 as an antisolvent to precipitate the nylon from its solution.

A problem with degradation techniques is that energy is required. They have the advantage that the products are of low molecular weight so that they can be readily separated from impurities and purified by conventional techniques such as filtration and distillation. This provides the flexibility for repolymerizing in a variety of ways and also of avoiding regulatory restrictions governing the use of products for applications such as those dealing with food. Techniques are familiar to chemical engineers, and the problem is one of optimization to make them economically attractive.

It is not clear which approach is best. This collection of articles represents a multifaceted approach which permits comparisons. It is hoped that such studies may help with decisions.

POLYM.–PLAST. TECHNOL. ENG., 38(3), 401–410 (1999)

PLASTICS, RUBBERS, AND TEXTILES IN MUNICIPAL SOLID WASTE IN THE UNITED STATES

SATISH KUMAR

School of Textile and Fiber Engineering
Georgia Institute of Technology
Atlanta, Georgia 30332-0295

Abstract

In 1996, 210 million tons of municipal solid waste was generated in the United States. Fifty-seven million tons of this waste was recovered for recycling, 36 million tons was combusted primarily for energy recovery, and the rest (110 million tons) of the waste was landfilled. In 1996, plastics, rubbers, and textiles accounted for 20% by weight and 41% by volume of the total municipal solid waste. Six percent (2 million tons) of plastics, rubbers, and textiles were recovered for recycling in 1996.

Key Words: Polymers; Landfill; Recycling; Combustion; Waste statistics.

INTRODUCTION

This article presents solid-waste statistics on plastics, rubbers, and textiles based primarily on the U.S. Environmental Protection Agency's report on municipal solid waste (1). Municipal solid-waste (MSW) generation grew from 88 million tons (2.68 lbs./person/day) in 1960 to 214 million tons (4.51 lbs./person/day) in 1994. In 1996, the waste generation decreased to 210 million pounds (4.33 lbs./person/day) (Fig. 1). Materials generated in the municipal solid-waste stream by weight and as a percentage of total waste are given in Fig. 2. Figure 3 shows that 27% (57 million tons) of this waste was recovered for recycling including composting, 17% (36 million tons) was used in combustion facilities, and 55% (116 million tons) waste was landfilled in the

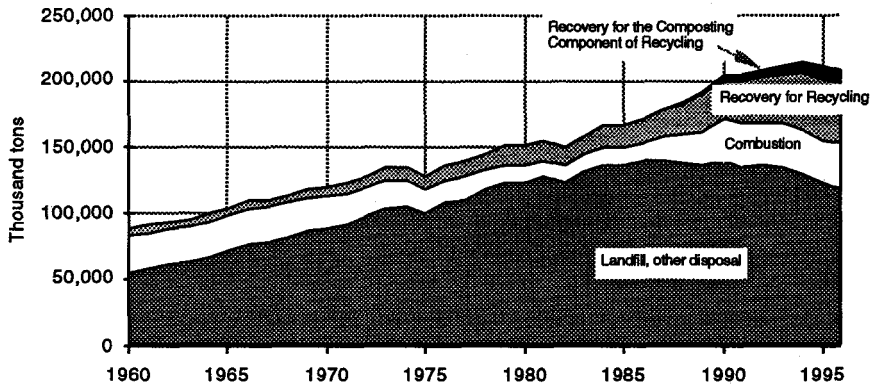

FIG. 1. Municipal solid-waste (MSW) management, 1960–1996. (From Ref. 1.)

2400 landfill facilities. By comparison, in 1986, 83% of municipal solid waste was landfilled.

Municipal solid waste includes the following: durable goods, nondurable goods, containers and packaging, food waste, yard trimings, and miscellaneous inorganic waste. Municipal solid waste does not include hazardous waste, municipal sludge, industrial nonhazardous waste, construction and demolition waste, agriculture waste, oil and gas waste, and mining waste.

The 1997 EPA report (1) uses the materials flow methodology for waste characterization. This method is based on production data (by weight). Ad-

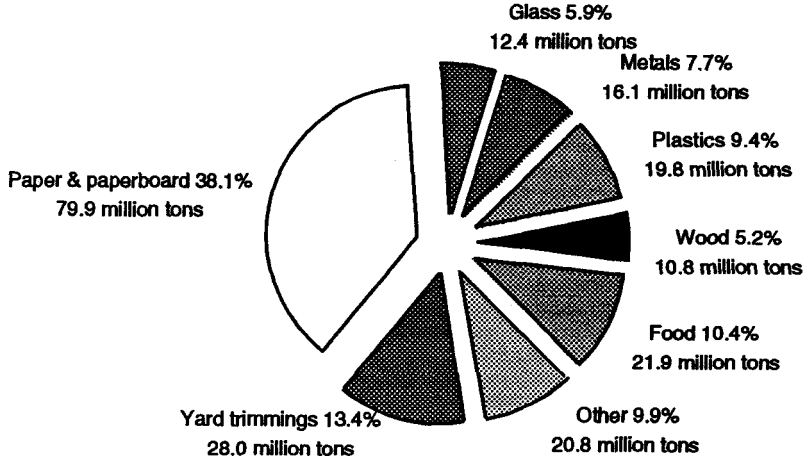

FIG. 2. Materials in MSW, 1996 (total weight 210 million tons). (From Ref. 1.)

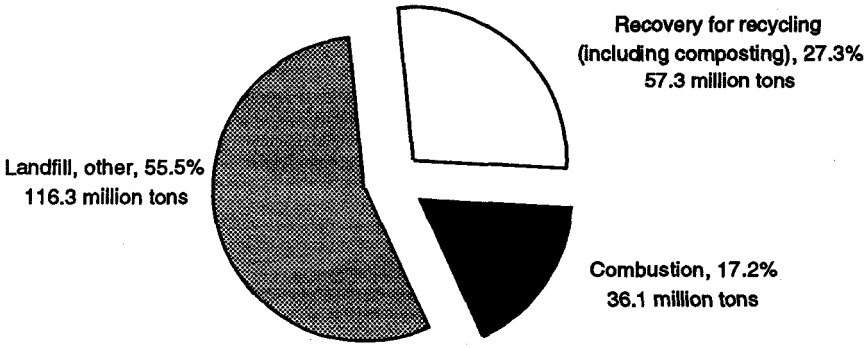

FIG. 3. Municipal solid-waste (MSW) management, 1996. (From Ref. 1.)

justments are made for imports, exports, diversion from waste stream, and product lifetimes.

TEXTILES AND RUBBERS

Textiles recovered for reuse as wiper rags and so forth eventually enter the waste stream. It was assumed that reused textiles enter the waste stream in the same year in which they are first recovered. In 1996, approximately 1 million tons of textiles were recovered for export or reprocessing and 6.8 million tons of textile waste was discarded.

It is also estimated that 2.3 million tons of carpets and rugs (carpet contains fiber, rubber, and inorganic filler) were generated into municipal solid waste in 1996, of which about 1% was recovered for recycling (Table 1). A number

TABLE 1
Selected Products in Municipal Solid Waste in 1996 (in Thousands of Tons)

Products	MSW generation	Recovered for recycling
Carpet and rugs	2310	30 (1.3%)
Rubber tires	3910	730 (18.7%)
Plastics plates and cups	810	10 (1.2%)
Trash bags	860	Negligible
Disposable diapers	3050	Negligible
Clothing and footwear	5340	700 (13.1%)
Towels, sheets, and pillowcases	750	130 (17.3)

Source: Ref. 1.

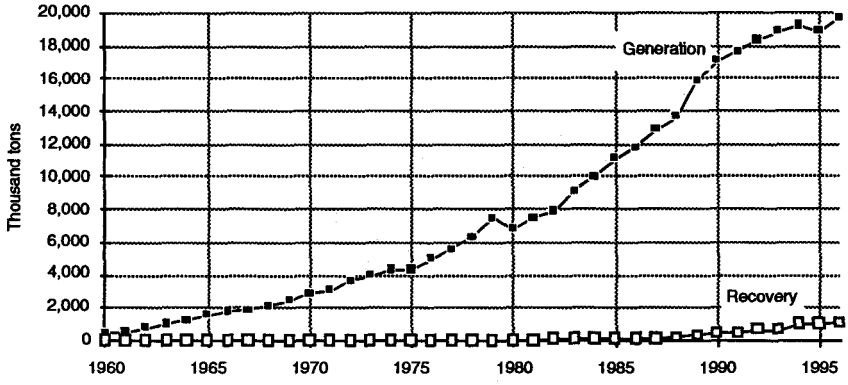

FIG. 4. Plastics waste generation and recovery, 1960–1996. (From Ref. 1.)

of carpet recycling initiatives are currently underway and we should continue to see growth in carpet recycling in the coming years. For example, AlliedSignal Inc., BASF, DuPont Co., Collins and Aikman, and some others have initiated postconsumer carpet recycling programs in recent years.

The generation of 3.9 million tons of tires was estimated in the municipal solid-waste stream in 1996, 19% of which were recovered for recycling, leaving 3.2 million tons to be discarded (Table 1).

PLASTICS

The growth of plastics in municipal solid waste is shown in Fig. 4 and a breakdown by products is shown in Fig. 5. Plastic products had the largest increase

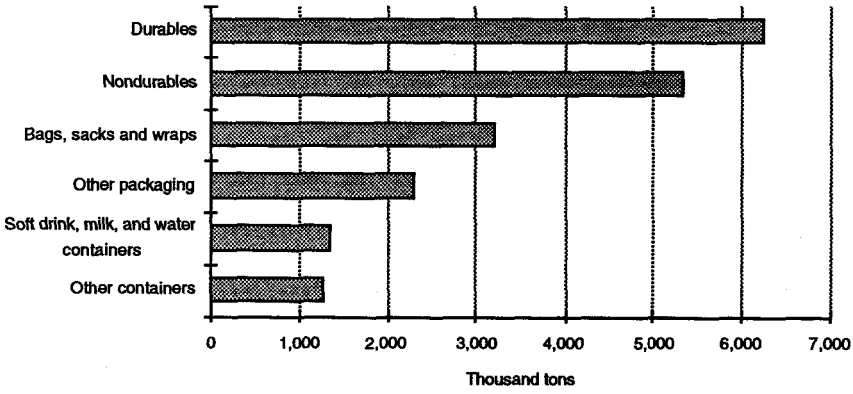

FIG. 5. Plastics products in MSW, 1996. (From Ref. 1.)

TABLE 2
Plastic Resins in Municipal Solid Waste in 1996 (in Thousands of Tons)

Resin[a]	MSW generation	Recovered for recycling
PET	1,700	350
HDPE	4,120	410
PVC	1,230	Negligible
LDPE/LLDPE	5,010	110
PP	2,580	130
PS	1,990	30
Other resins	3,130	30
Total plastics in MSW	19,760	1,060 (5.4%)

[a] PET = polyethylene terephthalate; HDPE = high-density polyethylene; PVC = poly(vinyl chloride); LDPE/LLDPE = low-density polyethylene/linear low-density polyethylene; PP = polypropylene; PS = polystyrene.
Source: Ref. 1.

in generation for all materials—increasing by nearly 1 million tons from 1995 to 1996 in MSW generation. Various plastic resins in the municipal solid waste are given in Table 2.

Polyethylene terephthalate (PET) and high-density polyethylene (HDPE) currently account for about 80% of plastics recovered from MSW. A complete list of plastics recovered is given in Table 2. Prices for recycled HDPE and recycled PET are presented in Figs. 6 and 7, respectively. High prices in the 1995–1996 period are believed to be a result of the lack of participation in the curbside recycling program. Relatively low prices for recycled PET are at-

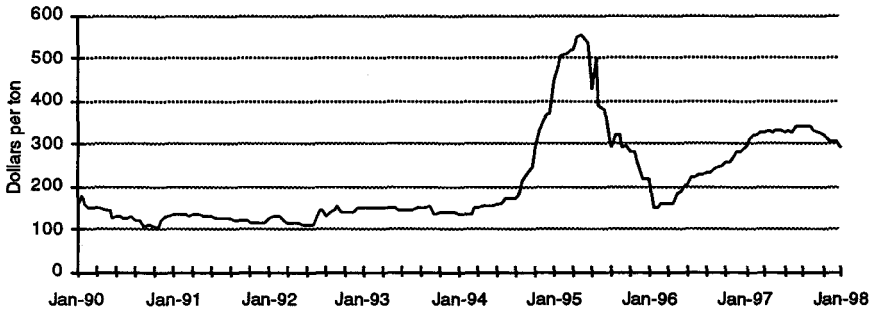

FIG. 6. Average price for baled HDPE from 1990 to 1998. (From Ref. 1; original source: *Recycling Times*.)

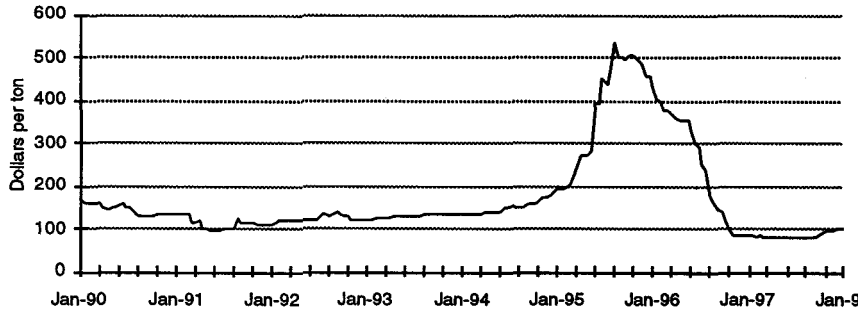

FIG. 7. Average price for baled PET from 1990 to 1998. (From Ref. 1; original source: *Recycling Times.*)

tributed to the large supply of off-class virgin PET resin. New bottles made with recycled HDPE content represent the largest market for this resin (Fig. 8). Recycled polyethylene is also used for drainage pipe, trash and grocery bags, pallets, and lumber. A high percentage of recycled PET is converted to fibers for use in carpets and as fiberfill in garments and sleeping bags (Fig. 9).

Plastic plates and cups are primarily made of polystyrene resin. It was estimated that 810,000 tons of waste from these products was generated in 1996, of which 11,000 tons were recovered for recycling.

Disposable diapers, including adult incontinence products, were estimated to contribute 3 million tons of material (e.g., wood pulp, plastics including su-

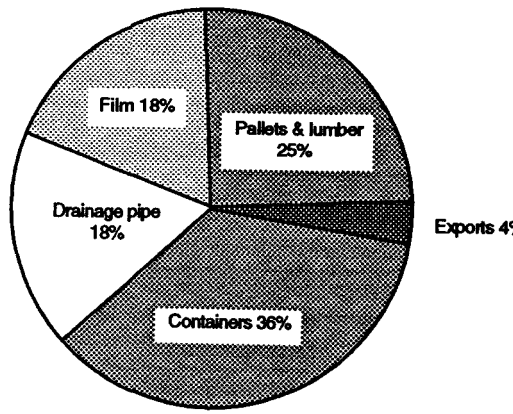

FIG. 8. End-user markets, by product category, for HDPE bottles. (From Ref. 1; original source: *Modern Plastics.*)

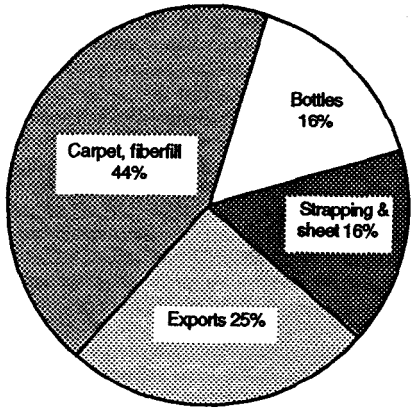

FIG. 9. End-user markets, by product category, for PET bottles. (From Ref. 1; original source: *Modern Plastics.*)

perabsorbant, tissue paper, nonwoven textiles, etc.) to MSW. No significant recycling or composting of these products was reported in 1996.

COMBUSTION

Combustion of municipal solid waste primarily involved waste conversion to steam, electricity, or fuel. In 1996, there were 110 waste-to-energy conversion facilities in the United States. There were also eight combustion facilities that utilized waste as fuel. A small amount (2450 tons/day) of waste was combusted without energy recovery. Nearly 40% of waste-to-energy recovery facilities are located in the Northeast. Energy values of a number of materials are listed in Table 3. In all, 36 million tons (17% of total MSW generated) of

TABLE 3
Energy Content of Selected Materials

Material	BTU/lb.
Bituminous coal	13,000
Nylon	8,500
Polyester	6,800
Polypropylene	9,300
Processed wood pellets	8,500

Source: Ref. 2.

municipal solid waste was combusted in 1996, of which 2.5 million tons of waste, mostly containing rubber tires and some wood, paper, and plastic waste, have been combusted as fuel. Approximately 25% of the dry weight of combusted municipal solid waste converts to ash. It is assumed that most of the ash is landfilled. However, in the EPA report (1), the combustion ash was not considered a part of the MSW, as it must be managed separately.

COMPOST

Composting is mostly limited to yard trimming, food waste, soiled paper, and the other biodegradable components in MSW. In 1996, over 3200 yard-trimming composting facilities, 15 MSW composting facilities, and 176 food-waste composting facilities were reported in the United States.

MATERIALS RECOVERY

Materials recovery facilities (MRFs) are used to process recyclable materials. There were 363 operating MRFs in 1996, with a total daily capacity of 29.4 thousand tons. Most of these MRFs are low-technology facilities, where materials are predominantly sorted manually. Some high-technology MRFs sort recyclables using eddy currents, magnetic pulleys, optical sensors, and air classifiers.

Mixed-waste processing facilities, less common than MRFs, receive waste just as if it were going to the landfill. Mixed waste, loaded on conveyers, is

TABLE 4
Estimated Volume of Selected Materials Discarded in MSW in 1996

Material	MSW generation[a] (million tons)	Discards[b] Weight (million tons)	Discards[b] Weight (% of MSW total)	Discards[b] Volume (% of MSW total)
Plastics	19.8	18.7	12.3	25.1
Rubbers/leather	6.2	5.6	3.7	7.8
Textiles	7.7	6.8	4.4	8.2
Total	33.1	31.1	20.4	41.1

[a] Municipal solid waste generation = recovery + combustion + landfill.
[b] Discards = combustion + landfill.
Source: Ref. 1.

TABLE 5
Per Capita Generation, Materials Recovery, Combustion, and Discards of MSW (in Pounds per Person per Day; Population in Millions)

	1960	1990	1996
Generation (all materials)	2.68	4.51	4.33
Plastics	0.01	0.38	0.41
Rubber and leather	0.06	0.13	0.13
Textiles	0.05	0.13	0.16
Recovery (all materials) (recycling and composting)	0.17	0.74	1.18
Combustion	0.82	0.70	0.70
Landfill	1.69	3.07	2.44
Population	180	249	265

Source: Ref. 1.

sorted both manually and mechanically for removing recyclables for further processing. In 1996, there were 58 mixed-waste processing facilities in the United States, handling 34,800 tons of waste per day.

CONCLUDING REMARKS

In 1996, plastics, rubbers, and textiles contributed 20% by weight and 41% by volume to the U.S. municipal solid-waste stream (Table 4). On a per capita basis, the contribution of the plastics, rubbers, and textiles increased from 0.12 lb./person/day in 1960 to 0.70 lb./person/day in 1996 (Table 5). This represents a loss of high-energy products through landfilling. Significant efforts are being made to develop technologies to recover these materials (3–8).

REFERENCES

1. *Characterization of Municipal Solid Waste in the United States—1997 Update,* U.S. Environmental Protection Agency Report EPA 530-R-98-007, Franklin Associates Ltd., Prairie Village, KS, 1998.
2. S. Kumar, Carpet recycling technologies, in *Book of papers, 1997 International Conference and Exhibition, American Association of Textile Chemists and Colorists,* Atlanta, GA, 1997, pp. 220–228.
3. R. J. Ehrig (ed.), *Plastics Recycling,* Hanser Publishers, New York, 1992.

4. G. D. Andrews and P. M. Subramanian (eds.), *Emerging Technologies in Plastics Recycling,* ACS Symposium Series 513, American Chemical Society, Washington, DC, 1992.
5. F. P. La Mantia (ed.), *Recycling of Plastic Materials,* Chem Tec Publishing, Toronto-Scarborough, Canada, 1993.
6. A. L. Bisio and M. Xanthos (eds.), *How to Manage Plastics Waste,* Hanser Publishers, New York, 1994.
7. C. P. Rader, S. D. Baldwin, D. D. Cornell, G. D. Sadler, and R. F. Stockel (eds.), *Plastics, Rubber, and Paper Recycling: A Pragmatic Approach,* ACS Symposium Series 609, American Chemical Society, Washington, DC, 1995.
8. Brandrup, M. Bittner, W. Michaeli, and G. Menges (eds.), *Recycling and Recovery of Plastics,* Hanser Publishers, New York, 1996.

POLYM.–PLAST. TECHNOL. ENG., 38(3), 411–431 (1999)

SEPARATION AND RECOVERY OF NYLON FROM CARPET WASTE USING A SUPERCRITICAL FLUID ANTISOLVENT TECHNIQUE

ARON T. GRIFFITH, YOONKOOK PARK, and
CHRISTOPHER B. ROBERTS*

Department of Chemical Engineering
Auburn University
Auburn, Alabama 36849

Abstract

This article presents a new process for the selective separation and recovery of nylon material from carpet waste using a solvent-based selective dissolution technique combined with supercritical fluid antisolvent precipitation. The process is described in three primary stages: (1) selective dissolution of nylon up to 2.31 wt.% from the model carpet with an 88 wt.% liquid formic acid solution is performed at 40°C, (2) recovery of the nylon product powder with supercritical CO_2 antisolvent precipitation at pressures between 84 and 125 bar at 40°C, and (3) recycle of both the solvent and antisolvent by flashing into two phases. Detailed studies on the supercritical fluid antisolvent precipitation (stage 2) of the nylon material from carpet waste were performed in which the influences of operating conditions were examined. Effective recovery of the nylon material was achieved with control over the morphology and particle size of the nylon powder. The particles obtained were typically less than 20 μm and spherical in nature, with exceptions observed at the highest operating pressure above 300 bar. In general, the experiments illustrate that changes in operating pressures (both upstream and down-

* To whom correspondence should be sent.

stream of the expansion nozzle), nozzle diameter, and solution concentrations had little influence on the particles' mean size and size distribution. The results suggest this process to be very controllable. In addition, analysis of the nylon product illustrated that this process shows promise in providing quality nylon material from waste carpet material.

Key Words: Carpet; Recycling; Supercritical fluid; Antisolvent precipitation; Nylon.

INTRODUCTION

We present a new method of separating certain mixed or commingled polymeric materials for recycle. Specifically, we will examine the separation of nylon from common carpeting materials. This new process (1) combines selective dissolution of the nylon materials in a liquid solvent and the subsequent recovery of the nylon in controllable powder form using a supercritical fluid antisolvent precipitation technique, as described below. This recovered material has many potential applications, including membrane materials, filter media, novel thermoplastic blends, chromatographic packing, and catalyst support materials.

Carpet is generally comprised of three primary polymer components: polypropylene (backing), latex (binding), and nylon (face fibers). Nylon face fiber is a major component in carpet, typically constituting more than 50% by mass (2). The high value of nylon material increases the recycle viability of carpeting material from an economic perspective. Unfortunately, much of the waste carpet being disposed of by consumers is done so through landfilling. In the United States, greater than 3 billion pounds of waste carpet was removed from homes and businesses in 1995 (3). An equal amount was reported in Western Europe (4).

There have been many approaches to mixed plastics and carpet recycling, including density-based separations, depolymerizations, solvent-based separations, and others. One mechanism gaining attention for the separation of polymeric mixtures involves selective dissolution techniques. Selective dissolution is the process in which one component of a mixture is preferentially dissolved in a solvent, leaving the other components of the mixture undissolved. Solvents for these selective dissolution techniques range from liquids at room temperature to supercritical fluids (SCFs). Methods of recovering the dissolved polymer from the solvent have included flash devolatilization (5,6), rapid expansion of a SCF solvent (7), and dilution with nonsolvents.

Supercritical fluid solvents have gained much attention in recent years as solvents in a variety of polymer processes, including extractions and separa-

tions (8,9) fractionations (9,10) and particle formation (8). This attention stems primarily from the ability to dramatically change the bulk properties of a SCF, such as density and solvent strength, with small variations in temperature and pressure. A supercritical fluid is any fluid heated above its critical temperature and compressed beyond its critical pressure. For example, the critical temperature of CO_2 is 31°C and its critical pressure is about 73 bar. In this supercritical region, the physical properties of the fluid can be "tuned" from gaslike to liquidlike by adjusting the temperature and pressure. Figure 1 illustrates the ability to "tune" the properties of supercritical fluids. The new process described herein takes advantage of the "tunable" properties of supercritical fluids.

Sikorski patented the use of a SCF solvent for the dissolution and recovery of components from carpet (7). It was proposed that the individual polymers in carpet could be sequentially extracted using SCF solvents such as alkanes and CO_2 by incrementing the temperature and pressure (hence changing density) of the SCF solvent. This would allow the polymers in the matrix to be sequentially separated (7). Unfortunately, fairly high operating temperatures and pressures are required to dissolve the various polymers in the SCF solvents.

Another recent application of SCF solvents in polymer processing involves the use of a SCF as an antisolvent (or nonsolvent) for inducing polymer precipitation from solutions and for the production of fine particles during precipitation. Gallagher et al. (11) introduced the process termed Gas Anti-Solvent (GAS) Recrystalization. GAS uses a SCF or a compressed gas as an antisolvent to precipitate a solute (e.g., polymer), which has been dissolved in a liquid solvent. The process takes advantage of the fact that a SCF can dissolve in and expand liquid solutions. The introduction of the SCF to the polymer–solvent solution expands the liquid solution and decreases the solubility

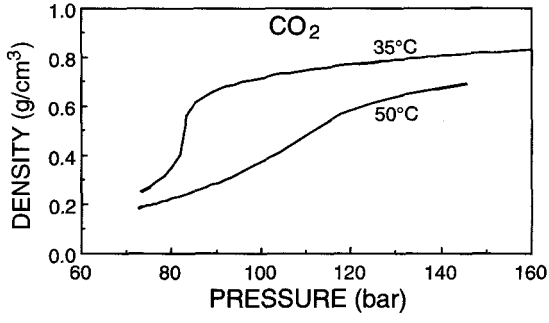

FIG. 1. Density of CO_2 in the supercritical region as a function of pressure along two isotherms.

of the polymer, which results in forced nucleation and growth of polymer particles. A slight twist on the GAS process is one introduced by Dixon et al. (8) termed Precipitation with a Compressed Fluid Antisolvent (PCA). In this process, a polymer and liquid solvent solution is sprayed into a compressed antisolvent, where the liquid solvent rapidly dissolves into the SCF. The polymer, which is insoluble in the SCF, precipitates out of solution. Both of these techniques have been widely used for a variety of materials processing to produce micron-sized particles (powders) with narrow size distributions. To determine the applicability of these processes to a particular system, (1) the solid must dissolve in a liquid solvent at mild temperatures, (2) the solid or polymer must be relatively insoluble in a supercritical fluid antisolvent, and (3) the liquid solvent must be at least partially miscible with the chosen supercritical fluid.

An extension of these two processes from the realm of particle size reduction to that of recycling can be readily performed. Given a polymeric mixture that needs to be separated, a liquid solvent can be chosen in which one polymer in the mixture is soluble and the other polymers are not. An appropriate SCF antisolvent can be chosen for the system, and the polymer–solvent system can then be separated via either antisolvent process discussed above.

Here, we present a new method of separating nylon from carpet material, taking advantage of this SCF antisolvent recrystallization technique for recovery of valuable resources (1,12). The details of the process are provided in the following section.

NEW PROCESS DESCRIPTION

In this process, the recovery of nylon from carpet will occur in three stages: dissolution of nylon in formic acid, antisolvent recovery of the nylon in SCF CO_2, and separation of the solvent and antisolvent via density manipulations. A flow diagram of the process is given in Fig. 2 (1). This new technique is a closed-loop process which uses environmentally benign SCF CO_2 and offers convenient recovery of the polymer as well as control over the morphology and particle size of the recovered nylon.

In the first stage (dissolution), the carpet is fed into a dissolution vessel, where the nylon is selectively dissolved by the formic acid solvent, leaving the polypropylene and latex matrix along with the filler material (usually calcium carbonate). A number of solvents can be identified for the dissolution of nylon at or near room temperature, such as formic acid and phenol, as well as some stronger acids. However, the use of the stronger acids can result in significant degradation and depolymerization even at short contact times. The solubility of nylon in an 88% formic acid solution (12% water) has been determined to be as high 2.5+ wt.%. Passing formic acid over the polymer matrix gives complete separation of the nylon. The polypropylene and latex are

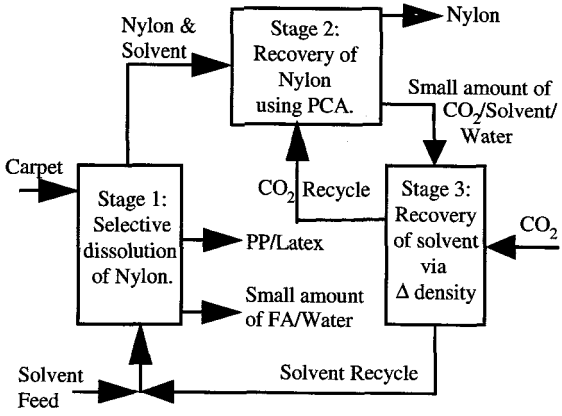

FIG. 2. Process flow diagram for recovery of nylon from carpet waste (PP: polypropylene; FA: formic acid).

left behind in the extraction chamber as the nylon is dissolved and swept away by the formic acid. In a commercial version of the process running in a continuous or semicontinuous fashion, some small amounts of formic acid and water will be discharged with the polypropylene and latex backings when the solids trap in stage 1 is opened and the material is filtered. This material can then be subsequently dried for disposal or recycle.

The second separation stage involves the recovery of the nylon from the liquid solvent (antisolvent precipitation stage). Of course, the formic acid–nylon solution could be simply diluted with water to precipitate the nylon material. However, the subsequent required separation of the solvent's formic acid and water is challenging. Here, we present the use of SCF CO_2 as an antisolvent which will provide convenient solvent separation (in stage 3). CO_2 is convenient for use as an antisolvent, as it is cheap and environmentally attractive and has a relatively low critical temperature and pressure. The nylon–formic acid solution is pumped into the second stage, where it is contacted with the SCF CO_2. The operating conditions can be chosen such that the formic acid and CO_2 are miscible, so that when contacted, the solution's solvent strength is lowered, which forces precipitation of the nylon. Again, in a commercial version of the process, some small amounts of CO_2, formic acid and water will be discharged with the nylon when the nylon trap in stage 2 is opened. This nylon material can then be subsequently filtered and dried for reuse. The ability to control particle size and morphology by manipulating recovery conditions has been investigated and the results of detailed investigations in stage 2 are presented in the following sections.

Finally, in the last stage of the process (stage 3), the CO_2–formic acid stream (with residual water) is separated with a simple adjustment in temperature or pressure so that the acid solution and CO_2 are no longer miscible. In other words, by simply decreasing the pressure of the system, this stream can be "flashed" into a CO_2-rich phase and a formic acid–water-rich phase. Therefore, the CO_2 and the formic acid are then recycled into the process. Many mixtures of CO_2 and carboxylic acids similar to formic acid (such as acetic, propionic, *n*-butyric acids) demonstrate the transition from a one-phase system to a two-phase system with small changes in pressure. Unfortunately, to the authors' knowledge, detailed phase behavior data for the formic acid–water–CO_2 system is not available in the literature to date. However, Figure 3 shows ternary diagrams at typical operating conditions in stage 2 and stage 3 for a similar solvent, acetic acid. In Fig. 3a, the circle symbol represents a typical operating condition in stage 2 of roughly 17% acetic acid and 82% CO_2, with a residual amount of water at the operating temperature and pressure of 313 K and 150 bar, respectively. This is a one-phase system at these operating conditions, as desired (solvent and antisolvent are miscible in stage 2). Figure 3b illustrates that with a decrease in pressure to 40 bar (stage 3), the system will phase split into a CO_2-rich phase and an acetic-acid-rich phase along the tie lines provided. This allows reuse of the solvent and antisolvent. The data in Fig. 3 were taken from Panagiotopoulos et al. (13).

This three-stage process provides effective separation of nylon from the polymer matrix; investigations into the specifics of each of the three stages are underway in our laboratory. In the following section, we present specific investi-

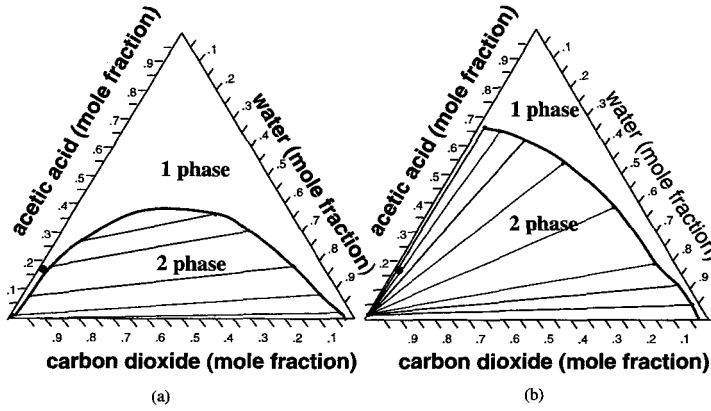

FIG. 3. Ternary phase diagram for the acetic acid–water–carbon dioxide system at (a) 150 bar and (b) 40 bar at 313 K. Circle symbol represents typical operating conditions of stages 2 and 3 (see text). (Data from Ref. 13.)

gations of the antisolvent recovery of nylon via the PCA process (stage 2), and the results of these separations are discussed. Unique nylon materials are produced, including the production of fine nylon powders of porous microspheres.

EXPERIMENTAL

Materials Used

Common carpet material was obtained from the Textile Engineering Department at Auburn University; it consisted of roughly 50 wt.% nylon fibers, with the remainder made up of polypropylene primary and secondary backings, a SBR latex binder, and calcium carbonate filler. Formic acid (88%) was obtained from Aldrich and used as received. Figure 4 is a photograph of the carpet material before processing with formic acid (Fig. 4a) and the remaining backing material after dissolution of the nylon fibers (Fig. 4b). Carbon dioxide (SFC grade) was obtained from BOC Gases (Bessemer, AL, U.S.A.).

Apparatus and Method

The experimental setup used for this study of the antisolvent precipitation of nylon from carpet waste (stage 2) is similar to that used by Dixon et al. (8) and is shown in Fig. 5. Nylon fibers from carpet waste were dissolved in formic acid to 2.31 wt.% and the liquid solution was placed in the sample side of a stainless-steel piston–cylinder assembly. We have measured the solubility of this nylon material in the 88 wt.% formic acid solution to be roughly 2.5 wt.%. The nylon concentration of 2.31 wt.% used in the experiments is just below the solubility limit. The piston–cylinder assembly was then compartmentalized with two valves, as shown in Fig. 5, and the pressure on the piston was then maintained with a high-pressure nitrogen tank (runs 6–15) or a model 260D Isco high-pressure syringe pump (runs 1–5). A Jerguson (Strongsville, OH, U.S.A.) sight gauge (model R-12) was used as the collection vessel. Capillary tubing of two different inside diameters (50 and 154 μm) were used as spray nozzles during these investigations and were attached to one end of the collection vessel. A glass plate for particle collection was placed inside the vessel.

Antisolvent (CO_2) was delivered to the collection vessel using another Isco 260D high-pressure syringe pump programmed to operate at a constant desired pressure. The system temperature was maintained at 40°C during all experiments by use of a water bath fitted with an immersion circulator. The system pressure was measured using a pressure transducer (Omega, Stamford, CT, U.S.A., model PX945). The computer-controlled syringe pump, jacketed for heating/cooling, was charged with CO_2, which was subsequently brought to and kept at experimental temperature and pressure. The jacket was also con-

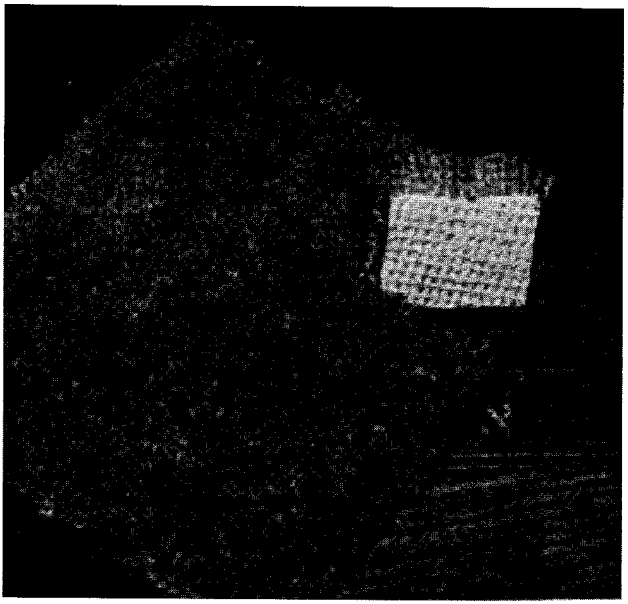

(a)

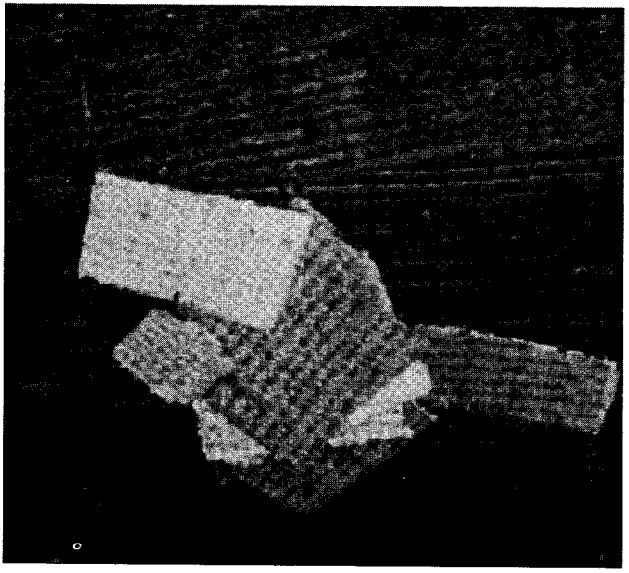

(b)

FIG. 4. Photographs of (a) postconsumer carpet used in experiments and (b) the remaining backing material after nylon dissolution.

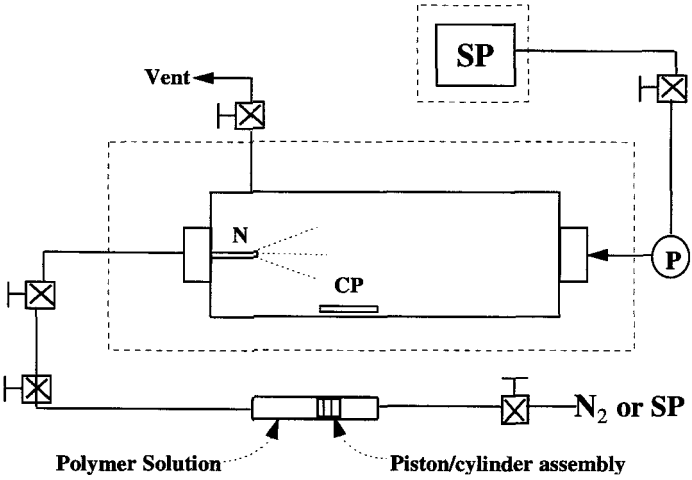

FIG. 5. Experimental apparatus for SCF antisolvent precipitation of nylon (CP: collection plate; N: 50- and 154-μm spray nozzle; P: pressure transducer; SP: Isco syringe pump).

nected to an immersion circulator operating at 40°C. The polymer solution pressure (upstream), antisolvent (CO_2) pressure (downstream), nozzle diameter, and polymer solution concentration were varied in order to determine the influence of process operating conditions on the product materials obtained. After the collection vessel was allowed sufficient time to equilibrate and the polymer solution was pressurized, the valve restricting the flow of the polymer solution was opened briefly, causing a liquid jet to spray into the collection vessel. The precipitation of the nylon was noted by the formation of a very cloudy region inside the vessel.

Following precipitation, the vessel was purged with more than three equivalent volumes of pure carbon dioxide at the experimental temperature and pressure to remove all of the liquid solvent from the system. The collection vessel was then depressurized slowly while being maintained at the experimental temperature so as to avoid the formation of liquid carbon dioxide within the cell. The glass collection plate was removed when atmospheric pressure was reached and the particles collected were analyzed on a Jeol (Peabody, MA, U.S.A.) JSM-840 scanning electron microscope (SEM). For SEM analysis, the collection plates were sputtered with a thin layer of gold and placed on the sample tray. Small strips of double-sided carbon conductive tape were used to attach the collection plate to the SEM sample tray to ensure that the surface was conductive. SEM micrographs of the recovered nylon were obtained and used for particle sizing (perimeter weighted-average size distributions) and investigation of morphology.

A series of experiments were performed to investigate the influence of upstream pressure, antisolvent pressure, nozzle diameter, and nylon solution concentration on the recovered nylon's particle size distribution and mean particle size. To investigate the influence of each process variable, experimental conditions were chosen such that a comparison of results could be made in which only one process variable was manipulated. Table 1 shows the experimental conditions used in all 15 runs. In the first set of experiments, a downstream pressure of 111.3 bar, a 154-μm nozzle diameter, nylon concentration of 2.31 wt.%, and a system temperature of 40°C were used, while the upstream pressure was varied between 173.4 and 327.0 bar. The second set of experiments was performed with a constant upstream pressure of 133.4 bar while varying downstream pressure from 83.7 to 125.1 bar. The third set of experiments was performed under the same conditions as the second set, except the nozzle diameter was changed from 154 μm to 50 μm. Finally, an experiment was performed under the same conditions as above with the nylon solution concentration of 0.63 wt.%.

Intrinsic viscosity, differential scanning calorimetry (DSC), and Fourier transform infrared (FTIR) spectroscopic analyses were performed on the nylon material to determine viscosity-average molecular weight (M_v), melting temperature (T_m), and chemical structure and purity. Unfortunately, the mass of the nylon recovered in our experimental apparatus was too small to be tested directly in the analysis methods mentioned earlier. Therefore, after dissolution in the formic acid, nylon material was also recovered by simply diluting the formic acid solution with water, thus causing the nylon to precipitate. This method allowed the collection of a larger mass of nylon powder material while still permitting investigation of the material's physical properties. The nylon powder was then collected by filtration prior to intrinsic viscosity, differential scanning calorimetry, and FTIR spectroscopic analysis.

The viscosity-average molecular weight (M_v) of raw nylon from carpet waste and the nylon powder from dilution were determined by intrinsic viscosity measurements conducted at 25°C. The solvent used was 90% formic acid (14) and an Ubbelohde calibrated viscometer tube (Fisher, Pittsburgh, PA, U.S.A.) was used. The molecular weights of the nylon materials were calculated from the intrinsic viscosity ([η] in mL/g) according to the equation $[\eta] = 2.5 + 0.0132M^{0.873}$ (15). A Perkin-Elmer (Norwalk, CT, U.S.A.) DSC-2 differential scanning calorimeter was used to analyze the melting temperature of raw nylon from carpet waste and the nylon powder. The analyses were performed at 10°C/min heating rate and 20 cm^3/min nitrogen flushing rate. Finally, recovered nylon from carpet waste was mixed with Fluorolube™ (Fisher), used as a mulling agent, following a method described in the literature (16). The mull was spread evenly on a NaCl salt plate and analyzed on a Perkin-Elmer Spectra 2000 FTIR spectrometer. The results of these studies are presented in the following section.

TABLE 1
Experimental Conditions

Run	Nozzle diameter (μm)	Nozzle length (mm)	Polymer conc. (wt.%)	Upstream pressure (bar)	Downstream pressure (bar)	Pressure differential (bar)	Mean particle size (μm)	Microstructure
1	154	110 ± 10	2.31	327.0	111.3	215.7	—	Porous, hollow, half-spherical
2	154	110 ± 10	2.31	276.8	111.3	165.5	3.63	Spherical
3	154	110 ± 10	2.31	242.3	111.3	131.0	2.92	Spherical
4	154	110 ± 10	2.31	207.9	111.3	96.6	2.17	Spherical
5	154	110 ± 10	2.31	173.4	111.3	62.1	2.11	Spherical
6	154	18 ± 2	2.31	133.4	83.8	49.6	1.54	Spherical
7	154	18 ± 2	2.31	133.4	97.5	35.9	2.81	Spherical
8	154	18 ± 2	2.31	133.4	111.3	22.1	2.64	Spherical
9	154	18 ± 2	2.31	133.4	125.1	8.3	2.98	Spherical
10	154	18 ± 2	0.63	133.4	97.5	35.9	1.78	Spherical
11	50	18 ± 2	2.31	133.4	83.8	49.6	2.09	Spherical
12	50	18 ± 2	2.31	133.4	97.5	35.9	2.01	Spherical
13	50	18 ± 2	2.31	133.4	103.7	29.7	3.14	Spherical
14	50	18 ± 2	2.31	133.4	111.3	22.1	1.89	Spherical
15	50	18 ± 2	2.31	133.4	125.1	8.3	4.28	Spherical

Note: Temperature: 40°C; material: nylon from carpet waste.

RESULTS AND DISCUSSION

A series of experiments were performed for CO_2 antisolvent recovery of nylon from the 2.31 wt.% nylon–formic acid solutions. A typical example of the nylon material obtained is illustrated in the SEM micrograph of Fig. 6. This figure displays particles obtained from expansion through a 154-μm nozzle with an upstream pressure of 207.9 bar and antisolvent pressure of 111.3 bar at 40°C. The particles obtained are spherical in shape and range in size from <1 to 20 μm. The results here are typical for the experiments run with upstream pressures ranging from 133.4 to 276.8 bars, downstream pressures ranging between 83.8 and 125.1 bar, and nozzle sizes of 50 and 154 μm. However, an exception to the spherical particles occurred at very high upstream pressures, such as the situation shown in Fig. 7a. In this experiment, expansion of the 2.31 wt.% solution at an upstream pressure of 327.0 bar was performed through a 154-μm nozzle into CO_2 antisolvent at 40°C. An abrupt change in the particle morphology occurred, resulting in the production of hollow half-spheres or "cusps." It is possible that as the nylon–formic acid liquid droplets are sprayed into the CO_2 antisolvent, precipitation rapidly occurs on the surface of the sprayed droplet, causing production of a nylon film (or skin)

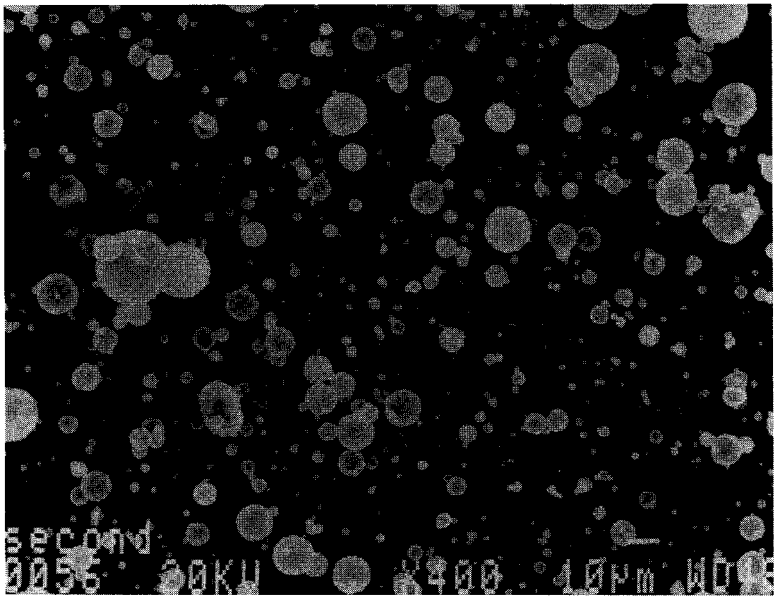

FIG. 6. SEM micrograph of nylon particles recovered using a 154-μm nozzle, an upstream of 207.9 bar, and a downstream pressure of 111.3 bar at 313 K.

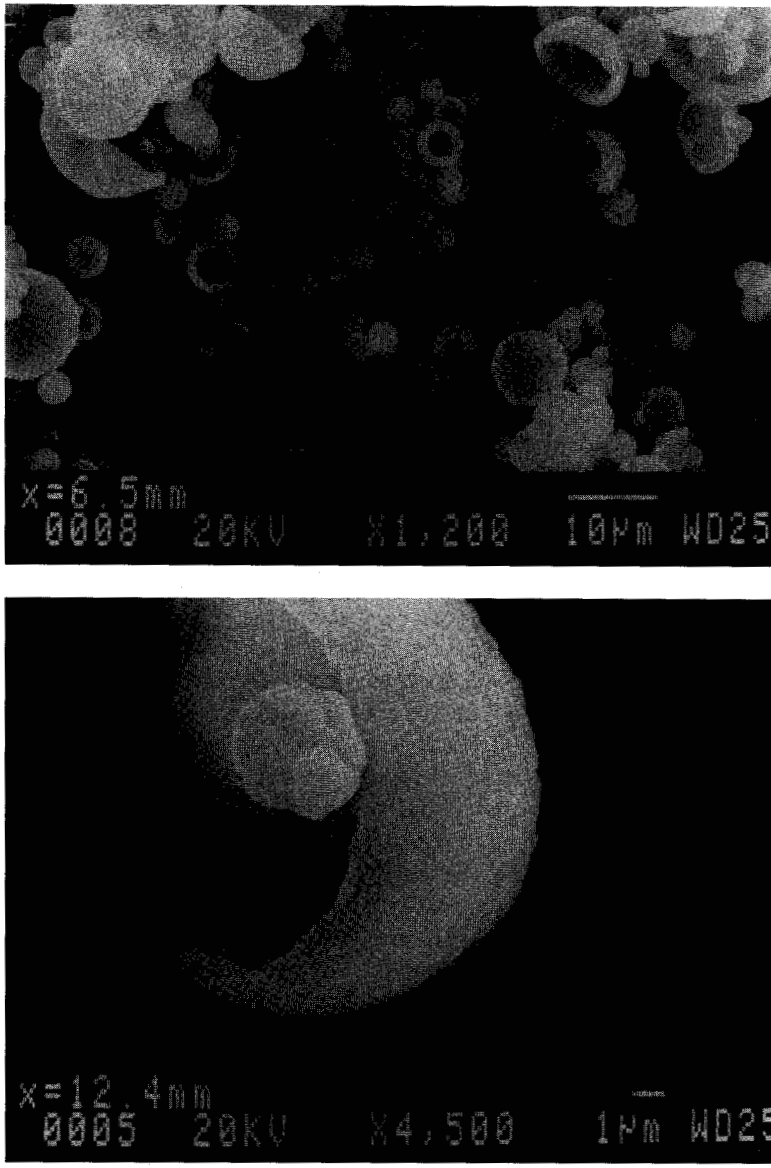

(a)

(b)

FIG. 7. SEM micrographs of nylon particles recovered using a 154-μm nozzle, an upstream pressure of 327.0 bar, and a downstream pressure of 111.3 bar at 313 K. The scale bar represents 10 μm (a) and 1 μm (b).

around the liquid droplet. As the CO_2 continues to penetrate and swell the formed nylon shell, and as the liquid solution continues to diffuse into the bulk CO_2, a rupture of the nylon shell may occur. An alternative explanation involves the increased shear that occurs at this larger pressure drop during expansion. A closer investigation of the particles from this high-upstream-pressure experiment is illustrated in Fig. 7b. The higher magnification illustrates a porous, hollow, half-spherical morphology.

Multiple experiments were performed to investigate the influence of upstream pressure, downstream pressure, nozzle diameter, and nylon solution concentration on the particle size and size distributions. In general, our experiments have shown little influence of these operating parameters on particle size and distribution. It should be noted that in all cases, the particles obtained are much smaller than the nozzle diameter, as observed in several other investigations (10,17).

Effect of Upstream Pressure

The upstream pressure is not only a very important factor in affecting particle morphology, as discussed earlier, but may also play an important role in impacting the mean particle size and size distribution, as seen in Table 1 and Fig. 8a. Figure 8a demonstrates a comparison of particles obtained at a downstream pressure of 111.3 bar, a nozzle diameter of 154 μm, and upstream pressures of 173.4, 207.9, 242.3, and 276.8 bar (comparing runs 2, 3, 4, and 5, respectively). From the SEM results obtained from each experiment, the size distribution (perimeter weighted size distribution) was determined. The particle size analysis was done by hand from the SEM micrographs. The maximum estimated error in the sizing of the particles is determined to be ± 0.5 μm. In general, the higher upstream pressures resulted in basically very little change in mean size. Figure 9 shows that the mean particle size increased only modestly with an increase in upstream pressure within the estimated error associated with the particle sizing. However, more than 90% of the particles obtained ranged from <1 to 6 μm in size. Notwithstanding, a very large fraction of the mass in the system is obvious with the larger diameter particles, even though they are few in number. To illustrate this, Fig. 8b presents a mass-weighted particle size distribution for the same data set as in Fig. 8a. Assuming the precipitated material to have roughly the same density as the bulk density of nylon from carpet waste ($\rho = 1.1$ g/cm^3), the mass of each diameter particle is estimated by

$$w_i = n_i \rho \frac{4}{3} \pi \left(\frac{d_i}{2}\right)^3 = \frac{\pi \rho}{6} n_i d_i^3 \tag{1}$$

where w_i is the estimated weight of a particle, n_i is the number of each diam-

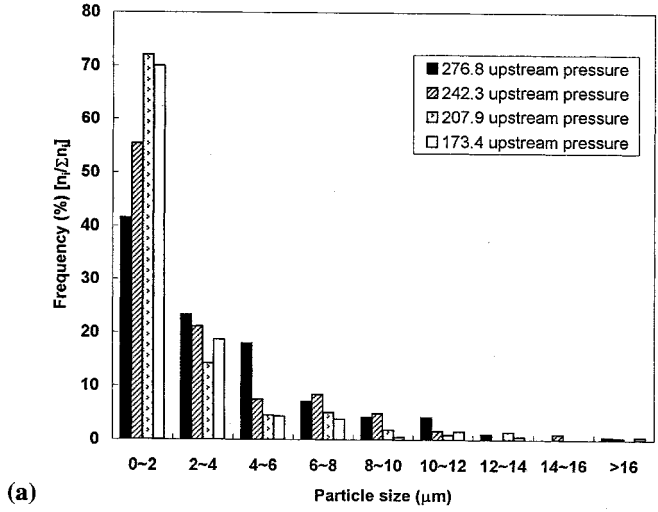

(a)

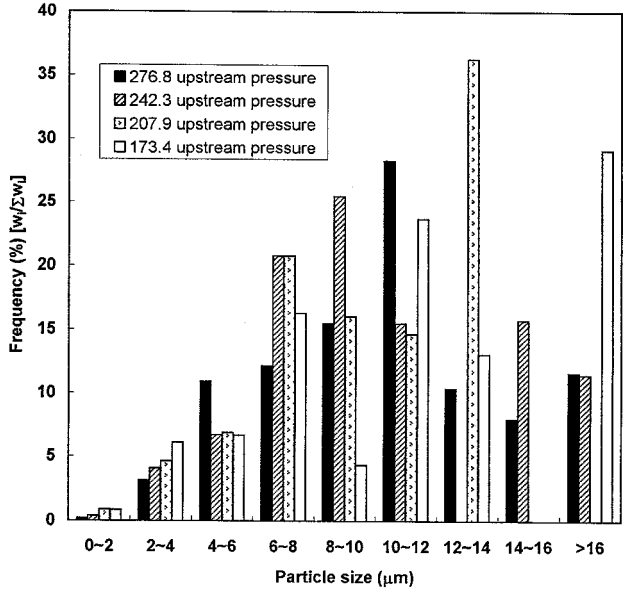

(b)

FIG. 8. (a) Comparison of number-average particle size distributions at different upstream pressures (downstream pressure of 111.3 bar and nozzle diameter of 154 μm). (b) Comparison of mass-weighted particle size distributions at different upstream pressures (downstream pressure of 111.3 bar and nozzle diameter of 154 μm).

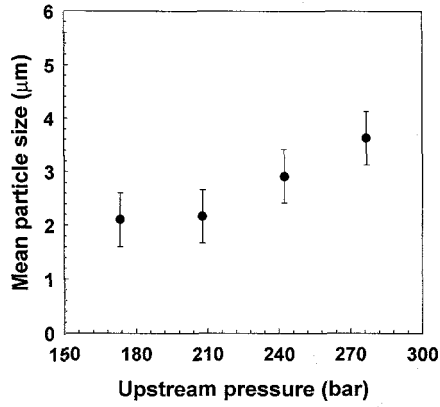

FIG. 9. Comparison of mean particle size obtained at different upstream pressures (downstream pressure of 111.3 bar and nozzle diameter of 154 μm; the estimated maximum error in particle size technique is ±0.5 μm).

eter particle, and d_i is the mean diameter value at each interval. The mass-weighted distribution could be obtained by taking the ratio between the mass at each diameter interval and the total mass over the whole range. The mass-weighted mean is shifted to more than 7 μm, as can be seen in Fig. 8b. In other words, although the larger particles are less frequent, they contain a large fraction of the mass in the system. Of course, this trend follows for all of the runs.

Effect of Downstream Pressure

Figure 10 illustrates a comparison of particle size distributions obtained at downstream antisolvent (CO_2) pressures of 83.8, 97.5, 111.3, and 125.1 bar with an upstream pressure of 133.4 bar and a 154-μm nozzle diameter (comparing runs 6, 7, 8, and 9, respectively). Changing the antisolvent pressure had little effect on the mean particle size, as can be seen in Fig. 11. The estimated error associated with the measurement of particle size is ± 0.5 μm and is nearly comparable to this change. In all, we observe only a minimal influence of the antisolvent pressure on the particle size distribution with 90+% of the particles between <1 and 6 μm. Similar results were obtained when using the 50-μm nozzle and the downstream pressure was varied (comparing runs 11–15). These results, along with those in the previous section, suggest that the operating conditions (stages 1 and 2) have little influence on the recovered product and would further suggest that, from a process viewpoint, this is an easily controllable method for generating powders in this size range.

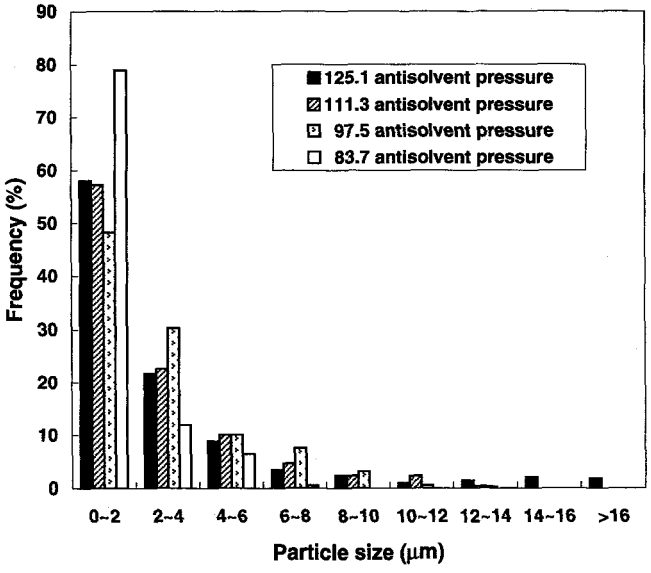

FIG. 10. Comparison of particle size distributions at different downstream antisolvent pressures (upstream pressure of 133.4 bar and nozzle diameter of 154 μm).

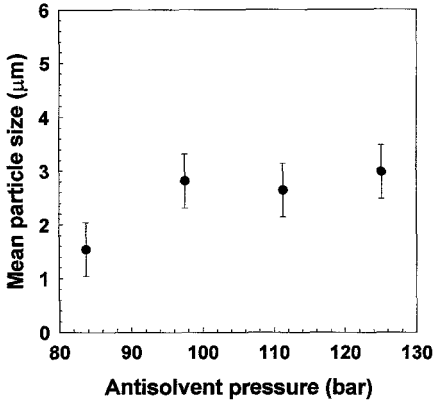

FIG. 11. Comparison of mean particle size obtained at different downstream antisolvent pressures (upstream pressure of 133.4 bar and nozzle diameter of 154 μm; the estimated maximum error in particle size technique is ±0.5 μm).

Effect of Nozzle Diameter

Figure 12 shows a comparison of the particle size distributions obtained at a constant upstream pressure of 133.4 bar, downstream pressure of 97.5 bar, and nylon solution concentration of 2.31 wt.% while varying the nozzle diameter from 50 to 154 μm (comparing runs 7 and 12). As can be seen at both nozzle diameters, the majority of the particles are less than 4 μm in size. Similar results are observed when comparing run 6 to run 11, run 8 to run 14, and run 9 to run 15, with the vast majority of the particles less than 6 μm. Overall, the nozzle configuration showed little influence on the particle characteristics.

Effect of Nylon Concentration

A set of experiments were performed in which the concentration of the formic acid–nylon solution was changed from 2.31 to 0.63 wt.% at an upstream pressure of 133.4 bar and downstream pressure of 97.5 bar, with a 154-μm nozzle (comparing runs 7 and 10). It might be anticipated that smaller particles would be obtained at the lower concentration due to the smaller amount of nylon contained within each droplet during the spray process. As can be seen in Fig. 13,

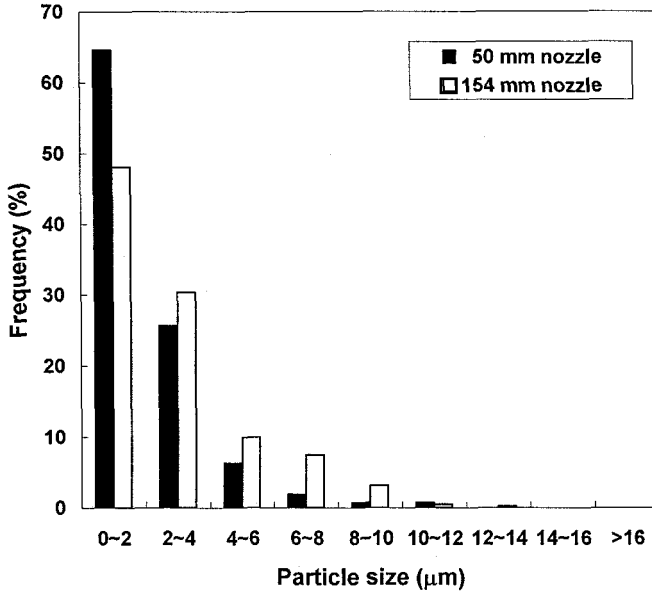

FIG. 12. Comparison of particle size distributions at two different nozzle diameters (upstream pressure of 133.4 bar and downstream pressure of 97.5 bar).

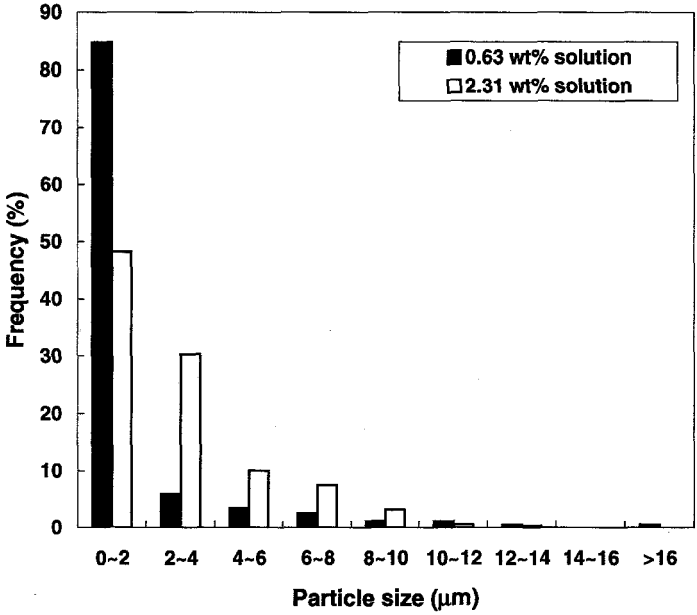

FIG. 13. Comparison of particle size distributions at two different nylon concentrations (upstream pressure of 133.4 bar and downstream pressure of 97.5 bar, and a 154-μm nozzle diameter).

while the particles obtained were within the same overall range for both concentrations, an increase in frequency from 48% to 85% of particles less than 2 μm in size was observed with the decrease in concentration. This suggests a small concentration dependence.

Analysis of Recovered Products

The melting temperatures of the raw nylon from carpet waste and the nylon powder from dilution were measured from DSC to be 258°C and 264°C, respectively. Based on this result, the carpet waste is likely composed only of Nylon 6/6 (18). The viscosity-average molecular weights (M_v) of raw nylon from carpet waste and the nylon powder are approximately 19,000 and 25,000 g/mol, respectively. Surprisingly, this suggests that the molecular weight increases. One possible explanation for this unexpected behavior is that the lower-molecular-weight nylon fractions and other additives were simply washed out through the dilution and filtration process. In all, the M_v of the recovered nylon material is estimated to be roughly between 19,000 and 25,000 g/mol. In order to further examine the structure of the recovered product and

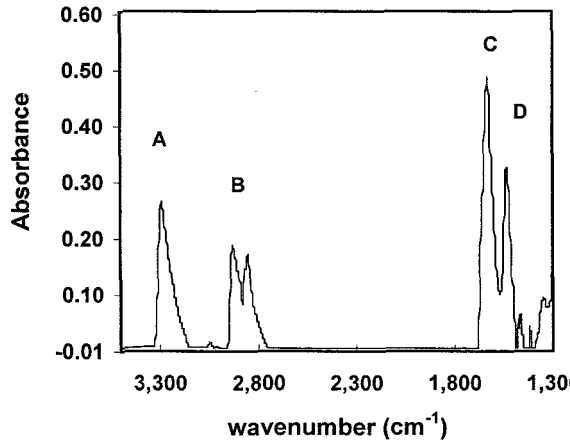

FIG. 14. FTIR spectrum of nylon material recovered through dilution (A: N—H, B: C—H, C: C═O, D: C—H).

the residual solvent content, FTIR spectroscopic investigations were performed as shown in Fig. 14. The characteristic amide bonds of N—H and C═O (19) in the recovered nylon appear at 3300 and 1640 cm^{-1}, respectively. However, the characteristic C═O bond of the solvent formic acid cannot be seen at 1700 cm^{-1}, suggesting that although formic acid can hydrogen-bond with the nylon, it is easily displaced during recovery and drying. Therefore, the nylon in this waste carpet was composed only of Nylon 6/6 as determined by DSC, and the experiments demonstrate that this process shows promise in delivering a high-purity nylon product from waste carpet.

CONCLUSIONS

A new process for the separation of nylon from carpet waste using selective dissolution and SCF antisolvent precipitation was described. The process proceeds in three stages: (1) selective dissolution of nylon from the carpet with a liquid solvent, (2) collection of the nylon product through SCF antisolvent precipitation, and (3) separation and recycle of the solvent and antisolvent through a phase change induced by a change in density. Investigations of the SCF antisolvent precipitation (stage 2) were performed and convenient recovery of the nylon material was achieved, as well as control over the morphology and particle size of the nylon powder. Although exceptions were observed at the higher upstream pressures, the particles obtained were typically spheri-

cal and less than 20 μm. Multiple experiments were performed to investigate the influence of operating variables on the nylon product. The experiments showed little influence on the particles' mean size and size distribution, suggesting this to be a very controllable process. Furthermore, product analysis illustrated that this process shows promise in providing quality nylon product from waste carpet material.

REFERENCES

1. C. B. Roberts and A. T. Griffith, U.S. Patent Appl. No. 06/809,050 (June 1997).
2. D. J. David, J. L. Dickerson, and T. F. Sincock, U.S. Patent No. 5, 294,384 (1994).
3. H. Gardner, *Int. Fiber J., 10*(4), 36 (1995).
4. B. Holtkamp, *High Perform. Textiles, 5*(5), 13 (1996).
5. R. J., Ehrig, *Plastics Recycling: Products and Processes,* Oxford University Press, New York, 1992.
6. J. C. Lynch and B. Naumann, *Chem. Eng. Prog., 87*(11), 22 (1991).
7. M. E. Sirkorski, U.S. Patent No. 5,233,021 (1993).
8. J. D. Dixon, K. P. Johnston, and R. A. Bodmeier, *AIChE J., 39,* 127 (1993).
9. M. A. Meilchen, B. M. Hasch, and M. A. McHugh, *Macromolecules, 24,* 4874 (1991).
10. M. A. McHugh and V. J. Krukonis, *Supercritical Fluid Extraction: Principles and Practice,* Butterworth Heinemann, Boston, 1994.
11. P. M. Gallgher, M. P. Coffey, V. J. Krukonis, and N. Klasutis, *Gas Antisolvent Recrystallization: New Process to Recrystallize Compounds Insoluble in Supercritical Fluids,* ACS Symposium Series No. 406, American Chemical Society, Washington, DC, 1989.
12. C. B. Roberts and A. T. Griffith, in *Proc. 4th Int. Symp. on Suprecritical Fluids,* 1997, Vol. A, p. 391.
13. A. Z. Panagiotopolus, R. C. Willson, and R. C. Reid, *J. Chem. Eng. Data, 33,* 321 (1988).
14. J. Brandrup and E. H. Immergrut, *Polymer Handbook,* 3rd ed., John Wiley and Sons, New York, 1989.
15. E. G. Elias and R. Schumacher, *Makromol. Chem, 76,* 23 (1964).
16. G. A. Robbins, R. A. Winschel, and F. P. Burke, *ACS Fuel Chem. Div. Prepr., 40,* 92 (1995).
17. T. W. Randolph, A. D. Randolph, M. Mebes, and S. Yeung, *Biotechnol. Prog., 9,* 429 (1993).
18. J. R. Fried, *Polymer Science and Technology,* Prentice-Hall, London, 1995.
19. F. Rodriguez, *Principles of Polymer Systems,* Hemisphere Publishing, New York, 1989, p. 537.

POLYM.–PLAST. TECHNOL. ENG., 38(3), 433–444 (1999)

CARBON-DIOXIDE-BASED MICROSORTATION OF POSTCONSUMER POLYOLEFINS AND ITS EFFECT ON POLYOLEFIN PROPERTIES

EDDY KARMANA, SINDEE SIMON,* and
ROBERT ENICK

Department of Chemical and Petroleum Engineering
University of Pittsburgh
Pittsburgh, Pennsylvania 15261

Abstract

Postconsumer polyolefin flake has been sorted using liquid carbon dioxide as a float–sink medium. This separation of PP and LDPE from HDPE was conducted at ambient temperature and a pressure that yielded a CO_2 specific gravity of 0.955, causing the HDPE to sink and the LDPE and PP to float. Although this process provided a high-purity (99+%) HDPE product stream, the effect of immersing the plastics in liquid carbon dioxide at these conditions was not previously measured. Therefore, six HDPE samples, two LDPE samples, and five PP samples were exposed to high-pressure carbon dioxide for 20 min. After this exposure, the polyolefins did not foam when the carbon dioxide was rapidly vented from the vessel. The weight reduction averaged 0.17%, which was attributed to the dissolution of low-molecular-weight additives or contaminants present on the surface of the plastics. No significant change in the melting point or latent heat of melting was observed, indicating that the degree of crystallinity was not affected by the exposure to carbon dioxide. No reduction was observed in the temperature at which the onset of thermal degradation occurred, because of the low solubility and degree of extraction of thermal stabilizers during the immersion in car-

* To whom correspondence should be sent.

bon dioxide. These results indicated that no deleterious effects on the polyolefin properties were associated with this separation technique.

Key Words: Carbon dioxide; Density; Latent heat of melting; Polyolefins; Microsortation; Recycling; Thermal stability.

INTRODUCTION

The recycling of plastics has been accomplished by the dissolution of the mixture into a solvent and the subsequent series of precipitations, the macrosortation of entire containers, or the microsortation of shredded postconsumer flake. Each separation technique was based on differences in chemical, mechanical, or physical properties of the plastics (1–5).

Many technologies have been proposed for the microsortation of postconsumer containers that have been shredded to reduce storage volume requirements; for example, hydrocyclones can be used to separate polyolefins [polypropylene (PP), low-density polyethylene (LDPE), and high-density polyethylene (HDPE) are less dense than water] from the nonolefins [poly(vinyl chloride) (PVC), polyethylene terephthalate (PET), bulk polystyrene (PS) are more dense than water] (4). Other technologies proposed for separating these products include flotation (6), float–sink separations with gas–liquid mixtures (5), froth flotation (1), separation based on differences in dielectric properties (7), x-ray fluorescence scanners for PVC detection, exposure to electrostatic fields (5), and cryopulverization/size separation (9,10). The PET–PVC separation can also be achieved by immersing both plastics in liquid carbon dioxide and flashing the system to ambient pressure. The rapid diffusion of carbon dioxide out of the PVC will cause it to foam, enabling it to be subsequently sorted from the PET using water as a float–sink medium (11). The only currently available technology for commercial-scale microsortation is based on camera detection of color and/or transparency differences in a feedstream (green PET soda bottles from clear PET soda bottles; natural HDPE milk jugs from opaque lids) traveling on a conveyor belt (12). After identification, precise pneumatic jets are employed to direct the "reject" to a different collection bin than the desired product as they pass off the edge of the belt (12).

In the 1990s, a new technology was proposed for the efficient microsortation of postconsumer plastics (13–15). The flake was sorted in a series of float–sink separations, as illustrated in Fig. 1. The separation medium was a fluid with a density intermediate to the densities of the plastics being sorted; for example, water [specific gravity (SG) = 1] was used in the initial step to

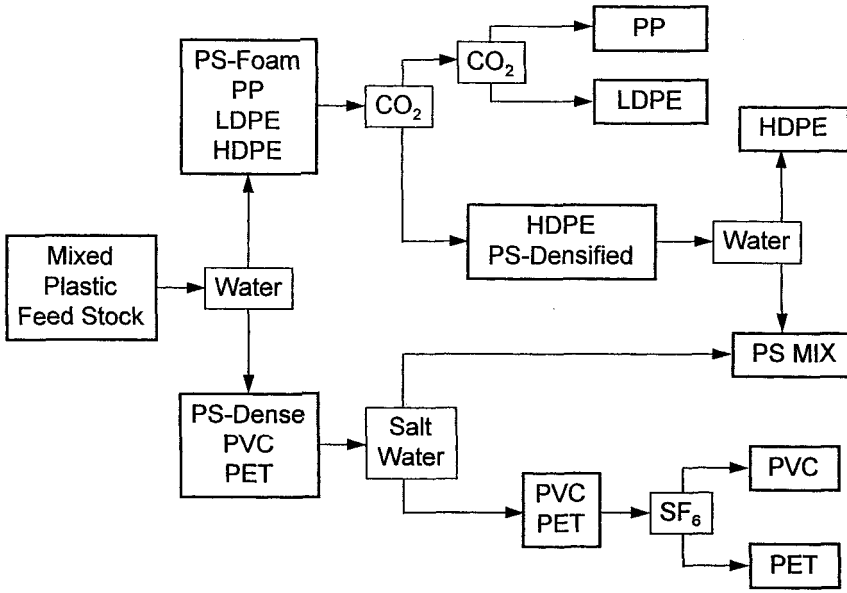

FIG. 1. Flow diagram for the float–sink separation of recyclable thermoplastics.

separate the "light" polyolefins and foamed polystyrene (HDPE, LDPE, PP, foamed PS) from the "heavy" nonolefins (bulk PS, PET, PVC). The bulk polystyrene was then removed as a "light" from the PET–PVC mixture using salt water as the float–sink medium. PVC and PET were then sorted by density using sulfur hexafluoride as the separation medium. The postconsumer polyolefin mixture was refined into an HDPE–densified PS "heavy" product and an LDPE–PP "light" stream using liquid carbon dioxide as the separation medium. The PP and LDPE could be further refined using carbon dioxide, if desired. The HDPE–densified PS mixture could also be further sorted using water as the float–sink medium. The bulk PS and the densified PS could then be combined to form a PS mixture product.

The most promising aspect of this technology has been the microsortation of polyolefins using carbon dioxide. Table 1 shows that the density of carbon dioxide can be adjusted via pressure to a value that is intermediate to HDPE and LDPE, or LDPE and PP. The density range for each plastic was based on postconsumer samples obtained from multiple sources (i.e., HDPE milk jug, HDPE shampoo bottle, HDPE detergent container, etc.). Figure 2 illustrates the six steps of a typical high-pressure batch microsortation (15). This diagram illustrates that the separation can only be accomplished if the density of the carbon dioxide, ρ_f, is greater than the density of the less dense plastic, ρ_l, but

TABLE 1
Density Ranges of Postconsumer Polyolefins and CO_2

Plastic or fluid	Sources	Density (kg/m^3)
Polypropylene	13	916–925
Low-density polyethylene	10	935–955
High-density polyethylene	34	956–980
CO_2 at 298 K and 6.44–69 MPa		780–1000

Source: Ref. 15.

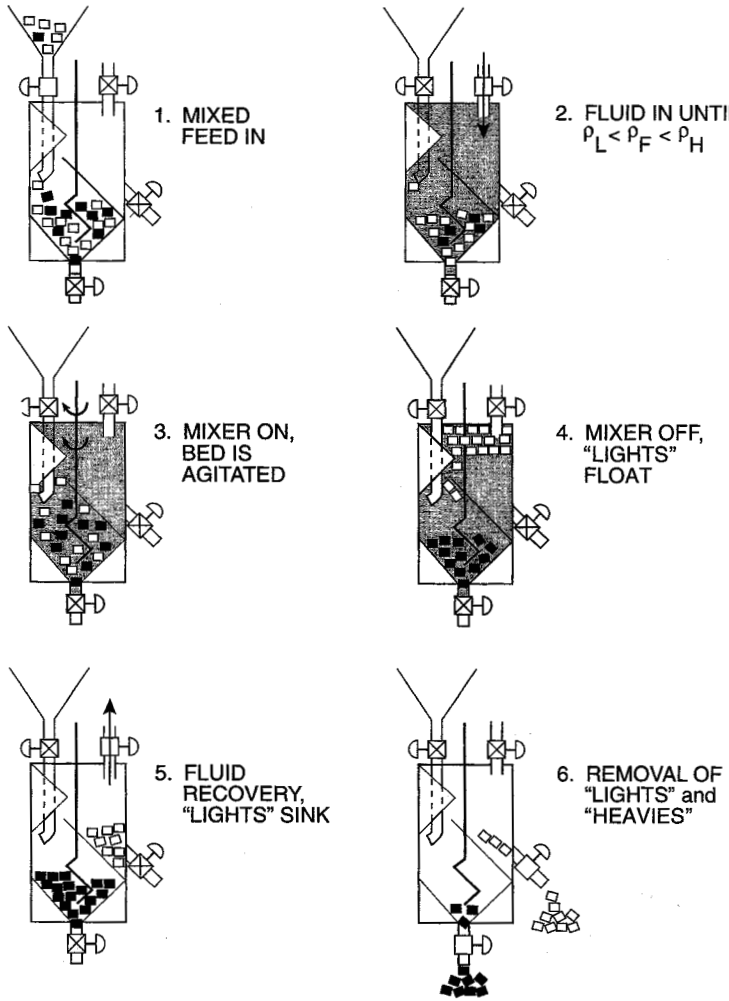

FIG. 2. The six-step batch microsortation process.

lower than the density of the more dense plastic, ρ_h. The viscosity of liquid carbon dioxide is approximately one-tenth that of water, resulting in increased velocities of the plastic particles as they fall or rise through the carbon dioxide. Polyolefins are hydrophobic; therefore, the carbon dioxide can easily displace any residual water from the flake and dissolve small amounts of water or residual oil found on the surface of the plastic. Upon removal from the high-pressure environment, the carbon dioxide will rapidly diffuse out of the flake, leaving no residue behind. Other attributes of this colorless, odorless fluid include its low cost, nonflammability, nontoxic nature, and non-VOC classification. The foremost economic disadvantage of a carbon-dioxide-based microsortation process is the high capital cost associated with high-pressure equipment. The primary safety concern is the oxygen displacement/dilution upon sudden release of large amounts of carbon dioxide into the room if there is a catastrophic equipment failure, such as a ruptured pipe, gasket, or pressure vessel weld. The most common safeguards employed to prevent such releases are the ventilation of the area containing the high-pressure equipment and the inclusion of pressure relief valves or burst plates into the apparatus. These relief devices are vented, allowing any carbon dioxide that is released through them to be discharged safely to the environment.

Separations of postconsumer mixtures (85% HDPE and 15% LDPE/PP) have yielded HDPE products with 99+% recovery and purity in lab-scale experiments; see Fig. 3 (15). One hundred percent purity was not attainable, however, because a few "heavy" flakes were lifted into the "lights" product by groups of the "light" flakes while several "light" flakes were forced into the "heavies" product by sinking groups of the "heavy" flakes. These effects were minimized by slightly agitating the plastic bed during the separation process with a slowly spinning, close clearance impeller. Estimates of process costs at the commercial scale fell into the \$0.07–0.09/kg range (15) for the batch microsortation of clean, dry flake. These technical and economic results are favorable enough to permit the current development of this process at the pilot scale.

The polyolefin flake was sorted using the six-step procedure illustrated in Fig. 2. The mixed feed was metered into the empty vessel through a rotary feeder and a high-pressure ball valve (Step 1). This feed ball valve was then closed and the carbon dioxide was introduced until the desired fluid density was attained (Step 2). A slowly spinning close clearance impeller was used to slightly agitate the particles, enabling them to float or sink (Step 3). The lights and heavies were permitted to accumulate (Step 4), and the carbon dioxide was vented from the vessel (Step 5). High-pressure ball valves were then opened, allowing the separated fractions to be recovered (Step 6).

Although it has been demonstrated that the high recovery and purity of HDPE product can be obtained in this manner, the effects of immersion in

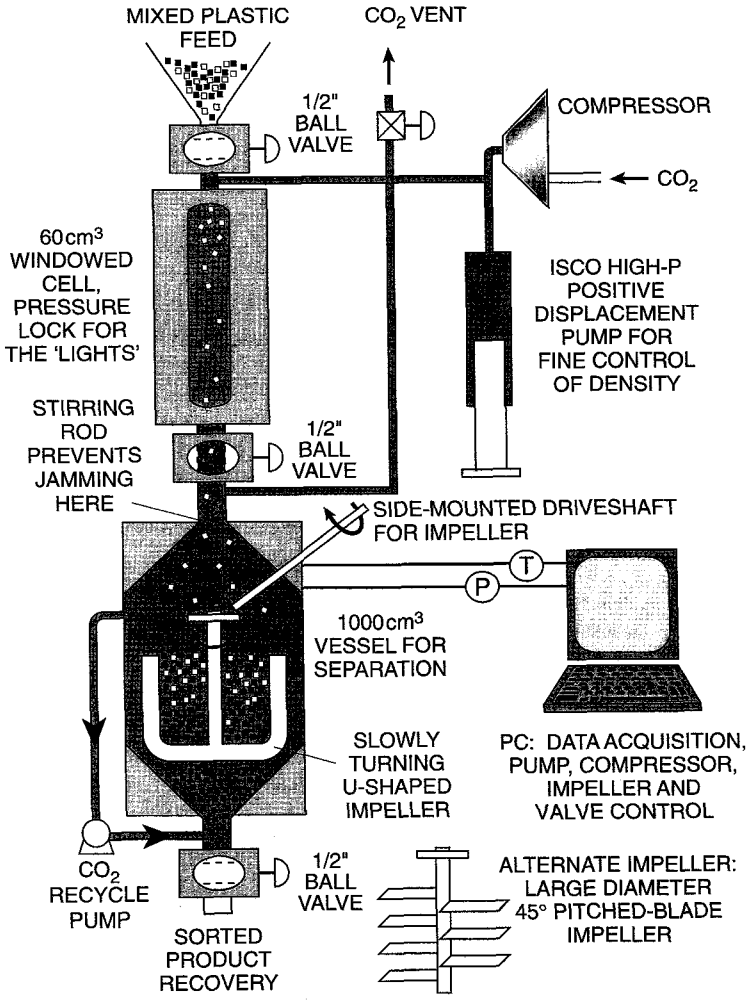

FIG. 3. The lab-scale, high-pressure, microsortation batch process.

CO_2 on the physical properties of the flake have not been previously determined. Significant changes in the properties of a piece of plastic exposed to liquid carbon dioxide would need to be accounted for prior to being used as a feedstream for the manufacture of items with a specified postconsumer content. For example, the extraction of additives used to inhibit the effects of radiation, thermal degradation, or oxidation would diminish the mechanical integrity of the final product unless these additives were reintroduced. The large

reductions in plastic density due to foaming upon removal from the high-pressure environment would necessitate increased volumetric feed rates to maintain the desired mass flow rate of the product.

OBJECTIVE

The objective of this study was to determine the effect of immersion in liquid carbon dioxide on the properties of postconsumer polyolefins. Postconsumer plastic flake from six HDPE sources, two LDPE sources, and five PP sources were selected as representative samples. The change in weight of each flake was measured to determine if a significant amount of low-molecular-weight (MW) additives or surface impurities were removed from the plastic. The density of the plastic was determined after the separation to determine if any foaming of the plastic had occurred. The melting point and latent heat data were used to determine if the degree of crystallinity had been altered by the exposure to carbon dioxide. The onset of thermal degradation by thermogravimetric analysis (TGA) of the plastics was measured to determine if the extraction of thermal stabilizers had occurred. A significant decrease in the density, degree of crystallinity, or thermal stability of the products would have indicated that the carbon-dioxide-based microsortation would have to be accounted for in subsequent processing of this material in products with postconsumer plastic content. The extraction of ultraviolet (UV) stabilizers was not evaluated.

EXPERIMENTAL

Postconsumer Plastics

Small pieces, approximately 0.5-cm squares, were cut from the clean, dry, HDPE, LDPE, and PP containers listed in Table 2. A brief description of these samples is provided.

Fluid

Bone-dry grade liquid carbon dioxide (99.9%) from Praxair was used in all experiments.

Exposure

The 13 samples (combined mass of approximately 260 mg) were placed on the top of a packed bed of stainless-steel balls (volume of balls = 100 cm^3) within a 1-L high-pressure vessel (Fig. 3). The vessel was then charged with about

TABLE 2
Change in the Properties of Postconsumer Thermoplastics Due to Immersion in Dense Carbon Dioxide

Plastic	Δ Wt. (%)	ρ (kg/m^3) unexp.	ρ (kg/m^3) exp.	Δρ (%)	T_m (K) unexp.	T_m (K) exp.	ΔT_m (K)	ΔH (J/g) unexp.	ΔH (J/g) exp.	$\Delta(\Delta H)$ (%)	T_{degrad} (K) unexp.	T_{degrad} (K) exp.	ΔT_{degrad} (K)
HDPE													
Cool Whip	−0.12	945.9	950.2	0.45	395.87	395.32	−0.55	167.20	171.90	2.73	704.58	700.79	−3.79
Era Detergent	−0.16	958.3	962.5	0.44	395.85	395.51	−0.34	160.80	168.80	4.98	702.02	699.29	−2.73
Flex Shampoo	0.00	945.9	950.2	0.45	394.88	395.52	0.64	167.80	161.10	−3.99	701.91	702.27	0.36
Pharmor H_2O_2	0.00	953.2	957.7	0.47	394.76	395.41	0.65	180.00	184.10	2.28	700.03	703.76	3.73
Ultra Downy Softener	−0.26	958.3	962.5	0.44	396.27	395.37	−0.90	194.60	194.00	−0.31	696.63	696.39	−0.24
Giant Eagle Milk Jug	−0.33	951.1	955.3	0.44	398.91	397.51	−1.40	210.90	212.00	0.52	696.87	696.39	−0.48
LDPE													
Cool Whip Lid	−0.09	927.9	930.0	0.23	384.25	383.98	−0.27	140.60	140.90	0.21	682.64	684.65	2.01
French's Mustard	−0.20	933.1	936.5	0.36	376.71	377.37	0.66	114.80	106.90	−6.88	689.25	688.14	−1.11
PP													
Italian Oven Cup	−0.10	905.0	906.9	0.21	416.62	417.06	0.44	80.34	80.42	0.10	675.12	675.12	0.00
Land 'O Lakes Sour Cream	−0.37	913.6	918.6	0.55	425.93	426.18	0.25	87.25	88.21	1.10	674.93	674.93	0.00
Soda Bottle Cap	−0.37	907.1	910.6	0.39	427.79	427.98	0.19	85.06	79.92	−6.04	674.43	673.52	−0.91
Reynold's Deli Container	−0.85	909.6	915.1	0.60	427.98	427.18	−0.80	99.73	98.04	−1.69	672.31	667.88	−4.43
Prescription Bottle	−0.24	907.1	910.6	0.39	428.40	426.52	−1.88	100.60	95.93	−4.64	638.73	635.11	−3.62

Note: Wt. = weight; ρ = density; T_m = melting point; ΔH = heat of melting; T_{degrad} = temperature of onset of thermal degradation; unexp. = the unexposed sample—prior to immersion in liquid carbon dioxide; exp. = the exposed sample—24 h after exposure to liquid carbon dioxide.

900 cm^3 of carbon dioxide at 293 K to a pressure of 27.58 MPa (4000 psi) for 20 min. This loading (plastic volume/vessel volume) was much lower than that realized in our previous lab-scale separations (15); therefore, our results should be conservative in that the carbon dioxide is present in greater amounts than that experienced in future pilot-scale and commercial-scale operation. (Plastic loadings of 50 vol% are proposed for commercial operation.) The vessel was then vented, resulting in the rapid elimination of the liquid carbon dioxide. The particles were then removed from the vessel. The rapid depressurization led to a cooling; therefore, the flake retained a small amount of "dry ice" and moisture from the environment after being removed from the vessel. The weight of the particles was measured hourly until no detectable change in weight was observed ($\pm$0.0001 g). It was determined that 24 h was sufficient for the evaporation of water from the plastic and the diffusion of carbon dioxide from the plastic, as evidenced by the constant weight of the samples that were dried for this amount of time.

Weight

The change in weight of the individual pieces of plastic was determined using a Mettler balance with a precision of 0.0001 g. Although the polyolefins are insoluble in carbon dioxide at these conditions, other constituents of the plastic flake could be soluble in carbon dioxide. Surface dirt or water could dissolve in the carbon dioxide or be displaced from the plastic by the liquid carbon dioxide. Plastic additives, such as UV absorbers, antioxidants, acid acceptors, thermal stabilizers, lubricants, flame retardants, and dyes, have much lower MWs than polypropylene or high-density polyethylene and could exhibit slight solubility in dense carbon dioxide.

Density

Although it has been established that the polyolefins do not swell or foam during short exposures to high-pressure carbon dioxide (13–15), changes in plastic density upon removal from this environment were not previously investigated. Therefore, the density of each plastic piece was determined in a 100-cm^3, high-pressure, variable-volume view cell. Each particle was quickly immersed in liquid carbon dioxide. The system density was then adjusted until the particle was suspended in the fluid. The particle density was estimated to be equivalent to the fluid density, which was estimated from the Lawal–Lake–Silberberg equation of state (16). The sample was then subjected to the 20-min immersion conditions, and then the cell was vented. After 24 h, the plastic density was estimated again.

These results are qualitative in nature because the density of the plastic is altered by the carbon dioxide that is absorbed into the plastic under high-pres-

sure conditions and the mechanical compression of the sample. The main objective of this experiment, however, was to determine if any foaming of the polyolefins would occur during the depressurization of the system. PVC, for example, shows a significant decrease in density due to irreversible foaming which occurred during the sortation in liquid carbon dioxide (11).

Melting Point and Latent Heat

The melting point and latent heat of melting for the exposed and unexposed samples were determined by differential scanning calorimetry (DSC). A TA Instruments DSC 2910 was used at ambient pressure in all experiments. The system was initially cooled with liquid nitrogen to a temperature 70–80 K lower than the nominal glass transition temperature of the polymer. The temperature was then ramped at 20 K/min until the melting point was passed. The sample was then cooled at 60 K/min and rescanned in order to obtain data on samples with a known thermal history.

Onset of Thermal Degradation

A TA Instruments high-resolution TGA 2850 was used to determine the onset of thermal degradation using thermogravimetric analysis with nitrogen purge. Individual samples were equilibrated at 473 K, and then their weight was continuously monitored as the temperature was increased at 3 K/min to 773 K. The temperature of the onset of thermal degradation was estimated by extrapolating the linear portion of the percentage weight versus temperature data back to 100% weight.

RESULTS

All of the results of this study are presented in Table 2.

Weight

The weight loss for the samples due to immersion in liquid carbon dioxide was in the 0–0.85% range. Because the polymers are essentially insoluble in liquid carbon dioxide at these conditions, this weight loss can be attributed to the extraction of low-molecular-weight additives (but not thermal stabilizers, as shown in a subsequent section) and/or impurities on the surface of the samples.

Density

The density of the samples increased by 0.21–0.55% after immersion in liquid carbon dioxide. This slight increase may be attributed to the mechanical

compression of the samples. There was no indication of foaming of any sample.

Melting Point/Latent Heat

The melting point remained consistent for all samples, as indicated by the deviations being less than the 1 K precision of the measurement. This was expected because the exposure of the sample to liquid carbon dioxide did not alter the composition of the polymer. The experimental melting temperatures reported are lower than the values of the equilibrium melting temperature reported in the literature, as should be expected (17). These published equilibrium melting temperatures are those for perfect crystals comprised of infinite-molecular-weight chains (17). The postconsumer samples were neither infinite in molecular weight nor able to form perfect crystals; consequently, the melting point was lower.

The differences between the latent heats of the exposed and unexposed samples for the same thermal history were also within the 5% precision of the apparatus. Therefore, no significant change in the degree of crystallinity occurred as a result of immersion in liquid carbon dioxide. [The degree of crystallinity for any sample can be estimated by dividing the heat of melting by the latent heat of the crystalline solid, 232 J/g polyethylene and 209 J/g polypropylene (17).]

Onset of Thermal Degradation

The most important property to be considered in this study was the onset of thermal degradation. A decrease in the thermal stability could be caused by the extraction of stabilizers into the carbon dioxide. The change in mass results indicated that approximately 0.2 wt.% of the sample was removed due to exposure to the dense CO_2. If the lost mass consisted of thermal stabilizers, a significant decrease in thermal stability could have occurred. This would render the sorted plastics unacceptable to manufacturers unless the stabilizers were reintroduced. The TGA results clearly indicated, however, that no discernible change in thermal stability occurred. All of the changes were within the 5 K precision of the measurement.

CONCLUSIONS

Polyolefins can be efficiently sorted using liquid carbon dioxide as a float–sink medium. The immersion of the flake in the high-pressure fluid at separation conditions has no deleterious effect on the properties of the plastic. Very small decreases in weight and increases in density were observed. No significant changes in the melting point, latent heat of melting, or onset of

thermal degradation were detected. Therefore, a high-purity HDPE stream obtained from the carbon-dioxide-based microsortation of mixed polyolefins can be used as a feedstream for the manufacture of items with a specified post-consumer HDPE content.

ACKNOWLEDGMENTS

This study was funded by Normex, International. The authors would like to thank the directors of Normex, David Gilbert and Lou Jullien, for their generous support.

REFERENCES

1. K. Saitoh, I. Nagano, and S. Izumi, *Res. Conserv. Recycl., 2,* 127–145 (1976).
2. I. Mishra, J. Koutsky, and N. Braton, *Polym. News, 9,* 32 (1975).
3. *Chem. Eng. Prog.,* 22 (November 1991).
4. A. E. Martin, *Small Scale Resource Recovery Systems,* Noyes Data Corporation, Park Ridge, NJ, 1982.
5. J. J-C. Hsieh, Separation of Solids by Varying the Bulk Density of a Fluid Separating Medium, U.S. Patent No. 3822015.
6. *Proceedings of the 14th Meeting of the Plastics Recycling Foundation Industrial Advisory Council,* 1992.
7. E. Gregory, Sorting plastic containers for recycling using frequency dependent dielectric properties, First Year Report (June 1991) and Second Year Report (June 1992) to the Plastics Recycling Foundation, Rutgers University Center for Plastics Recycling Research.
8. E. Sereni, in *Recycling of Plastic Materials,* ChemTec Publishing, Toronto, Canada (1993).
9. I. B. Mishra, J. A. Koutsky, and N. R. Braton, *Polym. News, II*(9/10), 32–38 (1975).
10. N. R. Braton, and J. A. Koutsky, in *Proceedings of the 4th Mineral Waste Utilization Symposium,* 1974, pp. 3–39.
11. G. Serad and T. Thorburg, Separation of PET and PVC Using Supercritical Carbon Dioxide, U.S. Patent 5462973 (1995).
12. S. Lancaster, SRC Vision, personal communication, 1998.
13. M. Super, R. Enick, and E. Beckman, *Res. Conserv. Recycl., 9,* 75 (1993).
14. B. Altland, D. Cox, R. Enick, and E. Beckman, *Res. Conserv. Recycl., 15,* 203 (1995).
15. E. Karmana, B. Eiler, D. Mainiero, M. Bedner, and R. Enick, *Res. Conserv. Recycl., 20,* 143 (1997).
16. A. Lawal, E. Van der Laan, and R. Thambynayagam, in *SPE AIME,* 1985, paper 14269.
17. J. Brandup and E. Immergut, *Polymer Handbook,* 3rd ed., John Wiley & Sons, New York, 1989.

POLYM.–PLAST. TECHNOL. ENG., 38(3), 445–457 (1999)

SOLID-STATE SHEAR PULVERIZATION OF PLASTICS: A GREEN RECYCLING PROCESS

KLEMENTINA KHAIT* and JOHN M. TORKELSON

Department of Chemical Engineering
and Polymer Technology Center
Northwestern University
Evanston, Illinois 60201-3140

Abstract

A novel process called solid-state shear pulverization (S^3P) has been developed at Northwestern University to recycle single or commingled postconsumer or preconsumer polymeric waste without sorting by type or color. This continuous, one-step process converts shredded plastic or rubber waste into controlled-particle-size powder ranging from coarse (10 and 20 mesh) to fine (80 mesh) or ultrafine (200 mesh). As a result, the pulverization product is usable in applications ranging from direct injection molding without prior pelletization, to rotational molding, to use in protective and decorative powder coatings, as well as to blending with virgin resins and compounding with additives. Scanning electron microscopy reveals that the fine particles have a unique elongated shape that is attributed to the high shear conditions occurring during the pulverization process. Injection-molded parts made from the powder product of the S^3P process have mechanical and physical properties comparable to or better than the properties resulting from direct conventional processing of recycled single or commingled plastics. In addition, the parts made from the powder product of the S^3P process are uniform in color, whereas parts injection-molded from multicolored recycled feedstock without prior pulverization via the S^3P process are streaked, re-

* To whom correspondence should be sent.

ducing their commercial applicability. The improved mixing achieved via the S^3P process is often accompanied by scission of the carbon-chain backbone of the polymers involved, as revealed by the generation of free radicals during S^3P processing, associated mechanochemistry, and modification of the melt flow rate of the polymers by the S^3P process. The implications of this chain scission process for *in situ* compatibilization of commingled plastic waste via S^3P processing are discussed.

Key Words: Plastics; Recycling; Pulverization; Mechanochemistry; Powders.

INTRODUCTION

The amount of plastics in the municipal solid waste (MSW) stream, both in absolute weight and as a percentage of total waste, is growing. The U.S. Environmental Protection Agency (1) reported that of a total of 208 million tons of MSW generated in 1995, plastics contributed 19.0 million tons or 9.1% by weight. Plastics in the MSW stream are projected to increase to 20.9 million tons in the year 2000 and to 24.7 million tons in the year 2010, accounting for 9.7% by weight of MSW. As a result of this growth in waste plastics, the plastics industry is committed to increase the rate of plastics recycling. As evidence of this commitment, according to the American Plastics Council (2) resin producers in the United States invested more than $1 billion from 1990 through 1995 in the reclamation and recycling of postconsumer and postindustrial plastics. Although some success has been achieved in plastics recycling as a result of this investment, most notably through blending of recycled high-density polyethylene (HDPE) with virgin HDPE and the use of recycled polyethylene terephthalate (PET), in reality the potential for plastics recycling has been largely unrealized. Among the factors contributing to this unrealized potential are the costs associated with sorting, cleaning (to remove original product residue and labels), grinding, and pelletizing (by melt extrusion) recycled plastics and problems with incompatibility of recycled plastics that have not been sorted into single-species materials.

Here, we present results achieved in recycling both single-species and unsorted, commingled plastic waste with a novel, continuous, one-step process called solid-state shear pulverization (S^3P). This mechanochemical, size-reduction process is based on high-pressure shear deformation. Unlike conventional recycling processes using sorting and size-reduction techniques followed by melt extrusion, S^3P produces powders that can be used to make high-quality products for various applications and markets, ranging from di-

rect injection molding, to rotational molding, to powder coatings. Furthermore, the S^3P process allows for simple compounding or blending with virgin resins during the pulverization process, along with homogenization of color for unsorted, multicolored feedstock.

The basic principles of S^3P have their origins in another principle of disintegration of plastics called elastic strain-assisted grinding developed at the Academy of Science in Moscow, Russia, where it was determined that elastic strain-assisted *high-temperature* grinding produced fine powders at lower energy requirements that that of cryogenic grinding. [This idea, in turn, has its origin in work done by Bridgman (3) in 1935, who studied transformation of solids under high shear and pressure.] Further research of the behavior of virgin polymeric materials, both thermosets and thermoplastics, under combined application of high shear and pressure using extrusion devices was conducted under the direction of the late N. S. Enikolopian (4,5). These researchers indicated that although the mechanism of the powder production process was not well understood, their data and physical observations supported the notion that polymers were pulverized by a sudden "rheological explosion"-type mechanism, similar to that found by grinding with Bridgman anvils.

In the S^3P process, plastics are processed at temperatures *below their melting points* (in the case of crystalline or semicrystalline polymers) or *glass transition temperatures* (in the case of amorphous polymers). The S^3P process utilizes a pulverizer that compresses the solid-state polymer at pressures equal to 0.2–0.7 MPa and then conveys the polymer at shear stresses from 0.03 to 5 N/mm^2 and pressures up to 50 MPa to a discharge. By controlling the temperature and process parameters, optimal fragmentation of the feedstock occurs, resulting in powder production of a given size range. Often accompanying this powder formation is the scission of bonds in the polymer backbone. This has been confirmed by measurement with electron spin resonance (6) of free-radical generation via the S^3P process and by observation by gel-permeation chromatography of a significant reduction in number-average molecular weight and polydispersity of polystyrene after pulverization (7). Finally, nuclear magnetic resonance spectroscopy (8) has revealed the formation of long-chain branches in linear low-density polyethylene (LLDPE) which has undergone S^3P processing, the equivalent of the formation of graft copolymers in blends.

In the present study, we report on the powder characteristics resulting from S^3P processing of single and commingled polyolefin waste. Additionally, we provide details on the mechanical and physical properties of injection-molded parts produced from S^3P-processed polymeric waste, demonstrating that reasonable properties can be achieved in materials made from multicomponent, commingled, traditionally incompatible polymeric waste when the S^3P process is employed.

RESULTS AND DISCUSSION

Highly crystalline polymers such as HDPE are traditionally troublesome to make into fine powders. In fact, Enikolopian and co-workers (9) indicated that it was impossible to pulverize HDPE into powders using their elastic-strain-assisted, high-temperature grinding approach. However, by employing high shear conditions and a temperature of 0°C in the solid-state shear pulverizer at Northwestern University, powder from 100% postconsumer recycled HDPE is easily made. Table 1 provides a sieve analysis (measurements made with a Gilson ultrasonic autosiever) of the resulting HDPE powder showing that just under 50% of the powder had a size of 125 μm or smaller. Using the same high-shear and temperature conditions, the sieve analysis of an S^3P-processed 70/30 mixture of 100% recycled HDPE/polypropylene (PP) reveals quite similar powder characteristics. (See Table 2.) The only key difference is associated with the reduction in the amount of the most coarse powder (35 mesh or $>$ 500 μm) in the 70/30 HDPE/PP mixture from 15.3% to 7.7%, compensated for by increases in the amounts of 50- and 80-mesh powder. The fact that there was a reduction in the amount of the coarsest powder upon addition of PP to HDPE is not unexpected, as PP, with a lower crystallinity than that for HDPE, is much more pulverizable than HDPE. This is evidenced by the fact that under less severe conditions of shear in the pulverizer, it is impossible to produce substantial powder from HDPE, whereas it is possible to produce a relatively coarse powder from PP. Table 3 shows the sieve analysis of a coarse powder produced from 100% recycled PP at relatively low-shear conditions where it is not possible to produce powder from HDPE. Under the conditions of relatively low shear, less than 3% of the PP powder has a size of 125 μm or finer. This demonstrates that although there is substantial tunability of powder size,

TABLE 1
Sieve Analysis of 100% Postconsumer Recycled HDPE (High-Shear S^3P @ 0°C)

Mesh	Size (μm)	Weight %
35	500	15.3
50	300	15.5
80	180	23.3
120	125	11.6
200	75	17.6
270	53	6.7
450	32	6.5
Fines		3.6

TABLE 2
Sieve Analysis of 100% Postconsumer Recycled 70/30 HDPE/PP (High-Shear S^3P @ 0°C)

Mesh	Size (μm)	Weight %
35	500	7.7
50	300	18.4
80	180	27.2
120	125	12.8
200	75	14.7
270	53	7.1
450	32	6.9
Fines		5.1

achieved by controlling the S^3P processing parameters, the parameters needed for particular powder characteristics are strongly polymer dependent. Nevertheless, with appropriate process optimization, it is possible to prepare powders from 100% recycled feedstock that meet requirements for direct injection molding (10 mesh) without pelletization (to avoid additional heat history and property degradation), rotational molding (average of 35 mesh), and protective and decorative powder coatings (80 mesh or finer).

In addition to the controlled production of differently sized powders via the S^3P process, scanning electron microscopy of powders has revealed interesting characteristics of the shapes of the particles. Whereas flakes or chips of

TABLE 3
Sieve Analysis of 100% Postconsumer Recycled PP (Relatively Low-Shear S^3P @ 0°C)

Mesh	Size (μm)	Weight %
35	500	75.67
50	300	14.26
80	180	6.38
120	125	2.01
200	75	0.84
270	53	0.67
450	32	0.17
Fines		0.00

(as-received) recycled feedstock have sharp, angular surfaces resulting from blade-grinding processes, all pulverized materials have smooth surfaces, indicative of a solid-shearing process. Fine powders resulting from S^3P processing have a unique, elongated shape (see Fig. 1), whereas larger fluff consists of fibrous, easily peeled particles.

Physical and mechanical properties of the S^3P-made coarse-powder materials were tested on ASTM specimens prepared with a 1-oz. Battenfeld injection-molding machine and a four-cavity family mold. Typical molding conditions were as follows: barrel temperatures of 320–400°F, mold temperature of 100°F, injection pressures of 200–600 psi, and holding pressures of 250–500 psi. Molded specimens were tested in accordance with ASTM D638 (tensile strength), ASTM D256 (impact strength), ASTM D790 (flexural strength), ASTM D468 (heat distortion temperature), ASTM D2340 (hardness), and ASTM D1238 (melt flow rate). Results for recycled homopolymers (flake and pulverized) and for mixtures of commingled, recycled plastics (flake and pulverized) are given in Tables 4 and 5, respectively.

Table 4 illustrates no deterioration in tensile strength, elongation, Izod impact strength, and flexural modulus and strength for parts injection-molded from pulverized (from flake) recycled HDPE, LLDPE, and polypropylene (PP) as compared to parts molded from the (as-received) flake recycled homopolymers. In fact, in one case, that of LLDPE, there was a significant improvement in elongation for the pulverized material as compared to the as-received flake, increasing by a factor of 5–6. This is particularly important given the fact that elongation properties are often found to decrease in recycled materials.

Table 5 provides a range of mechanical properties for mixtures of recycled polyolefins as well as PET, polystyrene (PS), and poly(vinyl chloride) (PVC). Also listed at the bottom of the table are data for several virgin polyolefin homopolymers. Several points of importance may be noted from this table.

First, it is well know that HDPE and PP are incompatible and that typically only up to 10 wt.% PP can be added to HDPE by conventional melt blending (10) while maintaining reasonable mechanical integrity of the blend. However, the S^3P process allows up to 30 wt.% incorporation of PP into HDPE while maintaining reasonable, although not necessarily optimal, mechanical properties. Similar observations can be made regarding copulverized blends of LLDPE and PP. As a further indication of their mechanical integrity, these traditionally strongly incompatible blends exhibited good surface appearance and did not exhibit delamination upon breaking.

Second, in a number of cases for the HDPE/LLDPE and HDPE/LLDPE/PP blends, the copulverized samples exhibited significant improvement in elongation properties as compared to the samples directly molded from the recycled flake. For example, in the case of the 40/60 HDPE/LLDPE system, the

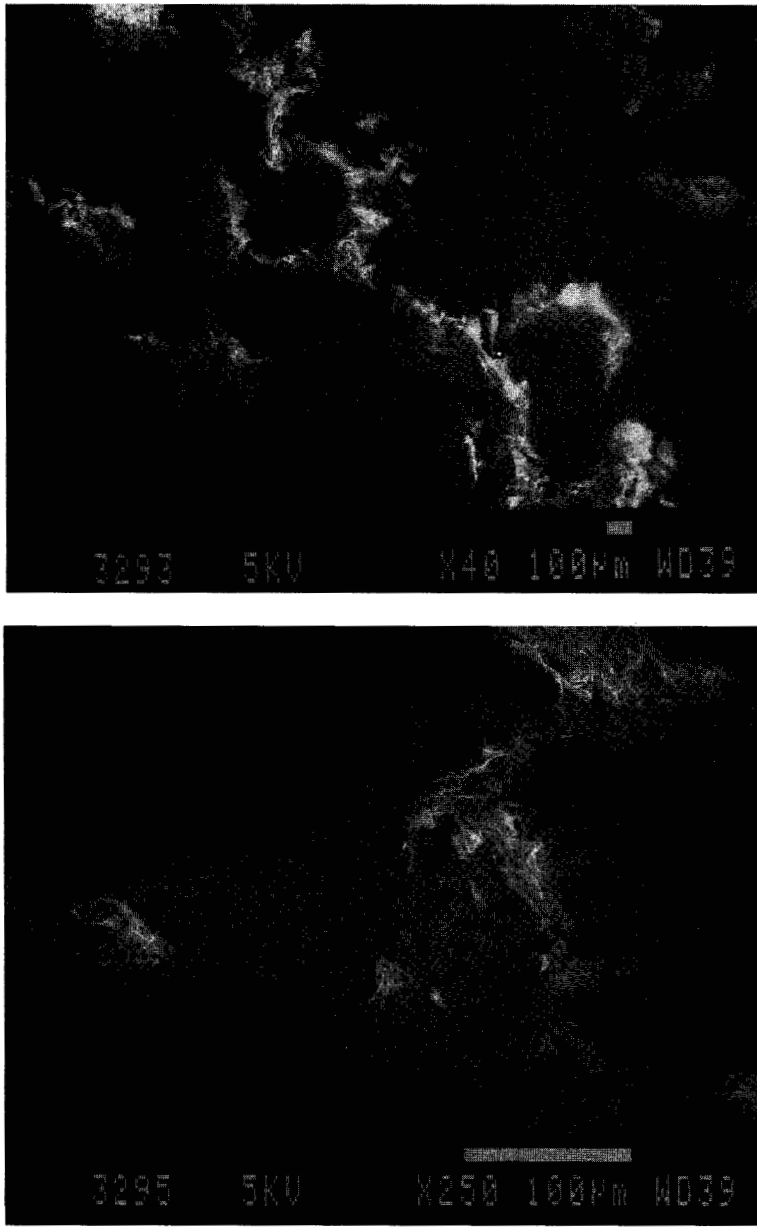

FIG. 1. Scanning electron micrographs at (a) low and (b) high magnifications (see 100-μm size scale on each micrograph) of powder resulting from solid-state shear pulverization of recycled HDPE.

TABLE 4
Key Properties of Postconsumer Polyolefins—Effect of S^3P Process

Feedstock	Tensile properties			Izod impact (J/m)	Flexural properties	
	Yield (MPa)	Ultimate (MPa)	% Elongation		Modulus (MPa)	Strength (MPa)
HDPE—not processed by S^3P	—	22.3 ± 1.2	12 ± 3	27 ± 2	—	—
HDPE—processed by S^3P	—	22.0 ± 0.3	16 ± 4	27 ± 1	1050 ± 100	36.2 ± 0.3
LLDPE—not processed by S^3P	13.6 ± 0.9	—	33 ± 30[a]	42 ± 3	—	—
LLDPE—processed by S^3P	13.4 ± 0.6	—	190 ± 9[a]	37 ± 1	540 ± 17	21.8 ± 0.2
PP—not processed by S^3P	33.3 ± 0.6	—	330 ± 160[a]	37 ± 3	1900 ± 120	59.3 ± 1.7
PP—processed by S^3P	32.5 ± 0.1	—	375 ± 250[a]	32 ± 3	1710 ± 70	64.3 ± 1.0

[a] Crosshead rate of 0.2 in./min.

TABLE 5
Key Properties of Blends of Postconsumer Plastics and Comparison to Properties of Virgin Polyolefins

		Tensile properties			Flexural properties	
Feedstock	S^3P	Ultimate (MPa)	% Elongation	Izod impact (J/m)	Modulus (MPa)	Strength (MPa)
HDPE/PP 90/10	Yes	19.8	12	21	880	25
HDPE/PP 80/20	Yes	20.1	9	21	860	26
HDPE/PP 70/30	Yes	19.6	8	11	960	27
LLDPE/PP 80/20	Yes	12.9	12	21	490	17
LLDPE/PP 70/30	Yes	12.9	8	32	510	19
HDPE/LLDPE 60/40	No	19.6 ± 0.5	13 ± 2	21 ± 2	810 ± 20	27
HDPE/LLDPE 60/40	Yes	18.1 ± 0.4	22 ± 6	27 ± 3	760 ± 50	29
HDPE/LLDPE 40/60	No	17.4 ± 0.3	17 ± 5	27 ± 3	740 ± 40	25
HDPE/LLDPE 40/60	Yes	16.4 ± 0.1 (yield)	130 ± 25	32 ± 2	660 ± 70	25
HDPE/LLDPE/PP 60/30/10	No	18.5 ± 0.4	9 ± 1	21 ± 2	790 ± 70	27
HDPE/LLDPE/PP 60/30/10	Yes	19.2 ± 0.9	13 ± 2	21 ± 2	970 ± 60	32
HDPE/LLDPE/PP/PVC 55/30/10/5	Yes	16.5	13	11	800	23

(continued)

TABLE 5
Continued

Feedstock	S^3P	Tensile properties		Izod impact (J/m)	Flexural properties	
		Ultimate (MPa)	% Elongation		Modulus (MPa)	Strength (MPa)
HDPE/LLDPE/PP/PET/PVC 40/30/5/20/5	Yes	16.1	9	11	980	25
HDPE/LLDPE/PP/PS/PVC 50/30/10/5/5	Yes	15.6	13	16	810	22
HDPE/LLDPE/PP/PET/PS/ PVC 40/30/5/15/5/5	Yes	13.7	6	5	910	22
HDPE/PET/PP/PS 50/30/10/10	Yes	30.8	10	32	1490	46
HDPE Q LB5602 copolymer virgin (Quantum Chem. Co.)	No	20.1	24	380	1120	36
LLDPE Q GA601 virgin (Quantum Chem. Co.)	No	16.5	480	—	300	13
PP Q 8020 virgin (Quantum Chem. Co.)	No	28.2	38	21	1430	48

pulverized material had an elongation at break of 130%, whereas material processed without pulverization had an elongation at break of only 17%, a difference of a factor of 7–8. Also noteworthy for this system is the fact that the copulverized 40/60 HDPE/LLDPE material exhibited a yield tensile strength comparable to the ultimate tensile strength (no yield exhibited) for the material that was not copulverized. Thus, the mechanical response of the copulverized material was qualitatively different from that of the conventionally recycled material. Smaller, yet significant improvements in elongation properties were also observed in copulverized 60/40 HDPE/LLDPE and 60/30/10 HDPE/LLDPE/PP samples as compared to samples that had not been copulverized.

Finally, four-, five-, and six-component blends of recycled plastics can be made via S^3P processing which have ultimate tensile strength, hardness, flexural modulus, and flexural strength properties that are highly competitive with the properties of virgin HDPE and LLDPE. The % elongation in these blends averages to about 40% of that for the virgin HDPE material, and the Izod impact strength is typically about half that of virgin PP. Thus, these multicomponent blends of recycled plastics could be useful in applications where flexural properties and ultimate tensile strength need to be comparable to common virgin polyolefin properties, but where some loss in impact strength and elongation is acceptable. When impact strength must be preserved to levels comparable to or better than that of virgin PP, greater amounts of PET (see the 30% PET blend) and reduced levels of LLDPE can restore impact properties to values 50% greater than that of a typical virgin PP. Especially important about four of the multicomponent blends is the presence of 5 wt.% PVC in the blends, including two cases containing 15 and 20 wt.% PET. The fact that S^3P processing results in uniform, melt-processible powder containing both PET and PVC is an important advance in recycling technology, as it known that PET waste contaminated with PVC cannot be melt-processed by conventional methods due to the high melting temperature of PET; in such cases, PVC degrades at temperatures well below the melt temperature of PET.

The extraordinary capability of the S^3P process for producing materials with relatively robust properties starting with complex mixtures of traditionally incompatible polymers is an issue of current interest. It has been recently demonstrated, via characterization of glass transition temperatures for the polystyrene-rich phase in PS/PP blends, that mixtures processed via S^3P methods achieve much more intimate mixing of components than is normally observed in conventional melt processing alone (7). This effect, along with the known capacity of S^3P to result in chain scission and to produce reactive free radicals, has the potential to lead to a self-compatibilization of the blends via block copolymer formation at the phase interfaces. Unequivocal evidence for the production of compatibilizing block copolymers as a result of S^3P pro-

cessing of incompatible blends is currently being sought by a variety of approaches.

Beyond the issues of mechanical and physical property modification resulting from solid-state shear pulverization, it is also important to note the ease in processing feedstock consisting of a wide variety of melt flow rates once the materials have been copulverized. For example, one of the recycled HDPE feedstocks studied consisted of multicolored flakes. When these flakes were separated by color, the different colors were found to have melt flow rates ranging from 12 to 56 g/10 min (at 190°C, 2.16 kg load). However, these variations in melt flow rate did not interfere with the conversion via the S^3P process of the multicolor HDPE flakes into a homogeneous, pastel-color powder (11). This homogenization of color via the S^3P process may alleviate the problems and cost associated with sorting recycled plastics, both single-component materials and blends, by color, as is commonly done at present. Thus, the S^3P process is not only capable of addressing problems related to deleterious effects of recycling on physical and mechanical properties of thermoplastics but can also eliminate certain aesthetic problems that may prevent efficient recycling of thermoplastics.

Finally, it should be noted that the S^3P process may also be applied in the recycling of certain thermosets. Limited studies have been done on recycling thermoset phenolic and acrylic resins, whereas more substantial work has been undertaken in the recycling of used tire materials with this pulverization technology (12). In particular, the S^3P process has been applied to crosslinked rubber from used tires as well as to whole-tire processing (including both fiber and tread rubber), yielding fine powders in both cases. Currently, used tire rubber is reused conventionally as a filler. However, applications are under study with the S^3P process in which combinations of used tire rubber and postconsumer plastics can be employed as feedstock, yielding materials with relatively robust properties while minimizing solid waste output. Thus, S^3P can be used not only with materials that by design (thermoplastics) are at least conceptually simple to reuse with melt-processing methods but also with materials (thermosets) typically designed to be used in one form and not reprocessed again into useful products.

SUMMARY

Solid-state shear pulverization technology has important potential for converting discarded commingled or single multicolored plastic products, postindustrial scrap, or rubber into high-quality powders of leveled color that can be used in virtually any existing plastic-fabrication process. This energy-efficient, pollution-free technology will facilitate the recycling of both

single-component and multicomponent polymeric waste, diverting it from landfills. The results illustrated here have confirmed that processing of recycled polymers by the S^3P technique followed by conventional melt-processing results in mechanical and physical properties typically no worse than and sometimes significantly better than those of polymer recycled by conventional techniques alone. Furthermore, certain recycled, copulverized, multicomponent blends have properties rivaling even those virgin homopolymers. Additionally, the S^3P process homogenizes the color of multicolor feedstock, eliminating certain aesthetic issues that often stand as roadblocks for the effective recycling of plastics. Further study of this technique is underway at Northwestern University, especially with regard to understanding the relationships among the processing parameters, the particle size of the resultant powders, and the degree of mechanochemistry and molecular-scale compatibilization achievable in mixtures of various polymers, both recycled and virgin. Optimization of the processing for throughput and cost-effectiveness is also being performed.

ACKNOWLEDGMENTS

The authors are grateful for the financial support of the Department of Commerce and Community Affairs, State of Illinois, Springfield, IL. We would like to thank Mr. John Rasmussen at the Polymer Technology Center for sample preparation and testing.

REFERENCES

1. *Characterization of Municipal Solid Waste in the United States,* EPA Report 530-R-97-015, May 1997.
2. *Plast. Prod. Rev.,* 31 (April/May 1997).
3. P. W. Bridgman, *Phys. Rev., 48,* 825 (1935).
4. N. S. Enikolopian, *Pure Appl. Chem., 57,* 1707 (1985).
5. S. A. Wolfson and V. G. Nikolskii, *Polym. Sci. USSR, Ser. B, 36,* 861 (1994).
6. D. Ahn, K. Khait, and M. A. Petrich, *J. Appl. Polym. Sci., 55,* 1431 (1995).
7. N. Furgiuele, K. Khait, and J. M. Torkelson, *Polym. Mater. Sci. Eng., 79,* 70 (1998).
8. A. R. Nesarikar, S. H. Carr, K. Khait, and F. M. Mirabella, *J. Appl. Polym. Sci., 63,* 1179 (1997).
9. N. S. Yenikolopyan, Ye. L. Akopyan, A. Yu. Karmilov, V. G. Nikolskii, and A. M. Khachatryan, *Polym. Sci. USSR, 30,* 2576 (1988).
10. M. A. Wendorf, in *Proc. RETEC,* 1993.
11. K. Khait, in *Proc. Ann. Tech. Conf. ANTEC '96,* 1996.
12. K. Khait, *Rubber World, 216*(2), 38 (1997).

POLYM.–PLAST. TECHNOL. ENG., 38(3), 459–470 (1999)

NYLON 66, NYLON 46, AND PET PHASE-TRANSFER-CATALYZED ALKALINE DEPOLYMERIZATION AT ATMOSPHERIC PRESSURE

MALCOLM B. POLK,* LEIGHTON L. LEBOEUF, MUNISH SHAH, CHEE-YOUB WON, XIAODONG HU, and WEN DING

School of Textile and Fiber Engineering
Georgia Institute of Technology
Atlanta, Georgia 30332-0295

Abstract

The depolymerization of PET, nylon 66, and nylon 46 at high temperatures in an autoclave is well known in the patent literature. We sought to invent processes for the depolymerization of PET, nylon 66, and nylon 46 in alkaline solutions at low temperatures and atmospheric pressure. A method was developed for the depolymerization of polyethylene terephthalate (PET) which involved the use of quarternary ammonium salt phase-transfer catalysts in saponification processes at atmospheric pressure and temperatures as low as room temperature. Phenyltrimethylammonium chloride, hexadecyltrimethylammonium bromide, trioctylmethylammonium chloride, and trioctylmethylammonium bromide were found to be effective catalysts for the depolymerization of PET in 5% aqueous sodium hydroxide solutions at temperatures as high as 80°C and atmospheric pressure to form terephthalic acid in yields as high as 93%. The catalyst could be recycled. The alkaline phase-transfer-catalysis approach was then successfully applied for the depolymerizations of nylon 66 and nylon 46. Benzyltrimethylammonium bromide was discovered to be an effective phase-transfer catalyst in 50 wt.% sodium hy-

* To whom correspondence should be sent.

droxide solution for the conversion of nylon 46 to oligomers. The collected nylon 46 oligomers were repolymerized using solid-state polymerization techniques to form high-molecular-weight nylon 46. Nylon 66 fibers were depolymerized in the presence of benzyltrimethylammonium bromide in 50% sodium hydroxide to form oligomers and a monomer. Adipic acid was isolated.

Key Words: Nylon 66; Nylon 46; PET; Depolymerization; Alkaline phase-transfer catalysis.

INTRODUCTION

Plastic waste recycling is beneficial because it can lead to a reduction in the amount of waste generated, a decreased need for landfills, and a more rational utilization of resources. The recycling of PET, nylon 6, and nylon 66 has been reviewed recently (1). Recently, the chemical recycling of PET was reviewed by Paszun and Spychaj (2).

An important source of polyethylene terephthalate (PET) for recycling is physically cleaned postconsumer bottles ground to form flake, depolymerized, purified, and repolymerized to form recycled resin bottles. Methanolysis is the depolymerization method used by manufacturers such as Hoechst, Eastman, and duPont (1,2). The flake is treated with methanol under pressure in a catalytic process to form dimethylterephthalate (DMT) and ethylene glycol (EG). The reaction mixture is heated to a temperature of 180–280°C at 2–4 MPa pressure. In a typical methanolysis process, heating the mixture of PET and methanol to 160–240°C at pressures of 2–7 MPa gave a reported monomer yield of 99% in less than 1 h (3). Zinc acetate, manganese acetate, cobalt acetate, and lead oxide are used as transesterification catalysts. Also, depolymerization catalysts such as benzenesulfonic acid, naphthalenesulfonic acid, and *p*-toluenesulfonic acid may be used. After distillation of the DMT recovered by filtration, pure DMT that meets the rigorous requirements for step-reaction polymerization is obtained. Ethylene glycol and methanol are recovered by distillation of the mother liquor.

Glycolysis (1,2), the second most important commercial method for the depolymerization of PET, is a process which involves the reaction of PET with boiling ethylene glycol. Temperatures in the range of 180–250°C and pressures of 0.1–0.6 MPa have been reported. Because of the reversibility of the polyesterification process, the addition of ethylene glycol to PET flake at high temperatures results in the formation of the monomers used in the original polymerization, EG and bis(hydroxyethyl)terephthalate (BHET). The reaction

is catalyzed by transesterification catalysts such as manganese acetate, cobalt acetate, sodium acetate, and calcium acetate. Initially, oligomers of polyethylene terephthalate are formed. The oligomers are separated by filtration. Cooling of the filtrate, which contains BHET and EG, results in the formation of crystals of BHET that are collected by filtration. The filtrate is distilled in order to isolate excess EG. Properly purified BHET may be polymerized to form PET, which is almost equivalent to virgin PET. PET oligomers obtained may be purified and repolymerized or used for the manufacture of unsaturated polyester resins (2).

Waste PET (1) may be depolymerized with strong acids such as sulfuric and nitric acids at high temperatures. The depolymerization of PET with 87% sulfuric acid requires several minutes. The reaction mixture is poured into water to precipitate terephthalic acid. Ethylene glycol is obtained by extraction of the mother liquor with trichloroethylene followed by distillation.

Caustic treatment of polyester scrap involves cleavage of the ester linkages. The reaction of aqueous sodium hydroxide (8–10% by weight) with waste material in an autoclave at 210–250°C and elevated pressure goes to completion in about 3–5 h (4). The rate of hydrolysis may be enhanced by the presence of accelerants (5,6). Terephthalic acid and ethylene glycol may be recovered from the solution. Hall (5) used cetyl trimethylammonium bromide and lauryl dimethylbenzylammonium chloride as accelerants for the caustic reduction of PET.

Recently, Uku et al. (7) reported the recovery of terephthalic acid and ethylene glycol by hydrolysis of PET with equivalent or excess alkalis in alcohol–ether mixed-solvent systems. They reported a 95% decomposition rate for the hydrolysis of PET pellets with potassium hydroxide in ethanol–dioxane over 30 min at 50°C.

The depolymerization of nylon 66 and nylon 46 involves hydrolysis of the amide linkages which are vulnerable to both acid- and base-catalyzed hydrolysis. In a duPont patent (8), waste nylon 66 was depolymerized at a temperature of at least 160°C in the presence of a propyl or butyl alcohol with an aqueous solution of sodium hydroxide in the amount of at least 20% excess equivalents of the acid component to be recovered. Thorburn (9) depolymerized nylon 66 fibers in an inert atmosphere at what was reported to be a superatmospheric pressure of up to 1.5 MPa and at a temperature in the range of 160–220°C in an aqueous solution containing at least 20% excess equivalents of sodium hydroxide.

At the 2nd Annual Conference on Recycling of Fibrous Textile and Carpet Waste (10), Kasserra of the duPont Company reported a relatively new process for the recycling of nylon 66 called ammonolysis. The ammonolysis process can be applied to the recycling of nylon 6 and nylon 66 (11). The ammonolysis process utilizes nylon fiber waste from carpets and automotive

parts. First, the nylon fiber is separated and the reclaimed nylon is melt extruded. The molten nylon is reacted with ammonia to form adiponitrile (ADN), hexamethylene diamine (HMDA), 5-cyanovaleramide (CVAM), 6-aminocaproamide (ACAM), 6-aminocapronitrile (6ACN), and caprolactam (CL) at a pressure of ~7 MPa and temperatures in the range of 300°C. After separation and removal of CL by fractional distillation, the crude monomers undergo hydrogenation to form HMDA. The HMDA produced may be reacted with adipic acid to produce nylon 66. DuPont has built an ammonolysis pilot plant in Kingston, Ontario (Canada).

With the previous studies clearly in mind, we sought to develop low-temperature, atmospheric-pressure processes for the depolymerization of PET, nylon 66, and nylon 46.

EXPERIMENTAL

Materials

Polyethylene terephthalate staple fibers (Celanese, Charlotte, NC, U.S.A.) were washed with methylene chloride in order to remove finishes followed by repeated washings with water and drying in an oven at 130°C. Nylon 66 fibers used in the depolymerization studies were provided by the duPont Company and used as-received. Nylon 46 fibers (Stanyl™) used for the depolymerization studies were provided by DSM Chemicals and Fertilizers, Netherlands and used as-received. The chemicals used in the procedures were reagent grade. Benzyltrimethylammonium bromide, trioctylmethylammonium chloride, trioctylmethylammonium bromide, hexadecyltrimethylammonium bromide, tetraethylammonium hydroxide, and phenyltrimethylammonium chloride were obtained from the Aldrich Chemical Company (Milwaukee, WI, U.S.A.).

Depolymerization of PET Fibers

In a 300-mL round-bottom flask, a 5% sodium hydroxide solution (250 mL) was heated to 80°C in a constant-temperature bath. The catalysts were added in the following amounts in separate experiments: trioctylmethylammonium chloride (TOMAC) (0.04 g, 0.0001 mol); trioctylmethylammonium bromide (TOMAB) (0.045 g, 0.0001 mol); hexadecyltrimethylammonium bromide (HTMAB) (0.045 g, 0.0001 mol); tetraethylammonium hydroxide (TEAOH) (0.015 g, 0.0001 mol); phenyltrimethylammonium chloride (PTMAC) (0.02 g, 0.0001 mol). PET fibers (1.98 g, 0.01 mol) were added to the mixture and allowed to react for 30, 60, 90, 150, and 240 min. Upon filtration, any remaining fibers were washed several times with water, dried in an oven at 130–150°C, and weighed. The results are shown in Table 1.

TABLE 1
Results of the PET Depolymerization (Weight % PET Fibers Reacted) with Quaternary Ammonium Compounds at 80°C Without Agitation

Catalyst	30 min	60 min	90 min	150 min	240 min
Control (wt. % PET reacted)	3.99	4.69	12.7	22.6	32.8
TOMAC (wt. % PET reacted)	21.84	44.09	52.78	66.07	69.79
TOMAB (wt. % PET reacted)	24.81	44.71	54.44	64.58	90.15
HTMAB (wt. % PET reacted)	7.08	32.87	44.66	66.22	81.72
TEAOH (wt. % PET reacted)	3.28	5.11	8.01	8.86	22.52
PTMAC (wt. % PET reacted)	1.09	3.58	15.15	30.51	46.76

Depolymerization of PET Fibers with Agitation

The agitation studies for PET depolymerization were performed in the Atlas Launder-ometer (Waltham, MA, U.S.A.). The Launder-ometer is a device for rotating closed containers in a thermostatically controlled water bath. The procedure used in these experiments was adapted from an AATCC standard test method. The 5% sodium hydroxide solution (250 mL) was preheated to 80°C in a 1-pt. stainless-steel jar. The catalysts were added in the following amounts in separate experiments: TOMAC (0.04 g, 0.0001 mol); TOMAB (0.045 g, 0.0001 mol); HTMAB (0.045 g, 0.0001 mol). The PET fiber specimens (1.98 g, 0.01 mol) were placed in the containers along with 10, 0.25-in. stainless-steel balls to aid in the agitation process. The jars were sealed in the Launder-ometer, whose bath was at the desired temperature (80°C). The machine was allowed to run for the allowed treatment times (i.e., 30, 60, 90, 150, and 240 min) at 42 rpm. Upon decanting, any residual fibers were washed several times with water, dried in an oven at 144°C, and weighed. The results are shown in Table 2.

Depolymerization of Nylon 46

A 500-mL round-bottom flask containing aqueous sodium hydroxide (25 or 50 wt.%) and benzyltrimethylammonium bromide as the phase-transfer agent (0.2 g, 0.0008 mol) was placed in a constant-temperature oil bath and heated to the reflux temperature of 165°C. Chopped nylon 46 fibers (6 g, 0.030 mol)

TABLE 2
Results of the PET Depolymerization (Weight % PET Reacted) with Quaternary Ammonium Compounds at 80°C with Agitation

Catalyst	30 min	60 min	90 min	150 min	240 min
Control	3.5	11.33	13.71	26.05	41.74
TOMAC	79.8	92.41	99.52	100	
TOMAB	85.71	98.55	100		
HTMAB	26.31	50.97	60.68	88.96	100

were placed in the reaction flask. The reaction mixture was constantly stirred with a magnetic stirrer and the reaction was carried out at atmospheric pressure for a period of 24 or 36 h (see Table 3 for results). The aqueous sodium hydroxide solution containing products of depolymerization was concentrated by evaporation and 30 mL of 35% aqueous hydrochloric acid was added to the concentrate. The precipitate was filtered and washed with water. The product was dried in a vacuum oven at 120°C for 24 h.

Repolymerization of Nylon 46 Oligomers

Oligomers (2.0 g) obtained from the alkaline hydrolysis of nylon 46 were charged to a round-bottom flask. The flask containing the oligomers was heated in a mineral bath at 210°C for 16 h under vacuum.

Depolymerization of Nylon 66

In a 500-mL resin reaction kettle, fitted with a mechanical stirrer and a reflux condenser, was placed 6 g (0.025 mol) of nylon 66 fibers and 200 mL of 50%

TABLE 3
Properties of Alkaline Depolymerization Products of Nylon 46

Weight BTEMB (g)	Weight % NaOH	Volume NaOH (mL)	Weight % fibers hydrolyzed	Weight of oligomers formed (g)	Intrinsic viscosity (dL/g)	M_v (g/mol)
0.2	25	100	0			
0.2	50	100	38.4	3.7	0.14	1846
0.2	50	50	32.0	4.1	0.34	5946
0.2	50	100	39.3	3.6	0.13	1679
0.0	50	100	8.7	5.5	0.29	4704

aqueous sodium hydroxide solution. Benzyltrimethylammonium bromide (BTEMB) (0.2 g, 0.0008 mol) was added to the reaction mixture. The reaction mixture was heated for 24 h under reflux (130°C). Next, the unreacted nylon 66 fibers were removed by filtration and dried in a vacuum oven at 100°C for 24 h. The remaining aqueous solution was evaporated and the residue was extracted with isopropanol in a Soxhlet apparatus for 24 h.

Repolymerization of Nylon 66 Oligomer

The mixture of oligomers were heated in a flask to 200°C in a mineral bath [the differential scanning colorimeter (DSC) peak melting temperature of the oligomers was 230°C] while stirring and removing water formed with a vacuum pump.

Effect of Feed Ratio of the Depolymerization Reaction Mixture on the Molecular Weight

A known amount of nylon 66 fiber (MW = 30,944 g/mol) was mixed with 200 mL of a 50% aqueous solution of NaOH and 0.2 g of BTEMB in five different runs. The mixture was heated at 143°C for 24 h under reflux. After 24 h, on cooling, a white powder mixed with short whiskers settled at the bottom of the flask. The solid was collected by filtration. The reduced viscosity of the depolymerized nylon 66 was determined in 88% formic acid at 25°C in a Ubbelhode viscometer.

Isolation of Adipic Acid

Nylon 66 fibers (6.0 g) were depolymerized under reflux with 200 mL of 50% NaOH solution in the presence of 0.20 g of BTEMB to form 0.55 g of adipic acid (after acidification) and 4.52 g of oligomer. In a second step, the oligomer obtained in step 1 was depolymerized under the same conditions to form 0.72 g of adipic acid and 1.62 g of oligomer. In the third step, the 1.62 g of oligomer formed in step 2 were depolymerized with 50 mL of 50% NaOH solution and 0.54 g of BTEMB to form 1.05 g of adipic acid after initial exposure of the oligomer to heat in an attempt to obtain hexamethylenediamine by distillation.

RESULTS AND DISCUSSION

PET Depolymerization

We became interested in the application of phase-transfer agents for depolymerization of polymeric fibers while studying the alkaline depolymerization of PET. A phase-transfer catalyst is used in catalytic amounts in a two-phase

reaction system to cause the transfer of one of the reactants into the normal phase of the other reactant in such a form that high reaction rates are obtained. Our requirements were that the phase-transfer agent be cationic and have enough organic character such that it and the desired anion are partitioned into the organic phase with high potential reactivity. Crown ethers, quaternary ammonium compounds and *N*-alkyl phosphoramides have been used successfully as phase-transfer catalysts. Also, our plan was to develop an atmospheric pressure process. We discovered that PET fibers could be hydrolyzed with 5% aqueous sodium hydroxide at 80°C in the presence of trioctylmethylammonium bromide in 60 min to obtain terephthalic acid in 93% yield. We were unable to isolate the small amount of ethylene glycol produced.

The results of catalytic depolymerization of PET without agitation are listed in Table 1. The results of catalytic depolymerization of PET with agitation are listed in Table 2. As expected, agitation shortened the time required for 100% conversion.

Tetraethylammonium hydroxide was chosen because it was thought that the presence of the hydroxide counterion would aid in maintaining the hydroxide ion concentration in the reaction medium during the course of the reaction. As the results indicate (Table 1), depolymerization was somewhat inhibited. Conditions in the bath were favorable for a Hofmann elimination reaction, and the integrity of the catalyst was probably affected.

Results (Table 1) for the quaternary salts with a halide counterion were promising. Phenyltrimethylammonium chloride (PTMAC) was chosen to ascertain whether steric effects would hinder catalytic activity. Bulky alkyl groups of the quarternary ammonium compounds were expected to hinder close approach of the catalyst to the somewhat hidden carbonyl groups of the fiber structure. The results indicate that steric hindrance is not a problem for PET hydrolysis under this set of conditions because the depolymerization results were substantially lower for PTMAC than for the more sterically hindered quaternary salts.

Hexadecyltrimethylammonium bromide (HTMAB) was included in the investigation because it had been employed previously. The past success of HTMAB was attributed to its long-chain alkyl group. Mimicking a long polymer chain, the hexadecyl group probably aided in the solvation of PET. As expected, HTMAB made a respectable showing in these experiments.

Trioctylmethylammonium chloride (TOMAC) and TOMAB outperformed all other catalysts. It was postulated that the three octyl groups were the proper length for solvation of the polymer, while small enough to avoid sterically hindering the reaction.

In order to determine if TOMAB could be used to catalyze PET depolymerization for more than one treatment cycle, the catalyst was recovered upon completion of one treatment and added to a second bath for 60 min. The per-

cent PET conversion for the second cycle was 85.7% compared to a conversion of 90.4% for the first treatment cycle.

Nylon 46 Depolymerization

Trioctylmethylammonium chloride and TOMAB were found to be ineffective for the depolymerization of polyamides. Aqueous sodium hydroxide solutions containing BTEMB were successfully used to depolymerize nylon 46 to form low-molecular-weight oligomer fractions. The depolymerization efficiency (% weight loss) and the molecular weight of the reclaimed oligomers were dependent on the amount and concentration of the aqueous sodium hydroxide and the reaction time. Table 3 exhibits the effects of experimental conditions on the depolymerization efficiency and the average molecular weight of the oligomers. The viscosity-average molecular weight was calculated from the Mark–Houwink equation $[\eta] = KM_v^a$, where M_v is the viscosity-average molecular weight, $K = 4.64 \times 10^{-2}$ dL/g, and $a = 0.76$ at 25°C in 88% formic acid. Nylon 46 fibers ($M_v = 41{,}400$ g/mol) did not undergo depolymerization on exposure to 100 mL of 25 wt.% sodium hydroxide solution at 165°C. Out of 6.0 g of nylon fibers fed for depolymerization, 5.95 g were unaffected. When the concentration of sodium hydroxide was increased to 50 wt.%, the depolymerization process resulted in the formation of low-molecular-weight oligomers. Hence, even in the presence of a phase-transfer agent, a critical sodium hydroxide concentration exists between 25 and 50 wt.%, which is required to initiate depolymerization under the conditions used. Soluble amine salts were also obtained.

In order to establish the feasibility of alkaline hydrolysis in respect to recycling of nylon 46, it was necessary to determine whether the recovered oligomers could be repolymerized to form nylon 46. For this purpose, solid-state polymerization was performed on nylon 46 oligomers formed via alkaline hydrolysis with 50 wt.% NaOH at 165°C for 24 h. The solid-state polymerization process was carried out in a round-bottom flask at 210°C for 16 h under vacuum. Solid-state polymerization of the nylon 46 oligomers resulted in an increase in intrinsic viscosity from 0.141 to 0.740 dL/g. That corresponds to an increase in viscosity-average molecular weight from 1846 g/mol to 16,343 g/mol. In theory, higher molecular weights would be obtained by heating for a longer time interval.

Nylon 66 Depolymerization

The product of the depolymerization of nylon 66 with 50% aqueous sodium hydroxide solution was relatively low-molecular-weight oligomers. A series of experiments were run in order to examine the applicability and efficiency

TABLE 4
Effect of Feed Ratio on the Depolymerization of Nylon 66

	Experiment					
	1	2	3	4	5	6
Feed ratio of nylon/BTEMB (wt./wt.)	5	10.3	20.6	29.4	59.8	No PTA
Decrease in weight of oligomers	40.3	49.5	55.5	42.5	40.8	−15.9
M_v of oligomers	1556		1912	1697	2396	1644

of benzyltrimethylammonium bromide as a phase-transfer catalyst in the depolymerization of nylon 66. Table 4 shows the effect of the feed ratio of the nylon 66 to BTEMB on the viscosity-average molecular weight of the depolymerized nylon.

The product of the run with no phase-transfer agent showed a 15.9% increase in weight compared to the weight of the original nylon 66. The calculated percentage increase in weight for a 19-fold decrease in molecular weight (due to the addition of water) would be ~1%. Therefore, a large part of the increase must be due to leaching of silicates of the glass container (resin reaction kettle) by the strong alkali (50 wt.%) at the temperature of the reaction (130°C) over 24 h. The oligomer obtained had a viscosity-average molecular weight of 1644 g/mol (the original nylon 66 had a molecular weight of 30,944 g/mol). The runs with a phase-transfer agent produced oligomers with decreases in weight of 40–50%. Although the occurrence of leaching of silicates from the glass container makes quantitative assessment difficult, these results suggest that in the absence of a phase-transfer agent, only oligomers are formed; however, soluble low-molecular-weight products are formed in the presence of a phase-transfer agent. The oligomers obtained were repolymerized in the solid state by heating at 200°C in a vacuum. The viscosity-average molecular weight of the solid-state polymerized nylon 66 obtained was ~23,000 g/mol (the molecular weight of the oligomeric mixture was 1434 g/mol).

Isolation of Adipic Acid from the Depolymerization of Nylon 66

Nylon 66 fibers were depolymerized under reflux with a 50% NaOH solution in the presence of catalytic amounts of benzyltrimethylammonium bromide.

The oligomers formed in successive steps were depolymerized under similar conditions. The yields in steps 1, 2, and 3 were 57.8%, 38.7%, and 100+% theoretical. However, we were unable to isolate hexamethylenediamine. The overall yield of adipic acid was 59.6%.

CONCLUDING REMARKS

Alkaline depolymerization of PET at 80°C in the presence of phase-transfer agents resulted in the isolation of terephthalic acid in yields as high as 93%. Hydrolysis of PET occurred at temperatures as low as 20°C; however, the best results were obtained at the highest temperatures employed (80°C). Phase-transfer-catalyzed alkaline depolymerization of nylon 46 produced oligomers which could be repolymerized and soluble products believed to be amine salts. Catalytic depolymerization of nylon 66 produced oligomers and adipic acid in reasonable yields. The isolation of adipic acid on depolymerization of nylon 66 required a stepwise approach involving the catalytic depolymerization of intermediate oligomeric fractions. Future research would involve developing conditions whereby the nylon 46 and nylon 66 may be completely converted to monomers (1,4-diaminobutane and adipic acid in the case of nylon 46 and hexamethylenediamine and adipic acid in the case of nylon 66) while utilizing phase-transfer catalysts. These new conditions may require the discovery of new phase-transfer catalysts.

ACKNOWLEDGMENTS

The authors would like to acknowledge the National Textile Center and E. I. duPont de Nemours & Company for financial support of the research. Also, we thank the Polymer Associates Program at the Georgia Institute of Technology for the support of L. L. LeBoeuf, Jr.

REFERENCES

1. P. Bajaj and N. D. Sharma, in *Manufactured Fibre Technology* (V. B. Gupta and V. K. Kothari eds.), Chapman & Hall, New York, 1997.
2. D. Paszun and T. Spychaj, *Ind. Eng. Chem. Res., 36,* 1373 (1997).
3. H. Grushke, T. Neuenhain, W. Hammerschick, B. Nauheim, and H. Medem, U.S. Patent 3403115 (1968).
4. H. Ludewig, *Polyester Fibres: Chemistry and Technology,* John Wiley and Sons, New York, 1971.
5. A. J. Hall, *Textile World, 113*(9), 108 (1963).

6. S. M. Gawish, M. Gourgeois, and G. Ambroise, *Am. Dyestuff Rep., 73*(12), 37 (1984).
7. A. Uku, R. Ebisu, and E. Yamada, *Chem. Abstr., 128,* 230829t (1998).
8. B. M. Miller, U.S. Patent 2,840,606 (1958).
9. J. Thorburn, U.S. Patent 3,223,731 (1965).
10. H. P. Kasserra, *2nd Annual Conference on Recycling of Fibrous Textile and Carpet Waste,* 1998.
11. R. J. McKinney, U.S. Patent 5,302,756 (April 12, 1994).

POLYM.–PLAST. TECHNOL. ENG., 38(3), 471–484 (1999)

RECYCLING NYLON 6 CARPET TO CAPROLACTAM

M. BRAUN, A. B. LEVY,* and S. SIFNIADES

AlliedSignal Inc.
P.O. Box 1021
101 Columbia Road
Morristown, New Jersey 07962

Abstract

The recycling of nylon 6 carpet via depolymerization provides the potential for an environmentally benign new process to produce world-class caprolactam. This article describes the depolymerization of nylon 6 carpet in the presence of steam under medium pressure (800–1500 kPa, 100–200 psig). A small laboratory apparatus was set up to demonstrate the feasibility of the scheme. A total of eight runs were carried out using ~180 g of pellitized carpet and 2–6 g/min steam (at 101–1500 kPa, 0–200 psig, and 300–340°C). In our best run at 340°C, 6 g/min of steam, and 1500 kPa (200 psig) for 3 h, we obtained a 95% yield of crude caprolactam. The lactam purity was 94.4%, resulting in an overall 89.7% yield of caprolactam. The laboratory data were used to construct a computer model of the process for both batch and continuous-flow stirred reactors.

Key Words: Nylon 6; Carpet recycle; Depolymerization; Caprolactam; Waste carpet recycling.

INTRODUCTION

In 1997, the United States and Canada produced 3.2 billion pounds of fiber for carpets (1). The fiber was used in ~6.6 billion pounds of carpet, of which

* To whom correspondence should be sent.

~70% was for replacement. The vast majority of the replaced carpet ended up in landfills. At that disposal rate, carpet constitutes approximately 1.6% by weight of all material landfilled. Although carpet is not hazardous in a landfill, it is large, visible, and relatively difficult to handle. In addition, the number of landfills is decreasing. In 1995, there were only about 4500 active landfills. By the year 1999, this number is expected to be reduced to 2500. Thus, it seems inevitable that society will increasingly pressure the carpet industry to provide a recycle path.

A typical broadloom carpet consists of approximately 50% by weight face fiber (Fig. 1). Most of the face fiber produced in North America is nylon 6 or 6,6, with smaller amounts of polyester, wool, and polypropylene. Of the face fiber produced in North America, ~30% is nylon 6. Thus, the mixed carpet stream will require significant sorting prior to recycling. As a manufacturer of caprolactam and nylon 6, AlliedSignal is primarily interested in recycling nylon 6 to caprolactam.

Recycling of nylon 6 has been carried out for at least the past 30 years and has been reviewed (2). Chemical processing via depolymerization usually leads to caprolactam [Eq. (1)].

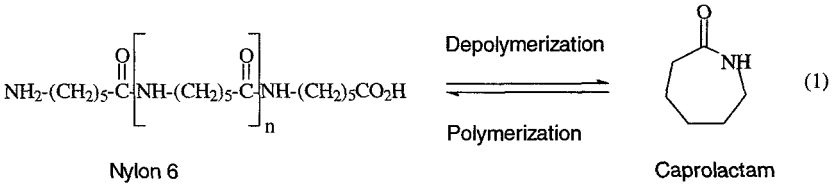

(1)

In order to achieve reasonable rates in the depolymerization, an acid catalyst is usually employed (3).

The recycling of nylon 6 carpet, however, is a more complicated issue due to its multicomponent construction and to the presence of the backing material and contaminants such as dyes and coatings. In addition to the nylon 6 face fiber, the typical broadloom carpet also contains ~10% polypropylene as primary and secondary backings, 9% styrene–butadiene latex adhesive, and about 35% calcium carbonate as filler. Furthermore, face fiber is treated with small amounts of dyes, pigments, antistatic compounds, and other surface treatments. Last, and perhaps most significant, is the fact that postconsumer carpet is dirty. A carpet that contains 50% nylon when new can add as much as 20% of its weight as dirt consisting of everything from dog hair, to food, to metal fragments. The presence of these impurities significantly complicates the recycling process.

Two distinct approaches, physical and chemical, have been investigated. The physical approach is characterized by mechanical separation of the face

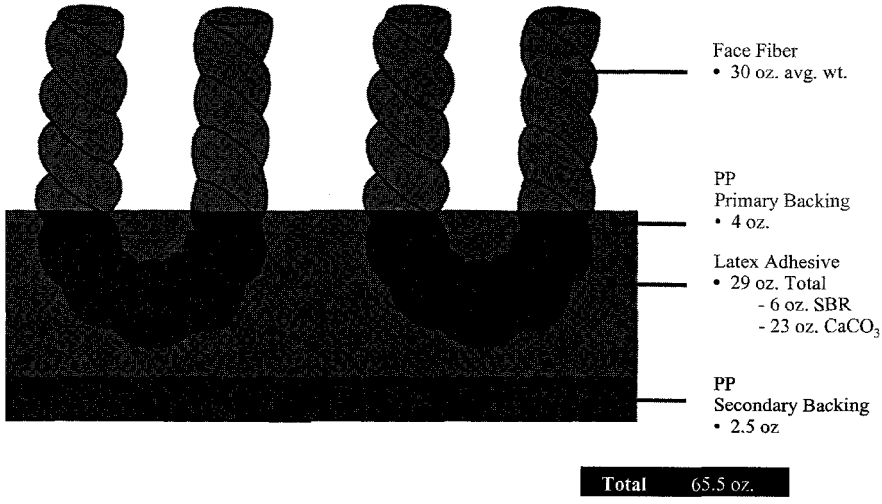

FIG. 1. Typical carpet construction and composition.

fiber from the backing and adhesive through a series of grinding and milling steps. At this point, typically a mix consisting of ~70–80% nylon 6 containing about 15% polypropylene and 5–10% calcium carbonate/styrene–butadiene rubber is obtained. Corbin et al. (4) have demonstrated that material from such a process can be depolymerized in the presence of phosphoric acid to caprolactam.

Further purification of the crude material through a wet separation process can give nylon 6 of 95–98% purity. The resultant fibers are usually colored and typically mixed with virgin polymer and used as a black engineering resin, or depolymerized to caprolactam via the classical phosphoric acid reaction (3).

We approached the problem differently. The segregation of face fiber from backing is a capital- and manpower-intensive process which would be best to avoid as a separate step. We concluded that it would be best to feed postconsumer carpet to a reactor containing the necessary reagents to separate the nylon from the carpet backing and provide a separate means of exit for the caprolactam produced and residue. Furthermore, because the major component of a typical backing is calcium carbonate, we are constrained from using acidic catalysts to depolymerize nylon 6 carpet. Finally, because of the environmental impact and potential costs, we considered only simple, inexpensive, and

environmentally benign solvents/reactants. This train of thought led to the conclusion that the simplest approach to depolymerizing nylon 6 carpet is to use water to recover caprolactam. The problem the literature suggests we face is getting the reaction to go at a commercially viable rate and at temperatures which commercial equipment can handle. We have previously reported a process involving depolymerization of carpet under pressure (~1100 psig) at 290°C in the presence of water followed by filtration and flashing the resultant solution in a hot tube (5). We now report a process involving steam distillation of caprolactam from raw carpet at moderate pressures, which results in high yields at commercially viable rates (6).

EXPERIMENTAL

General

Chemicals

Caprolactam (Aldrich Gold Label, Aldrich, Malwaukee, WI, U.S.A.) was dried in a vacuum dessicator to ~0.1% water content before using as an analytical standard. Carpet pellets were made by extruding nylon 6 preconsumer carpet.

Analytical

High-Performance Liquid Chromatography. The product was analyzed by high-performance liquid chromatography (HPLC) using a Waters 600E liquid chromatograph equipped with a Waters model 990 photodiode array detector and Waters model 715 Wisp autosampler. The analysis was carried out using acetonitrile/0.05*M* phosphoric acid on a Supelcosil™ LC-8DB, 4.6 mm by 25 cm column. The resultant chromatogram was monitored at 200 nm for cyclic oligomers and 230 nm for caprolactam quantification.

Gas Chromatography. The isolated caprolactam samples were analyzed for purity on a Hewlett Packard model 5880 GC using a 50-m capillary Carbowax 20M column.

Permanganate Number (ISO PN). For a typical sample, 0.1 g of crude lactam are weighed into a 250-mL volumetric flask and filled to the mark with distilled, deionized water. The pH of the sample is adjusted using dilute H_2SO_4 or NaOH to be within the range 6.2–6.5. One hundred milliliters of the sample are then quantitatively transferred to an Erlenmeyer flask and placed in a 25°C ± 0.5°C water bath for 15 min. Once equilibrated, 2.0 mL of a 0.01*N* potassium permanganate solution is added and a timer started. The absorbance of the sample is taken at 10 min after permanganate addition at 420 nm. If the resulting absorbance is outside the range of 0.025–0.080 absorbance units, the sample concentration must be adjusted and the test re-

peated. The ISO PN value is calculated as absorbance of the sample minus absorbance of the blank divided by the grams of lactam in 100 mL of sample times 500.

AlliedSignal Color. In a representative case, 2 g of crude lactam were weighed into a 5.0-mL volumetric flask and filled to the mark with distilled, deionized water. After mixing, the sample was filtered through a 0.45-μm Teflon syringe filter and the absorbance measured at 410 nm. Color was then calculated as absorbance times 1.625 times 1000.

Miscellaneous. The analysis for nitrogen was performed by Robertson Laboratory. The calcium, ammonia, and water analyses were carried out by AlliedSignal's Morristown Analytical Sciences Laboratories. Aminocaproic acid analysis was done at the Allied Technical Center using ion chromatography. Gas chromatography–mass spectroscopy was carried out at both the Allied Technical Center and the Morristown Analytical Sciences Laboratories.

Medium-Pressure Steam Depolymerization of Nylon 6 Carpet (Fig. 2)

Water was pumped using a Waters 590 HPLC pump at 2–6 g/min through two steam generators in series (1200 W total). Transfer lines and valves were

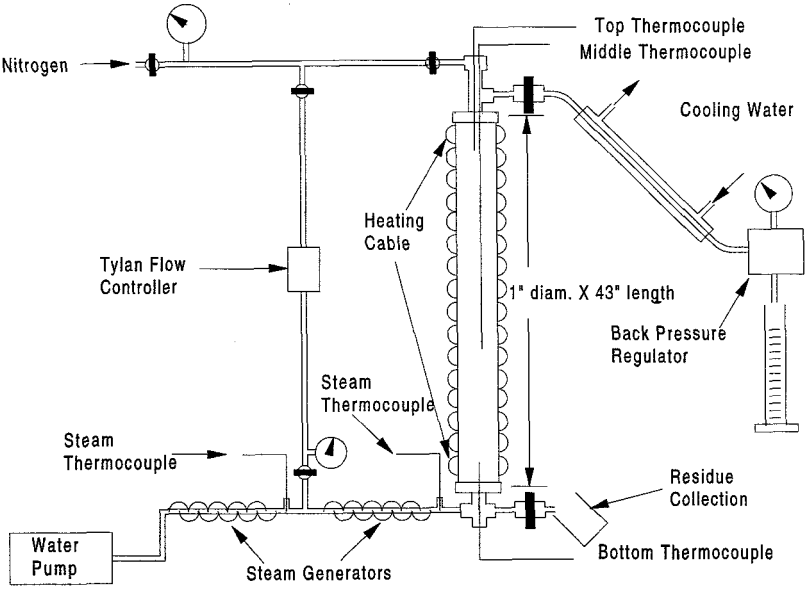

FIG. 2. Laboratory-scale medium-pressure depolymerization apparatus

heated using various lengths of heating tape. Reactor heating was configured as three zones using a 400-W cable heater for each zone. Three internal thermocouples monitored the temperature for each zone. High-temperature needle valves were used at the reactor overheads and bottoms exit points.

In a typical reaction, 180 g of chipped carpet extrudate was charged into a stainless-steel reactor 43 in. by 1 in. in diameter while the reactor was purged with nitrogen. Analysis of the extrudate showed 57.6% nylon. The system was then sealed and all zones not directly in contact with the carpet were brought up to temperature. Heat was then applied to the reactor body itself and steam flow was started when the reactor's internal temperature reached ~120°C (~20 min). The reactor was maintained at a moderate (410–450 kPa, 45–50 psig) pressure during heatup and increased to the desired pressure as reactor temperature reached ~180°C. Overheads condensate samples were collected throughout the reaction. At the end of the reaction, steam flow was shut off and the overheads exit valve closed. The nitrogen inlet valve at the reactor top was then opened and the system pressure was allowed to build up slightly. The residue was then discharged by carefully opening the valve at the bottom of the reactor and collecting into a metal beaker. After sampling for GC and HPLC analysis, the overheads fractions were combined and 50% of it rotoevaporated to constant weight. The resulting solid was analyzed by GC and HPLC. The permanganate number and color were also determined on the solid caprolactam. The solid bottoms samples were analyzed for residual nylon by nitrogen analysis.

RESULTS AND DISCUSSION

Medium-Pressure Steam Depolymerization of Carpet

The literature (2) on nylon depolymerization suggests that the rate of the reaction at atmospheric pressure is quite slow compared to the catalyzed process. Our results at atmospheric pressure (Fig. 3) corroborate the nylon data and suggest that at atmospheric pressure, the reaction is too slow for a commercial process.

It seemed to us that the use of pressure might have a beneficial effect on the rate. This may seem counterintuitive at first glance. Our rationale, however, is as follows. We expected that the rate of removal of caprolactam overhead would be dependent on pressure, temperature, and steam flow rate. We also suspected that pressure would have a significant positive effect on the rate. In general, at increased pressures, one expects a decreased mole fraction of a volatile component in the vapor phase at constant temperature and steam feed rate and, thus, a decrease in rate of removal overhead. However, the solubility

of water in nylon 6 increases with pressure, thereby increasing the rate of depolymerization, and hence the mole fraction of caprolactam in the polymer. Thus, given the two competing effects, one might predict a maximum in rate of removal of caprolactam overhead as the pressure is increased at constant temperature and steam flow.

We have run a total of eight experiments in the apparatus shown, at various combinations of pressures, temperatures, and steam flow rates. Figure 3 shows a comparison of the rates of lactam formation overhead obtained from these experiments.

In our first experiment at ~ 2 g/min steam flow, 930 kPa (120 psig), and 300°C, the rate, although considerably faster than our control at atmospheric pressure, was deemed to be too slow and the run was shut down at ~ 60% conversion. In all other cases, we obtain 87% conversion or higher by analysis in 3–6 h.

The lactam concentrations typically range from about 14% to 24% in the early fractions to about 1% at the end. Figure 4 shows a concentration profile for lactam and cyclic dimer in a reaction carried out at 1100 kPa (145 psig)

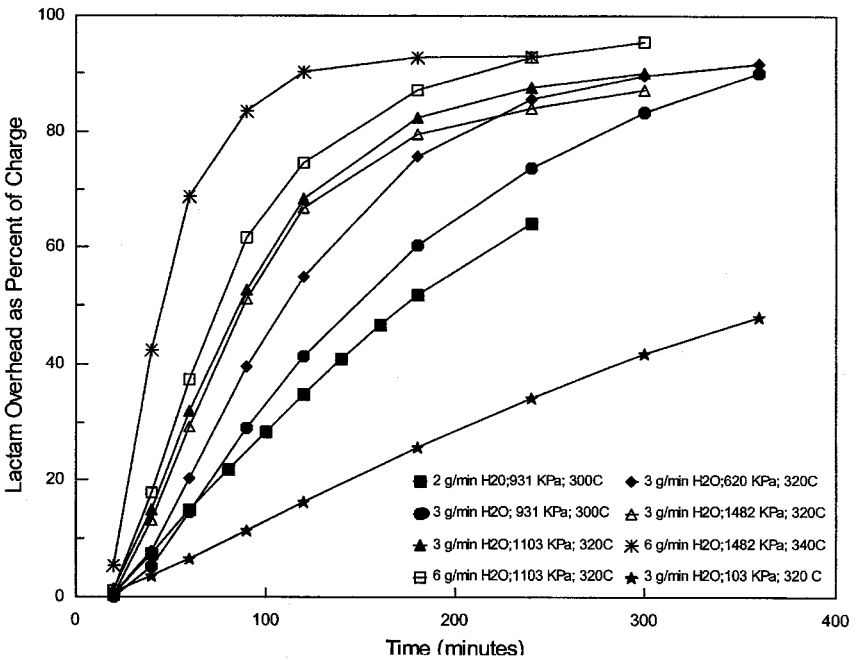

FIG. 3. Medium-pressure depolymerization of carpet extrudate. Lactam overhead (percentage of charge) as a function of time.

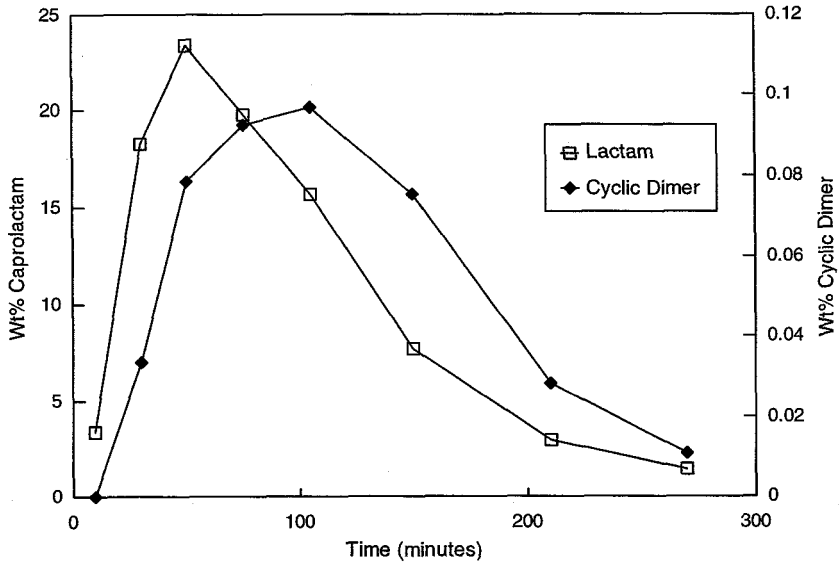

FIG. 4. Medium-pressure depolymerization of carpet extrudate, 182 g extrudate, 3 g/min steam at 320°C and 1100 kPa. Concentration profiles of lactam and cyclic dimers in the overheads.

and 320°C with 3 g/min steam. It is worth noting the relatively low level of cyclic dimer in the overheads after 200 min.

A comparison of reactions run at 320°C with 550, 1100, and 1480 kPa (75, 145, and 200 psig, respectively) in Figure 3 suggests that the pressure affects the rate between 550 and 1100 kPa, but going to 1480 kPa results in essentially no increase in rate. One reaction was run at 340°C, resulting in a large increase in initial rate (~ 1.5 g lactam overhead/min versus 0.4–0.9 g lactam overhead/min) compared to all other examples. Furthermore, under these conditions, the lactam concentration reaches ~ 25% in the aqueous overheads.

The results clearly demonstrate a relatively large effect of moderate pressures. Figure 5 summarizes the effect of pressure on initial rate and maximum concentration of caprolactam observed during the reaction. As can be readily seen, there is a large effect of an initial pressure increase (100–620 kPa, 0–75 psig) above atmospheric. Further increases in pressure lead to more modest increases in rate until the reaction reaches an optimum pressure, at which point the reaction rate seems to level off. As expected, the maximum concentration parallels the maximum rate at fixed steam flow and temperature.

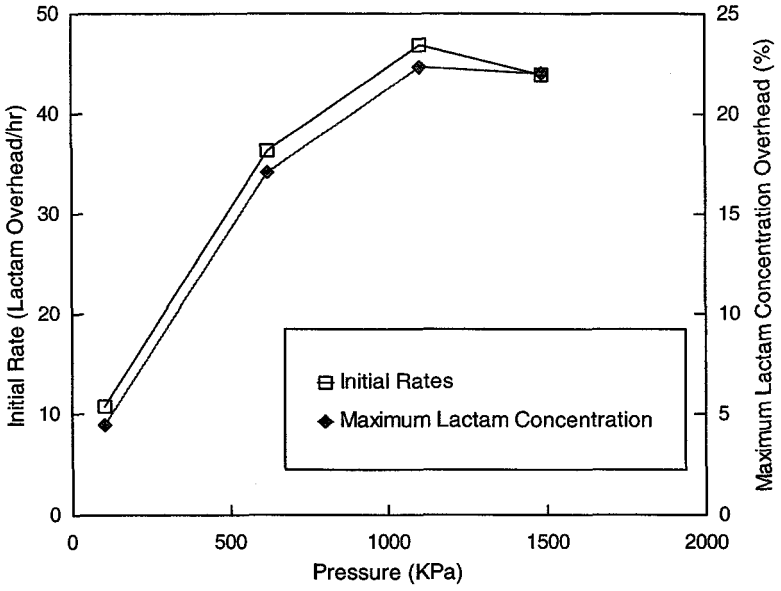

FIG. 5. The effect of pressure on the initial rate and maximum concentration of lactam in the overheads during medium pressure depolymerization. Conditions: 320°C and 3 g/min steam.

Impurities in the Medium-Pressure Depolymerization Process

Table 1 summarizes the analytical results for the six reactions carried out to high conversion. At temperatures between 300°C and 340°C, 3 or 6 g/min steam, and pressures of 620–1500 kPa (75–200 psig), we obtain crude caprolactam yields of 87–95%. We believe that the differences in isolated yields have more to do with the time the reaction was allowed to run rather than any inherent side reactions. GC and HPLC analysis of the lactam versus a standard shows the material to be ~ 95% pure in all cases, indicating that there is ~3% of high-boiling impurities that do not show up on the GC. Part of this missing material is caprolactam cyclic dimer, which HPLC shows to be present in ~ 0.5–0.6% yield.

Ammonia is present in the hydrolysate at 0.8–1.5% yield based on nylon. For every mole of ammonia present, we assume there must be 1 mol of 6-hydroxycaproic acid or 6-hexenoic acid present, which may contribute to heavies. In addition to ammonia, low levels of *N*-methylcaprolactam were observed, and in one case, some octahydrophenazine (OHP), as well as some 7-(5-aminopentyl)-3,4,5,6-tetrahydro-2H-azepine (APTA). It is also gratifying

TABLE 1
Medium-Pressure Depolymerization of Carpet Extrudate

Conditions/impurity level	Run 1	Run 2	Run 3	Run 4	Run 5	Run 6
Reaction temperature (°C)	300	320	320	320	320	340
Charge (g)	178.8	181.9	179.1	180.2	180.4	180.2
Steam rate (g/min)	3	3	6	3	3	6
Reaction pressure (kPa)	931	1103	1103	620	1482	1482
Reaction time (min)	360	300	300	360	300	180
Caprolactam yield (%)[a]	87.4	89.2	93.1	92.2	87.9	95.0[j]
Nylon material balance (%)[b]	N.A.	95.1	95.7	94.9	94.9	95.9
Carpet material balance (%)[c]	N.A.	92.1	92.7	91.8	92.1	88.7
Caprolactam purity (%)[d]	94.4	95.1	94.7	96.7	96.2	94.4
Ammonia yield (%)[e]	0.80	1.5	1.2	1.8	2.0	2.0
Cyclic dimer yield (%)[f]	0.52	0.48	0.65	0.75	0.39	0.54
Cyclic trimer (%)[f]	N.D.	N.D.	N.D.	N.D.	N.D.	*i*
N-methylcaprolactam (ppm)[g]	560	350	580	380	460	500
Caprolactone (ppm)[g]	N.D.	N.D.	N.D.	N.D.	N.D.	N.D.
Octahydrophenazine (ppm)[g]	N.A.	20	N.A.	N.D.	60	N.D.
APTA (ppm)[g,h]	780	830	790	2220	1010	1932
Aminocaproic acid (ACA) (%)[k]	0.39	0.52	0.64	0.45	0.52	0.64
Iso PN	820	1310	1300	2010	1030	1920
Color (410 nm)	860	930	890	1440	1260	1270
$CaCO_3$ (ppm)	<25	<25	<25	N.A.	N.A.	N.A.

[a] Based on nylon analysis. Crude yields are based on isolated weights plus weights calculated to be in analytical samples.
[b] Based on isolated weights plus ammonia analysis and nitrogen in residue.
[c] Based on isolated weights and ammonia analysis.
[d] Average of GC and HPLC purity of crude isolate.
[e] By ion chromatography.
[f] HPLC analysis.
[g] GC analysis; response as a percent of lactam, uncorrected.
[h] 7-(5-Aminopentyl)-3,4,5,6-tetrahydro-2H-azepine.
[i] Trace amount (~30 ppm) of possible cyclic trimer in first fraction by HPLC.
[j] At 4 h the yield is 95.2%.
[k] Analyzed by ion chromatography.

that no calcium was observed overhead, suggesting that scaling should be minimal in this process. The ISO PN and color were also measured. GC/MS analysis of the isolated caprolactam detected low levels of *N*-methylcaprolactam and low levels of aromatics, such as diphenylpropane and styrene dimer. The aromatic impurities presumably result from decomposition of the styrene–butadiene rubber present in carpet backing. A similar analysis of the aqueous overheads without removing the water shows additional volatiles, including cyclohexylamine, styrene and α-methylstyrene. The aromatics are presumably derived from the styrene–butadiene rubber present in the backing.

The cyclohexylamine is used as a terminator in many nylons and thus is expected to be present. Analysis of the isolated caprolactam also shows ~ 0.5% aminocaproic acid (ACA) in caprolactam isolated from the medium-pressure depolymerization (MPD) process. We conclude that the ACA is formed in the process and carried overhead.

The amount of caprolactam cyclic dimer overhead is suppressed as the reaction is carried out at increasingly higher pressure. Figure 6 demonstrates this dramatic effect.

Modeling of the MPD Process

Seven runs that were conducted under reasonably controlled conditions in the apparatus described in Fig. 2 were used to construct a model of the process. The following assumptions were made in developing the model:

1. The carpet melt is composed of two distinct phases: a nylon phase and a non-nylon phase. All reactions take place in the nylon phase. The non-nylon phase is assumed to be inert.
2. Caprolactam and dimer exit the reactor in proportion to their respective partial vapor pressures. These are generally lower than the corre-

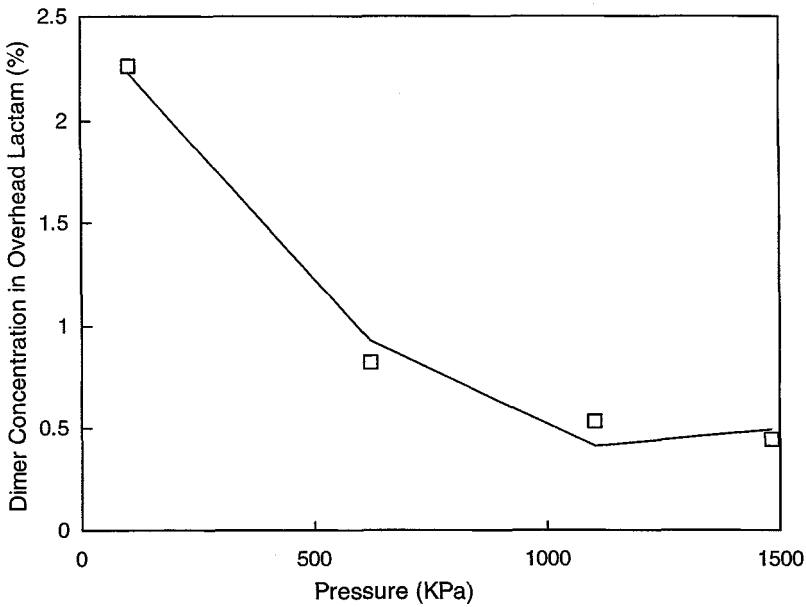

FIG. 6. The effect of pressure on cyclic dimer concentration in the overheads of medium-pressure depolymerizations of nylon 6 extrudate at 320°C and 3 g/min steam.

sponding saturation pressures due to mass transfer barriers between the liquid and the gas phases.

3. Ammonia is produced in proportion to the mass of the nylon phase, including caprolactam dissolved therein, has negligible solubility in the carpet melt, and its transport to the gas phase is not subject to mass transfer limitations. Dependence on the pressure, P, is accounted for by using the expression $k = A(1 + BP)\exp(-C/T)$ for the rate constant for ammonia formation, where A, B, and C are empirical constants fitted to match the data and T is the absolute temperature.

Medium-pressure depolymerization combines chemical reactions (nylon 6 depolymerization and ammonia formation) with mass transfer (removal of products overhead). To properly model the system, equations were developed that simultaneously addressed the reactions and mass transfer. The kinetics of nylon 6 depolymerization were simulated using AlliedSignal's proprietary nylon polymerization program which was specially calibrated for the temperature and water-vapor-pressure regime appropriate to MPD. Mass transfer coefficients for caprolactam and for caprolactam cyclic dimer were determined by fitting the MPD data to the model. Following are some of the predictions of the model for a batch reactor of similar mass transfer characteristics to the apparatus used in this work.

The effect of pressure on the rate of caprolactam production at constant temperature and steam flow is shown in Fig. 7. It is clear that increasing the pres-

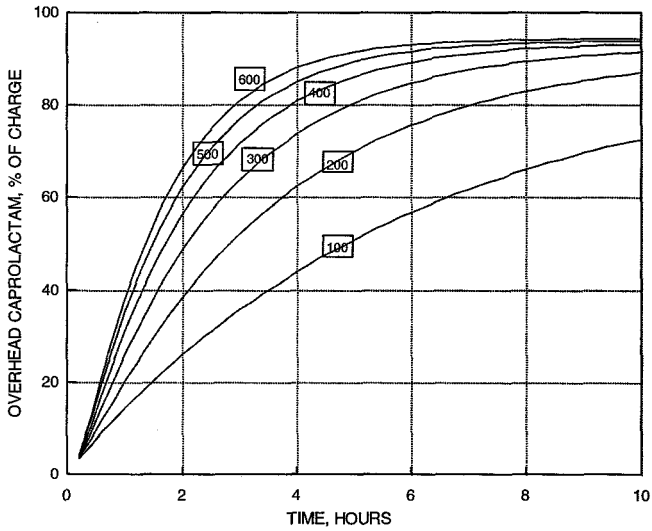

FIG. 7. MPD pressure effect on rate. Charge 180 g carpet pellets, 57.5% nylon 6, 180 g/h steam, 320°C. Numbers on curves are pressure (kPa).

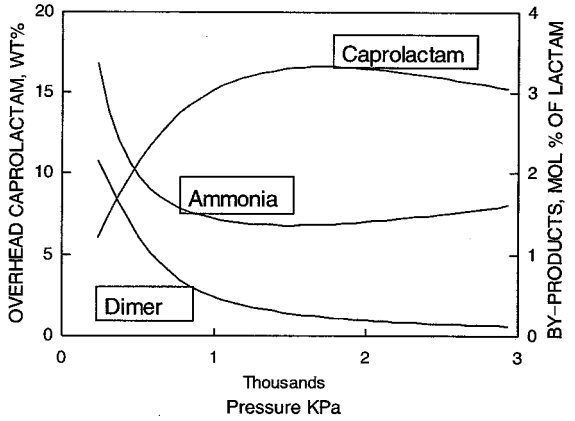

FIG. 8. MPD pressure effect on rate and selectivity. Charge 180 g carpet pellets, 57.5% nylon 6, 180 g/h steam, 320°C. Caprolactam yield 90%.

sure from 100 to 600 kPa (0–75 psig) increases the rate of caprolactam production, but the effect is most pronounced at the lower pressures. Figure 8 shows the effect of pressure at 320°C and constant steam flow on overheads caprolactam concentration at 90% caprolactam yield (under these conditions, the concentration is also an index of rate). It also shows the rates of formation of dimer and ammonia. It is clear that increasing pressure up to 1200–2000 kPa (160–275 psig) increases the rate of caprolactam production and suppresses the rates of dimer and ammonia production. Similar effects are shown at 340°C (Fig. 9).

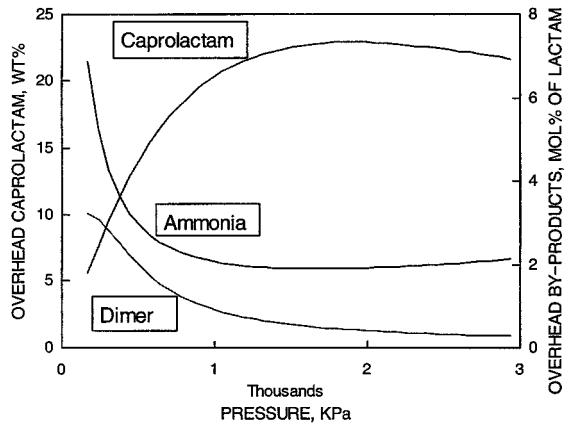

FIG. 9. MPD pressure effect on rate and selectivity. Charge 180 g carpet pellets, 57.5% nylon 6, 180 g/h steam, 340°C. Caprolactam yield 90%.

Comparing the two figures, we see that the lactam concentration increases at the higher temperature, but at the cost of increased dimer and ammonia formation.

REFERENCES

1. AlliedSignal Estimate (1998).
2. L. N. Dmitrieva, A. A. Speranskii, S. A. Krasavin, and Y. N. Bychkov, *Fibre Chem., 17,* 229 (1986).
3. J. H. Bonfield, R. C. Hecker, and O. Snider, U.S. Patent 3,182,055 (to Allied Chemical Corporation).
4. T. F. Corbin, E. A. Davis, and J. A. Dellinger, U.S. Patent 5,169,870 (to BASF Corporation).
5. S. Sifniades and A. B. Levy, U.S. Patent 5,457,197 (to AlliedSignal Corporation).
6. S. Sifniades, A. B. Levy, and A. J. Hentrix, U.S. Patent 5,681,952 (to AlliedSignal Corporation and DSM N.V.).

POLYM.–PLAST. TECHNOL. ENG., 38(3), 485–498 (1999)

RECYCLING CARPET WASTE BY INJECTION AND COMPRESSION MOLDING

YI ZHANG,[1] JOHN D. MUZZY,[2] and
SATISH KUMAR*,[1]

[1]*School of Textile and Fiber Engineering and*
[2]*School of Chemical Engineering*
Georgia Institute of Technology
Atlanta, Georgia 30332

Abstract

Studies have been carried out to convert carpet waste into valued products. Two common processes, injection and compression molding, can be used to recycle carpet waste. Three types of carpet waste have been recycled: (1) edge trim from carpet manufacturing, (2) polypropylene shear lint from cutting tufted carpet loops, and (3) separated polypropylene from postconsumer carpet waste. For injection molding, shredded carpet waste was debulked, ground, dried, and molded. For compression molding, the recycled carpet waste was combined with glass mat reinforcement. The compression-molding process consists of debulking, stacking with glass mats, and consolidation. The mechanical testing results are encouraging. The injection-molded samples showed properties acceptable for many applications. The glass-mat-reinforced carpet waste made by compression molding had properties comparable to commercial virgin thermoplastics reinforced with glass mat.

Key Words: Carpet waste; Recycling; Injection molding; Glass-reinforced thermoplastic.

* To whom correspondence should be sent.

INTRODUCTION

Carpet waste can be categorized into two basic types: preconsumer and postconsumer carpet waste. Preconsumer carpet waste consists of waste generated in carpet manufacturing and waste from the carpet fitting process. In carpet manufacturing, the edges of carpet need to be trimmed and the edge trim and off-cuts are disposed as carpet manufacturing waste. In Dalton, Georgia alone, over 20 million kilograms of carpet manufacturing waste is generated every year. The carpet waste from fitting is concentrated in the automotive industry. In the fitting process, a quantity of carpet waste is generated as the carpet is cut into various irregular shapes.

The other basic type of carpet waste is postconsumer waste. Approximately 2 billion kilograms of old carpet is removed from homes and businesses annually (1–3). Also, 0.7 billion kilograms of carpet waste are generated annually in Western Europe (4). Currently, most carpet waste is removed as part of the municipal waste and is disposed of by landfill. Compared to other municipal wastes, carpet waste provides a relatively simple resource with few components (approximately 80% of the carpet produced in the United States contains nylon, polypropylene, calcium carbonate, and SBR latex).

In this article, the technical feasibility of recycling carpet using two techniques is presented. In the injection-molding process, the carpet waste is recycled "as is," without any additive, and the baseline properties of the molded samples are evaluated. In the compression-molding process, the approach followed is to reinforce the carpet waste with fiberglass mat to form glass-mat-reinforced thermoplastics (GMT) (5). The market for GMT using virgin materials is growing, particularly for use in the automotive sector. Polypropylene is the most common matrix used in GMT (6). Therefore, carpet waste streams rich in polypropylene are emphasized in this study. The expectation is that glass-mat-reinforced carpet waste can be used in place of virgin polypropylene containing GMT.

EXPERIMENTAL METHODS

Material Analysis

Three types of carpet waste were recycled in this study: (1) carpet edge trim from Shaw Industries, (2) polypropylene shear lint from Advanced Textile Recycling, Inc., and (3) separated polypropylene from a postconsumer carpet waste recycling pilot plant operated by DuPont Co. The compositions of these carpet waste samples are given in Table 1.

The melt flow index of the carpet wastes was measured in a Melt Flow TQ (Ceast U.S.A.) instrument using a load of 2.16 kg. The mean of 12 readings is

TABLE 1
Approximate Compositions of Edge Trim, Separated Polypropylene, and Shear Lint

Carpet waste	Source	Appearance	Component
Edge trim	Shaw Industries	Chopped bales, many fibers >25 mm long, low-bulk density (<150 kg/m^3)	40% Polypropylene, 15% face fibers (mostly nylon 6 with some 66), 45% SBR plus calcium carbonate
Separated polypropylene	DuPont Co.	Lintlike, low-bulk density (<150 kg/m^3)	98% Polypropylene
Shear Lint	ATR Inc.	Lintlike, low-bulk density (<150 kg/m^3)	98% Polypropylene

listed in Table 2 along with the test temperatures. The procedure presented in ASTM D1238-90 was followed, except that the edge trim had to be tested at 260°C rather that the recommended 230°C for polypropylene. Because the edge trim contains at least 20 wt.% calcium carbonate as well as some nylon, it does not flow well.

A Seiko TG/DTA 220/320 was used to study the thermal properties of carpet waste. A heating range of 30–500°C and a rate of 10°C/min were selected. The samples used were from the carpet waste after the debulking step.

Debulking

Because the as-received chopped carpet waste had low-bulk density, less than 150 kg/m^3, it was difficult to feed it into the injection-molding machine with-

TABLE 2
Melt Flow Measurements for the Carpet Waste at 2.16 kg

Carpet waste	Temperature (°C)	MFI (g/10 min)
Edge trim	260	15.1
Separated polypropylene	230	10.7
Shear lint	230	22.2

out debulking. Also, it is necessary to convert them into sheets for stacking with glass mats in compression molding. A 89-kN (10-ton) Wabash press was used to debulk the carpet waste. The carpet waste was spread evenly on a foil and sent into the press, which had been preheated to a temperature lower than 232°C. A pressure lower than 700 kPa (100 psi) was then applied for less than 10 min. The compacted sheet of carpet waste was ground using a grinder (Model 46 SP, Double Angle Cut, Polymer Machinery Co.) for feeding in the injection-molding machine.

Injection Molding

A Van Dorn injection-molding machine with a 670-kN (75-ton) clamp force and 148-cm^3 (5-oz.) shot capacity was used to mold the samples. The ground carpet waste after debulking was vacuum-dried between 80°C and 110°C overnight. The molding temperature for edge trim carpet waste was set around 260°C due to the presence of nylon 6,6 (melting temperature: ~265°C). For the separated polypropylene (PP), a molding temperature less than 260°C was used. All the other settings were typical for polypropylene. At least 20 tensile samples (ASTM 638, type I) were obtained.

Compression Molding

A Wabash 445-kN (50-ton) vacuum compression press with 46-cm × 46-cm platens was used. A 30-cm × 30-cm mold was built for processing GMT samples. The compact sheets of carpet waste after the debulking step were interleaved with glass mat. The glass mats were from PPG and had two basis weights, 275 g/m^2 (0.9 oz./ft^2) and 450 g/m^2 (1.5 oz./ft^2). The glass mats were sized by PPG for unsaturated polyester resin. The stacked compact sheets of carpet waste and glass mats were placed in the mold. Then, the mold was placed in the preheated press set between 220°C and 260°C. The door of the press was closed and a vacuum of 0.2 atm obtained. After preheating for less than 5 min, a pressure of 350–1050 kPa was applied for less than 10 min. The mold was then cooled under pressure to room temperature. The laminate of GMT was removed, trimmed of excess flash, and cut into test samples.

Tensile Testing

Tensile samples were prepared to a size 165 mm long by 19 mm wide with a gauge section width of 12.7 mm (ASTM D638, type I). The injection-molded samples were directly molded using a standard mold. The compression-molded GMT samples were cut using a diamond saw. The gauge section of the

samples were shaped using a Tensilkut milling machine. All tensile tests were conducted at room temperature on an INSTRON 1125 universal test machine. The tensile speed was 50 mm/min. The procedure in ASTM D638-90 was followed. An extensometer 2630-106 (gauge length: 25 mm; travel: +12.5/−2.5 mm) was used for modulus measurements.

Impact Testing

Izod impact tests were performed on the injection-molded samples and by Dynatup™ testing on the compression-molded samples. An Izod impact tester, CS-137I, was used on the injection-molded samples. The injection-molded samples were cut into 130-mm-long strips and notched 65 mm from one end in the CSI CS-93 sample notcher machine. The notched depth was 1.0 mm. The procedure presented in ASTM D256 was followed.

A Dynatup 830-I impact tester was used on the compression-molded GMT samples. A dart with a mass of 15.9 kg was dropped on the 100-mm × 100-mm sample at a velocity of 284 mm/s. The procedure presented in ASTM D3763-92 was followed.

Density Measurement

The density of the compression-molded GMT is determined using a technique outlined in method A of ASTM D792. The samples were weighed both in air and water and then substituted into the following two equations to obtain their densities:

$$R = \frac{a}{a - w}$$

$$\rho = R\rho_{\text{water}}$$

where a is the weight in air, w is the weight in water, and ρ is the sample density.

RESULTS AND DISCUSSION

Injection Molding

The separated polypropylene was easy to mold after debulking and grinding. The molding conditions were typical for an injection-molding grade of polypropylene. The edge trim required a higher barrel and nozzle temperature, 260°C, which led to some gas formation from degrading polymer. Higher injection temperatures led to severe degradation. The SBR latex in the edge trim was probably the source of this degradation. No molding trials were conducted

on polypropylene shear lint. The shear lint should be slightly easier to mold than the separated polypropylene due to its higher melt flow index (MFI).

The mechanical test results of the injection-molded samples are shown in Table 3. A significant difference was observed between injection-molded edge trim and separated polypropylene. Separated polypropylene samples have about two times higher tensile strength than edge trim samples. Its elongation at break (32%) is also much higher than that of the edge trim. Compared to typical virgin polypropylene, separated polypropylene has comparable mechanical properties, including tensile strength, tensile modulus, and Izod impact strength. However, its elongation at break (32%) is much lower than that of typical virgin polypropylenes (200–500%). The separated polypropylene still contains 2% impurities. Those impurities could be detrimental to the elongation at break, which is sensitive to such inhomogenieties in the polymer. The edge trim properties are typical of a filled grade of polypropylene, except for the low modulus. The calcium carbonate present should raise the modulus; however, the SBR present should lower the modulus. The net result is a slightly lower modulus compared to separated polypropylene.

In order to explain the mechanical property differences, the tensile fracture surfaces of the two carpet wastes were examined (Fig. 1). The edge trim waste is characterized by a highly inhomogeneous microstructure. Both phase separation and calcium carbonate filler are observed on the fracture surface. In contrast to edge trim waste, the separated PP has a much more homogeneous microstructure. Therefore, the low mechanical properties of edge trim, compared to those of separated PP, at least in part is attributed to this inhomogeneous microstructure.

The results in Table 3 confirm that injection molding is feasible for recycling the carpet waste and that there was not much degradation during mold-

TABLE 3
Mechanical Properties of Injection-Molded Samples

Materials	Edge trim	Separated polypropylene	Typical virgin polypropylene
Tensile strength (MPa)	17.9	30.3	29.0–38.6
(ksi)	(2.6)	(4.4)	(4.2–5.6)
Tensile modulus (GPa)	1.43	1.51	1.03–1.72
(ksi)	(207)[a]	(220)	(150–250)
Elongation at break (%)	9.4	32	200–500
Izod impact strength (J/m)	16	27	21–32
(ft.-lb./in.)	(0.3)	(0.5)	(0.4–0.6)

[a] Estimated without use of an extensometer.

(a)

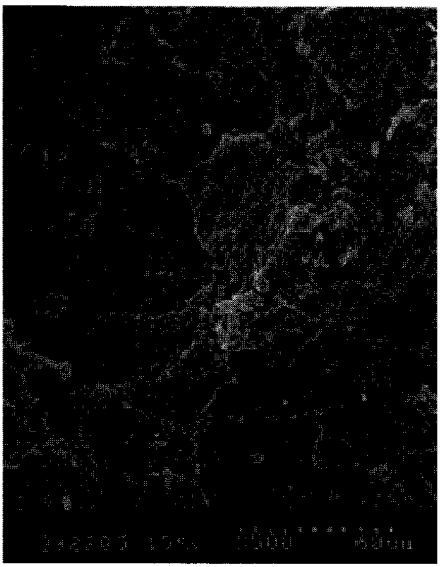

(b)

FIG. 1. Scanning electron micrographs of fracture surface of edge trim (a) and separated polypropylene (b).

ing for the conditions selected. Both of the two carpet wastes, especially separated polypropylene, have acceptable properties for many applications. Due to the high viscosity and thermal sensitivity of the edge trim, it is best suited for molding thick parts.

Compression Molding

The density measurements of the compression-molded GMT samples are shown in Table 4. Azdel PM 10400 is a continuous-strand fiber-reinforced polypropylene sheet manufactured by Azdel, Inc. and is presented here as an example of a GMT based on virgin polypropylene. The PM 10400 sheet is 3.7 mm thick and contains 40 wt.% glass. The GMT laminates prepared in this study contained nominally 40 wt.% glass; hence, the Azdel PM 10400 is a suitable reference for the mechanical testing.

As seen in Table 4, the density of GMT from edge trim is much greater than the densities of GMT from separated polypropylene, shear lint, or Azdel sheet. The edge trim contains high-density calcium carbonate. Based on the density for calcium carbonate of 2.85 g/cm^3, the GMT with edge trim contains approximately 21% calcium carbonate by weight.

The density provides an indication of the void content or degree of consolidation of the composite part. The theoretical density of completely consolidated 40 wt.% glass GMT is calculated to be 1.23 g/cm^3 (based on a density of 0.91 g/cm^3 for polypropylene and 2.58 g/cm^3 for glass fiber). Thus, the densities obtained in Table 4 imply that good consolidation was achieved using the separated polypropylene. The low density of the GMT from shear lint implies the presence of internal voids. The consolidation of the GMT from edge trim cannot be inferred solely from density measurements because the precise amount of calcium carbonate present is not known.

TABLE 4
Density Data of the Compression-Molded GMT from Carpet Waste

Samples	Density (g/cm^3)
GMT from edge trim	1.52
GMT from separated PP	1.18
GMT from shear lint	1.12
Azdel PM 10400	1.18

Note: All samples are nominally 40 wt.% glass.

TABLE 5
Tensile Properties of Compression-Molded GMT Samples Containing 40 wt.% Glass

Materials	Edge trim	Shear lint	Separated PP	Azdel PM 10400
Tensile strength (MPa)	109	84.1	95.8	95.2
(ksi)	(15.8)	(12.2)	(13.9)	(13.8)
Tensile modulus (GPa)	5.72	5.86	6.83	6.27
(msi)	(0.83)[a]	(0.85)	(0.99)	(0.91)

[a]Estimated without use of an extensometer.

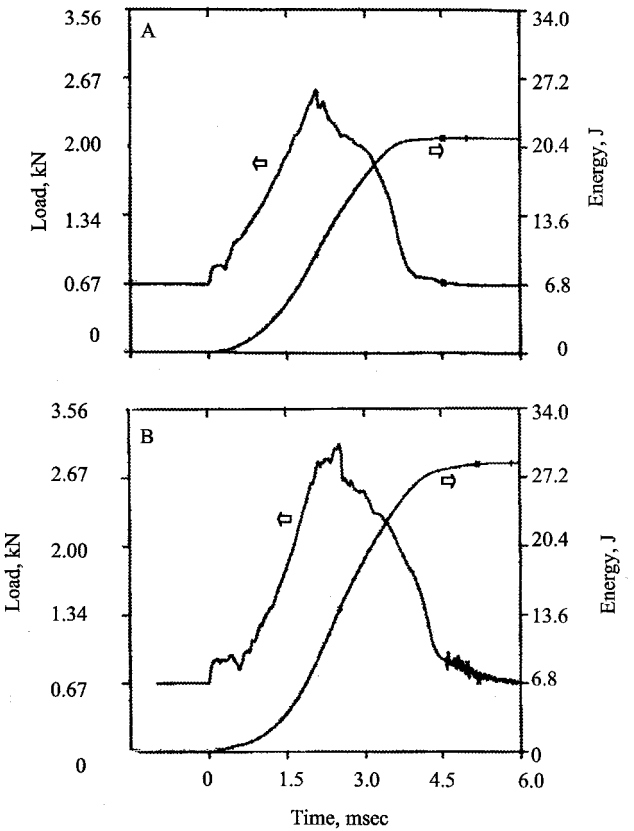

FIG. 2. Typical load and absorbed energy versus time curves generated in a Dynatup test of GMT from carpet waste and the molded Azdel: (A) GMT from edge trim; (B) GMT from separated polypropylene; (C) GMT from shear lint; (D) Azdel.

(continued)

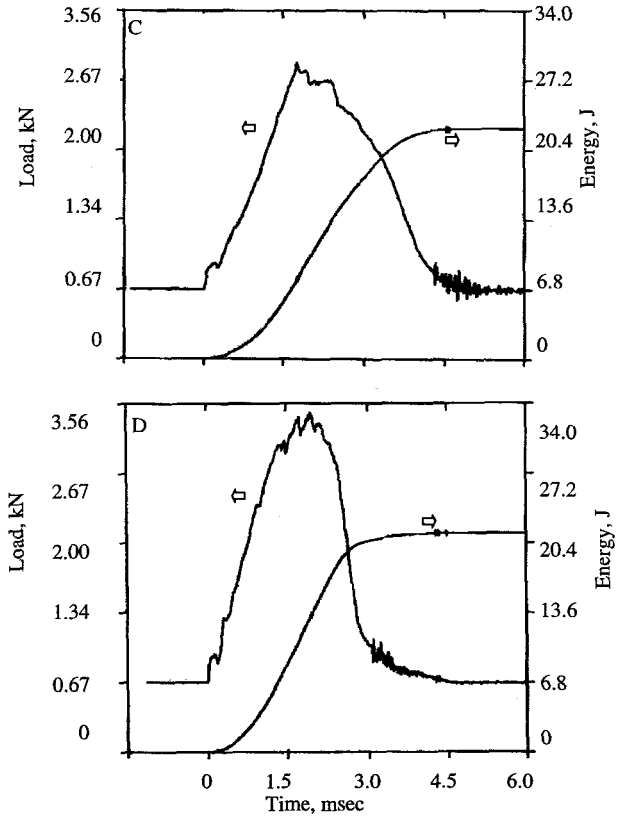

FIG. 2. Continued

The tensile properties of the GMT laminates are shown in Table 5. The GMT laminates from carpet waste all have tensile strengths and moduli similar to that of the Azdel product. The primary basis for this similarity is that the presence of the long glass fibers dominates the performance of these composites. Even a GMT with a heterogeneous matrixlike edge trim performs comparatively well.

One of the primary reasons for long-fiber-reinforced thermoplastic composites, including GMT, is their excellent impact resistance (7). This feature is one of GMT's advantages in automotive applications. In this study, special attention was given to the impact behavior of the GMT from carpet waste. The load and absorbed energy versus time curves generated in Dynatup impact testing GMT from carpet waste and Azdel 10400 are given in Fig. 2. All

four materials show a similar response, which is between ductile and brittle deformations (8,9). The impact dart produced a clean punch in each GMT (Fig. 3).

The impact resistance of a composite is determined by the total energy dissipated in the material before final fracture occurs. Good interfacial adhesion of matrix materials and reinforcements is required for the high-impact resistance. The total energy absorbed is generally selected to be the characteristic parameter to compare the impact resistance. These impact data are given in Table 6.

It is necessary to point out that the data are dependent on the sample thickness. Because energy is absorbed both by crack initiation and crack propaga-

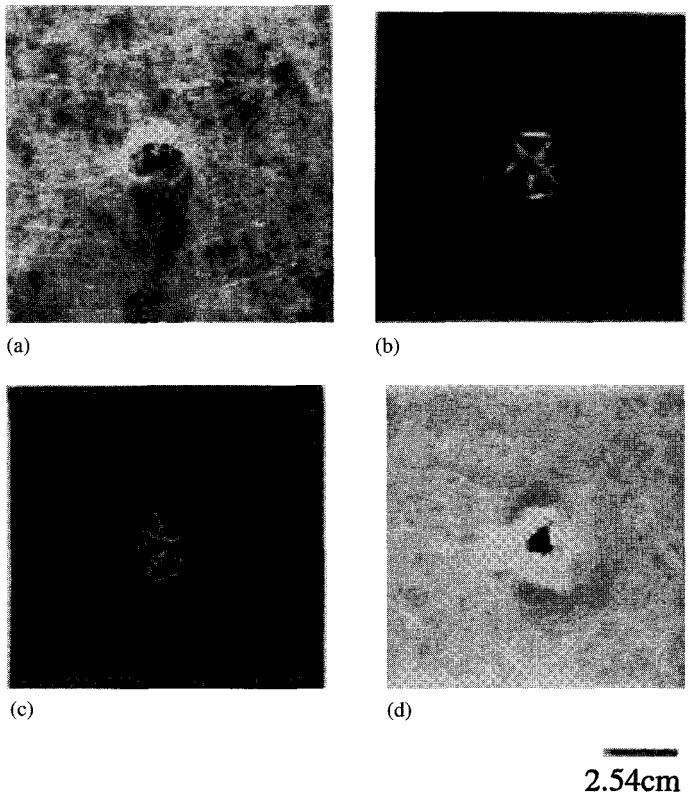

FIG. 3. Fracture surfaces of the impact tested GMT samples: (a) edge trim; (b) separated polypropylene; (c) shear lint; (d) Azdel.

TABLE 6
Impact Data of Compression-Molded GMT Samples Containing 40 wt.% Glass

Properties	GMT samples			
	GMT from edge trim	GMT from separated PP	GMT from shear lint	Molded Azdel
Maximum load, kN (lb.)	3.23 (725)	3.31 (745)	3.71 (835)	3.48 (783)
Deflection at max. load, mm (in.)	7.1 (0.28)	6.9 (0.27)	8.6 (0.34)	8.6 (0.34)
Total energy absorbed, J (ft.-lb.)	21.4 (15.8)	28.3 (20.9)	21.7 (16.0)	22.4 (16.5)
Sample thickness, mm (in.)	3.0 (0.12)	4.0 (0.158)	3.7 (0.145)	3.6 (0.14)

Note: Impact velocity 3.4 m/s (11.2 ft./s).

tion, the total energy absorbed cannot be normalized by the sample thickness. Because thicker samples should absorb more energy, the thickness of the laminates tested is reported in Table 6. Considering these thickness differences, it is concluded that GMT laminates from carpet waste have total energy absorptions comparable to the GMT from virgin polypropylene. Similar to the tensile properties, the presence of the long glass fibers in the GMT is more im-

TABLE 7
Effect of Glass Content on the Mechanical Properties of GMT from Shear Lint

Samples	Properties		
	Tensile strength, MPa (ksi)	Tensile modulus, GPa (ksi)	Impact strength, J (ft.-lb.)[a]
Shear lint, 0% glass	25.5 (3.7)	1.72 (250)	5.6 (4.1)
Shear lint, 20% glass	40.7 (5.9)	2.12 (310)	15.6 (11.5)
Shear lint, 30% glass	55.2 (8.0)	2.76 (400)	18.3 (13.5)
Shear lint, 40% glass	84.1 (12.2)	5.90 (855)	21.7 (16.0)

[a] Based on a thickness of 3.7 mm (0.145 in.).

portant than the purity of the matrix. Thus, long-fiber-reinforcement provides an attractive route for enhancing the properties of recycled thermoplastics. It remains to be determined what level of impurity can be successfully tolerated in reinforced recycled thermoplastics.

Because these thermoplastic waste streams are considerably less expensive than glass fiber and virgin polypropylene, a study was conducted on the effect of glass content on tensile and impact properties. These results for polypropylene shear lint are summarized in Table 7. It is evident that significant increases in all three properties are achieved with only 20 wt.% glass. The energy absorbed in drop impact testing increased dramatically for the 20 wt.% glass laminate compared to no reinforcement.

CONCLUSIONS

The following conclusions are drawn from this study:

1. The recycling of both production and postconsumer carpet waste by injection molding and compression molding has been successfully demonstrated.
2. The GMT from carpet waste has comparable mechanical properties to GMT from virgin polypropylene.
3. Significant improvements in the impact strength of shear lint samples are achieved by adding just 20 wt.% glass mat.

ACKNOWLEDGMENTS

The support of the Consortium on Competitiveness for the Apparel, Carpet and Textile Industries (CCACTI) is appreciated. The authors also wish to thank Advanced Textile Recycling, Dupont Co, Shaw Industries, and PPG for the carpet waste and glass mat samples, and to Dr. Ming Kao and Mr. Alan Kovicich for their help in impact testing at Johnson Controls.

REFERENCES

1. R. Otero, in *Conference on Recycling of Fibrous, Textile, and Carpet Waste,* Cartersville, GA, June 12–13, 1996.
2. H. Gardner, Carpet recycling technology, *Int. Fiber J.* 36 (August 1995).
3. Y. A. Gowayed, R. Valdyanathan, and M. El-halwagi, Synthesis of composite materials from waste fabrics and plastics, *J. Elastom. Plast., 27,* 79 (1995).

4. B. Holtkamp, Carpet waste recycling project launched, *High Perform. Textiles* (13 February 1996).
5. J. Muzzy, Patent pending.
6. M. Begemann and L. W. Stadlbauer, Isobaric long-fibre based GMT, *Kunstsoffe Plast. Eur* (May 1994).
7. D. M. Bigg, "Processing-property relationships for PET sheet composites, *Makromol. Chem., Macromol. Symp., 70/71,* 245 (1993).
8. H. I. Kau, A study of the impact behavior of chopped fiber reinforced composite, *Polym. Compos, 11*(5), 253 (1990).
9. T. L. Lin and B. Z. Jang, Fracture behavior of hydrid composites containing both short and continuous fibers, *Polym. Compos, 11*(5), 291 (1990).

POLYM.–PLAST. TECHNOL. ENG., 38(3), 499–511 (1999)

CONVERSION OF RECYCLED POLYMERS/FIBERS INTO MELT-BLOWN NONWOVENS

GAJANAN BHAT,* VASANTH NARAYANAN,†
LARRY WADSWORTH, and MAUREEN DEVER

Textiles and Nonwovens Development Center (TANDEC)
The University of Tennessee
Knoxville, Tennessee 37996

Abstract

Being a simple one-step process for converting polymer directly into a nonwoven fabric, melt blowing is ideally suited for processing of several recycled plastics. The process uses hot air to draw the fibers and does not require precise, individual control of each filament as in the conventional fiber-spinning processes. Recycled polypropylenes (PPs) from several sources were investigated as candidates for melt blowing. Waste from spun-bond line and spun-bond–melt-blown–spun-bond (SMS) fabrics were pelletized and then melt blown at our facility. The feasibility of using a melt-blowing line with an extruder gear pump unit to remelt the waste fibers/web and feed it with the molten virgin polymer stream coming from the main extruder was explored. A 1000 MFR virgin PP resin and fabrics produced from that polymer were used for this investigation. Fabrics were characterized in all the cases for their performance properties. Some of the relevant data are reported here. It was observed that in most of the cases, fabrics with good properties could be produced at high throughputs, thus demonstrating that most of the plant waste can be reused.

Key Words: Nonwovens; Melt blowing; Fibers; Polypropylene; Recycling.

* To whom correspondence should be sent.
† Present address: Techmer PM, #1 Quality Circle, Clinton, TN 37716.

INTRODUCTION

Being a simple one-step process for converting polymer directly into a nonwoven fabric, melt blowing is ideally suited for processing of several recycled plastics. The process uses hot air to draw the fibers and does not require precise, individual control of each filament as in the conventional fiber-spinning processes (1,2). In preliminary studies using a 508-mm (20-in.) melt-blown line at The University of Tennessee, Knoxville (UTK), two postconsumer recycled polyethylene terephthalates (PET), one industrial-waste copolyester, and a virgin PET were melt blown (3). Additional research utilizing the 508-mm Accurate Products melt-blown pilot line at Textiles and Nonwovens Development Center (TANDEC) at UTK demonstrated that recycled postconsumer PET can be processed into usable melt-blown webs. Compared with the virgin PET used, which was tailor-made to have a relatively low intrinsic viscosity (IV) for melt-blown processing, the recycled polymer had a higher IV, which may have been largely responsible for the larger average fiber diameters, larger pore size, and higher air-permeability values obtained (4).

Research was carried out to understand and improve the melt-blowing technology for recycled polyester and to determine the performance properties of the melt-blown nonwoven webs produced (5,6). In order to improve the melt-blown processing of the recycled PET, attempts were made to decrease the apparent viscosity of recycled PET during processing. Three alternate methods (viz. hydrolytic degradation, thermal degradation, and blending with other polymers) were investigated. Generally, the PET polymer must be intensively dried before it is processed, because of its high sensitivity to water at higher temperatures. The hydrolytic degradation that takes place in the presence of moisture and heat during processing, although considered unsuitable in most of the applications, helped in improving the melt-blowability by decreasing the melt viscosity of recycled PET. Alternatively, use of a higher processing temperature to reduce the melt viscosity was investigated.

Blending provides a straightforward, versatile, and relatively inexpensive method to develop new polymeric materials with superior combination of useful properties. Several researchers have studied the blending of PET and polybutylene terephthalate (PBT) polymers in processing and the results have shown that the system behaves as a compatible polymer pair and can serve as a good guide to solve practical problems (7–9). Apparently, significant improvement in properties of PET fiber could be achieved by blending with PBT. Low-molecular-weight PET was also used to blend with recycled PET to decrease the viscosity during processing.

It was shown that recycled polypropylenes of different grades could be melt blown as long as they were fairly clean (10). In those cases, having the

appropriate viscosity grades for the melt-blowing process was important so that fabrics with good performance properties could be produced. For melt blowing, a process where drawdown takes place due to low melt viscosity of the polymer, with no positive takeup mechanism as in a typical fiber-spinning process, higher melt-flow-rate (MFR) resins process better, resulting in fine fiber webs.

The waste coming from a spun-bond (SB) line and spun-bond–melt-blown–spun-bond (SMS) lines are different because of significantly different melt flow rates. It was important to actually process these reclaimed fibers and evaluate the melt-blown fabrics produced from them. Another objective of this work was to investigate the feasibility of using the J and M line in conjunction with the extruder gear pump (EG) unit to remelt the waste web and feed it with the molten virgin polymer stream coming from the 63.5-mm extruder on that line. If this technique could be shown to work effectively, it would be an ideal system to recycle the inplant fabric waste. As there is increased interest by the industry into melt-blowing 1000 MFR and higher melt-flow-rate resins, it was decided that the feasibility of processing and recycling this grade of PP be investigated.

EXPERIMENTAL PROCEDURE

Materials

The materials used in the study are listed in Table 1. All of these are industrial wastes only, not postconsumer. Both the SB and SMS reclaimed fabric were pelletized at Stevens Technical Institute, Brooklyn, NY. Standard conditions suggested by the ASTM D-1238 method were used to determine the MFR of all the samples using the Tinius Olsen melt indexer. The MFR of the pellets are shown in Table 1. For the nominal 1000 MFR PP, the actual MFR of reclaimed fiber could not be determined, as it was higher than the range that could be measured using the Tinius Olsen melt indexer.

TABLE 1
Polypropylenes Used in This Study

	MFR
Recycled SB fabric (pelletized)	48
Recycled SMS fabric (pelletized)	118
Virgin PP	1000
Melt-blown fabric from 1000 MFR resin	—

Processing

The first series of melt-blowing trials were performed on the Accurate Products 508-mm- (20-in.) wide melt-blowing pilot line (Fig. 1) at TANDEC. The line consists of a 50.8-mm extruder with 30/1 length/diameter (*L/D*), screen changer, metering pump, and a horizontal die with 501 holes with individual diameters of 0.4 mm. Hot air is supplied by a rotary-screw air compressor, which has a maximum capacity of 18.4 m^3/min and a furnace for heating the air. The processing conditions used for both the polymers are given in Table 2. The processing temperatures were higher than those typically used for PP polymers. Because the viscosities of these polymers with relatively low MFR were higher for melt blowing, higher temperatures had to be used to achieve some degradation and lowering of melt viscosity. In all these trials, efforts were made to adjust the collector speed to achieve web basis weights of 35 g/m^2 (1.0 oz./yd^2).

Studies with 1000 MFR PP were conducted using the J and M melt-blowing line at TANDEC consisting of a Davis-Standard (Pawcatuck, CT, U.S.A.) 63.5-mm extruder for melting the polymer, metering system, melt transport to the die, melt-blowing die (vertical), the hot-air supply (compressor was used in this work instead of the blower because of the higher operating air pressure), and the winding system for collecting the web. In addition to the extruder, there exists an extruder gear pump system for melting and pumping of the polymer. The extruder gear pump melt systems process a polymer utilizing the "progressive melt theory," which means that the polymer is heated gradually through various stages of heat zones. Once the polymer is placed in the hopper or premelt section, it contacts heated grids at the bottom. The molten material flows to the main melt zone by gravitational feed, where

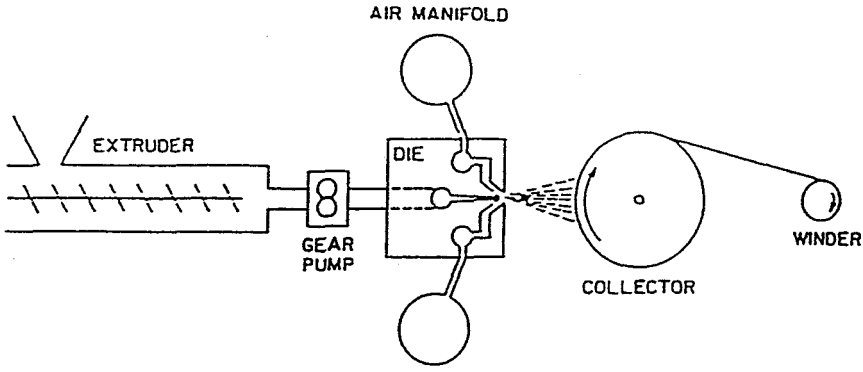

FIG. 1. The Accurate Products melt-blowing pilot line at TANDEC (horizontal die).

TABLE 2
Processing Conditions Used for Melt-Blowing of PP (Accurate Products line)

	Recycled polymers	
	SMS (118 MFR)	SB (48 MFR)
Polymer throughout (g/hole/min)	0.4	0.4
Die temperature (°C)	327	331
Air temperature (°C)	305	299
Air flow (m^3/min)	9.4	9.4
Die-to-collector distance (cm)	30	35

the temperature is further elevated. From the main melt, the molten material is fed to a precision gear pump by an auger screw. The melt is then metered, pressurized, and filtered before entering the transfer hose.

Although the extruder gear pump system was designed as a stand-alone system for melting of adhesives for melt blowing, the UTK system is designed such that the polymer melt from the extruder gear pump unit can be fed into the melt stream of the extruder at the final mixing zone (Fig. 2). This enables one to use either the extruder or extruder gear pump unit, or the combination

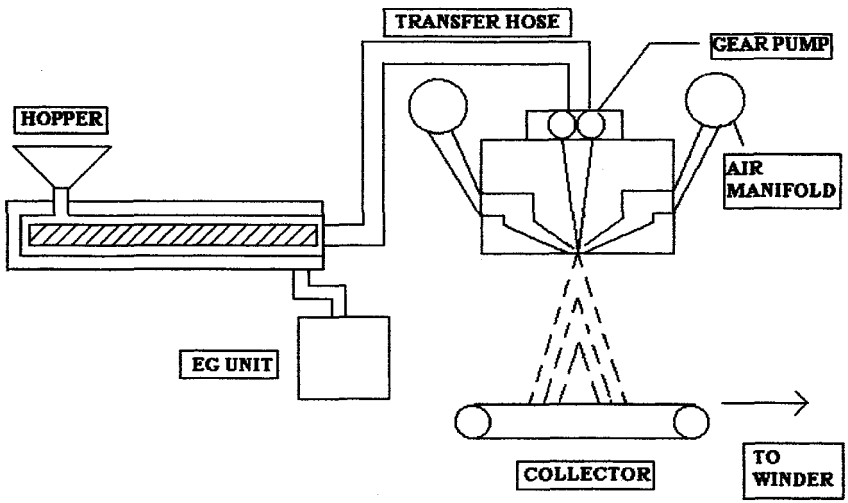

FIG. 2. The J and M melt-blowing pilot line at TANDEC with the extruder gear pump unit (vertical die).

TABLE 3
Processing Conditions for 1000 MFR PP (J and M Line)

Sample No.	Sample identification[a]
1	Virgin PP in extruder
2	Fabric (1000 MFR) in extruder gear pump
3	50/50, Resin/fabric
4	75/25, Resin/fabric

[a] Processing conditions for the samples were as follows: throughput: 0.8 g/hole/min; extruder gear pump temperature: 246°C; melt temperature: 268°C; melt pressure: 0.3 MPa; air temperature: 243°C; air flow: 9.6 m^3/min; die-to-collector distance: 254 mm.

of the two in feeding the molten polymer to the die. In the current project, the feasibility of using both the units, with the extruder gear pump unit as a supplier of the recycled material to the virgin polymer melted by the extruder, was investigated. The processing conditions used are summarized in Table 3. Efforts were made to produce webs of about 35 g/m^2 (1 oz./yd^2).

Determination of Web Properties

The standard tests performed to evaluate the physical properties of the melt-blown webs are listed in Table 4, with their corresponding ASTM methods.

TABLE 4
Test Methods for Physical Properties of Melt-Blown Web

Property measured	Standard method
Basis weight	ASTM D 3776-85
Thickness	ASTM D 1777-64
Air permeability	ASTM D 737-75
Bursting strength	ASTM D 3787-80A
Stiffness	ASTM D 1388-64
Pore size	ASTM F 316-86
Melt flow rate	ASTM D-1238
Tenacity and elongation to break	Tensile testing
Fiber diameter	Electron microscopy
Filtration efficiency	Filtration tester

Tests performed that did not have a corresponding ASTM method are described below.

The diameters of the fibers were measured from high-resolution scanning electron microscopic (SEM) photographs obtained from different areas of the webs using a Hitachi (Gaithersburg, MD, U.S.A.) S-800 model instrument. The webs were coated with between 2 and 5 nm of chromium, deposited by Baltech MS-12 ultrahigh-vacuum ion beam sputter coater. Chromium is used to both minimize charging and to enhance the image contrast. Five photomicrographs were taken for each web. The magnifications used ranged from 300 to 600 times. The reported fiber diameter values represent an average of 50 such measurements. For some of the samples, diameter values were obtained from the pressure drop during filtration testing using an aerosol of 0.1 μm NaCl at a velocity of 5 cm/s, instead of using SEM photographs. This method has been shown to correlate well with fiber diameters obtained from SEM photographs (11). Filtration efficiency was determined using the automated TSI (St. Paul, MN, U.S.A.) Model 8110 tester. Tests were carried out with 0.1-μm NaCl particles at different face velocities.

The tensile properties of the fabrics were determined by testing 25.4-mm-wide, 254-mm-long samples in a United (Huntington Beach, CA, U.S.A.) tensile tester (Model SSTM-1-E-PC). A gauge length of 127 mm with an elongation rate of 127 mm/min was used for the study according to ASTM D1117-80. An average of five readings is reported for each sample tested. The elongation at maximum load is reported as the breaking elongation. The shot rating was done using the comparative standard photographs developed at TANDEC at UTK. A rating of 0.5 indicates minimum shots and a rating of 5.0, highest among the samples. The rating was given by looking at the overall surface of the web and the standard photograph side by side under standard lighting.

RESULTS AND DISCUSSION

SB and SMS Fabrics

The properties of the melt-blown fabrics produced from both reclaimed SB and SMS are shown in Table 5. Both fabrics were of almost the same basis weight. The thickness of the SMS fabrics was slightly higher; indicating the differences in the densities of these fabrics. This higher thickness may also be due to the larger-diameter fibers in them. Although the SMS material resulted in a relatively larger diameter, both samples had fiber diameters close to 3 μm. which is very good. Air permeability and tenacity are comparable for both sets. The machine-direction breaking elongation is lower for melt-blown nonwovens from SMS and shows higher stiffness values as well. These properties are due to the lower molecular weights of the material as seen by higher MFR values.

TABLE 5
Properties of Melt-Blown Webs Produced from Recycled SMS and SB Polypropylene Nonwovens

Properties	SMS[a]	SB
Basis weight (g/m^2)	36.7	36.6
Thickness (μm)	357.0	331.0
Fiber diameter (μm)	3.3	2.7
Air permeability ($m^3/s/m^2$)	0.5	0.5
MD[b] tenacity (mN/tex)	15.6	15.5
CD[b] tenacity (mN/tex)	8.3	9.8
MD elongation to break (%)	19.0	33.0
CD elongation to break (%)	76.0	45.0
MD stiffness (mg cm)	414.0	370.0
CD stiffness (mg cm)	205.0	166.0
Bursting strength (kPa)	57.0	55.0

[a] Experimental SMS (without repellent finish).
[b] MD = machine direction; CD = cross direction.

Not only were the MFR values of the starting material for SMS higher (118 compared to 48 for SB), the MFR value of the melt-blown fabrics was also higher (352 for SMS and 266 for SB). From the MFR values of the melt-blown fabrics, it becomes clear that the values are still in the range that can be used for melt blowing. In fact, these fabrics can be pelletized and melt blown at least one more time, as the current resins used in melt-blown applications have MFR values in the range of 800 or higher. Another observation is that higher processing temperatures had to be used for these samples because of their very high molecular weight and correspondingly higher melt viscosity. On the other hand, a higher-MFR polymer has an advantage that the material can be processed at a much lower temperature to achieve samples with comparable fiber diameter and corresponding performance properties.

1000 MFR Polymer

The virgin polymer was fed into the extruder, whereas the recycled webs were fed into the EG unit. The results are summarized in Table 6. The basis weight and thickness of the webs collected with different compositions (100/0, 50/50, 75/25, 0/100, virgin/recycled) were almost the same in all the cases. The fiber diameter was marginally higher in the case of blends compared to 100% virgin or recycled material. Nevertheless, the fiber diameters achieved were low enough to produce high-quality webs. For samples produced from blends of

TABLE 6
Physical Properties of Melt-Blown Webs Produced from 1000 MFR PP

Sample ID[a]	Basis weight (g/m^2)	Thickness (μm)	Air permeability ($m^3/s/m^2$)	Fiber diam. (μm)	Tenacity (mN/tex)		Elongation (%)		Stiffness (mg cm)		Bursting strength (kPa)
					MD	CD	MD	CD	MD	CD	
1	36.0	379	0.24	1.85	8.6	3.7	2.5	4.2	313	124	13.8
2	33.9	382	0.40	2.10	7.3	2.6	1.8	2.9	186	111	11.1
3	35.3	370	0.56	2.57	7.4	2.8	1.7	2.3	344	179	12.4
4	34.6	347	0.51	2.47	8.0	3.1	1.7	2.1	337	205	13.1

[a] Sample numbers correspond to those identified in Table 3.

virgin and recycled-material fiber diameters were slightly higher with a wider scattering of data points. This is probably due to the degradation of the polymer and change in molecular-weight distribution. Also, at the throughputs that were used, there is very little time for complete mixing of the two streams of melt and this incomplete blending can have some inherent variability that leads to property variations in the fiber and the web.

As can be seen from Figs. 3 and 4, lower fiber diameter values in the webs were accompanied by correspondingly smaller pore size and higher filtration efficiency. All these properties are expected, as they are very much dependent on the fiber diameter. The effect of reprocessing is seen in lower stiffness (Table 6) and higher shot rating (Fig. 5) of the 100% recycled webs compared to that of 100% virgin, and webs made of blends of recycled and virgin PP. Tensile properties indicate that the addition of recycled content into the polymer stream reduces tenacity only slightly. The breaking elongation (Table 6) of the webs produced from recycled polymers is slightly lower. The webs are more brittle compared to the SMS and SB polymers, which is the expected result because of lower-molecular-weight material and having recycled content contributes to only a slight increase in brittleness.

Overall tensile properties of the 1000 MFR polymers are much poorer compared to that of the SMS and SB fabrics. This is obviously due to the lower molecular weights of the polymer as the differences between 50–100 MFR and 1000 MFR lead to large differences in melt viscocities. However, the ad-

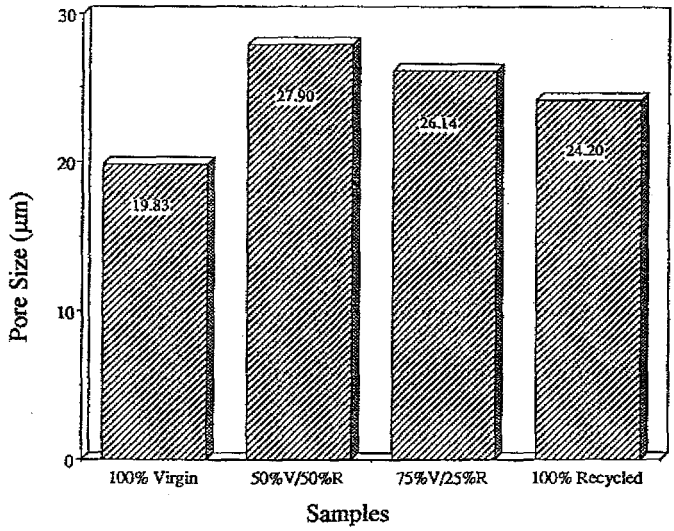

FIG. 3. Pore size of 1000 MFR melt-blown webs.

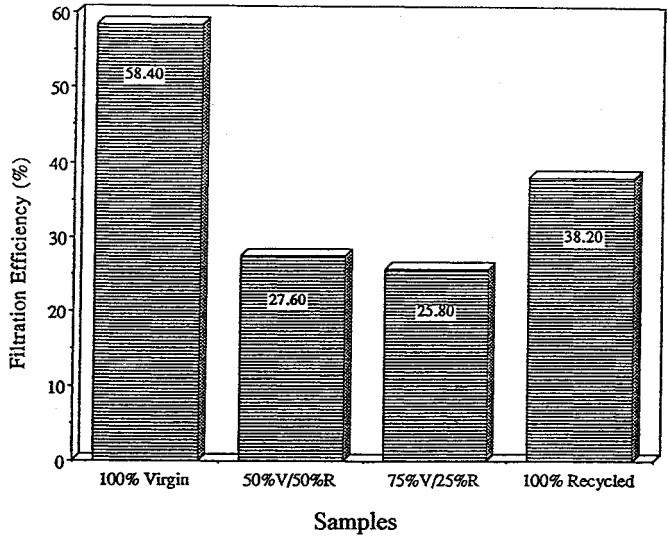

FIG. 4. Filtration efficiency of 1000 MFR melt-blown webs.

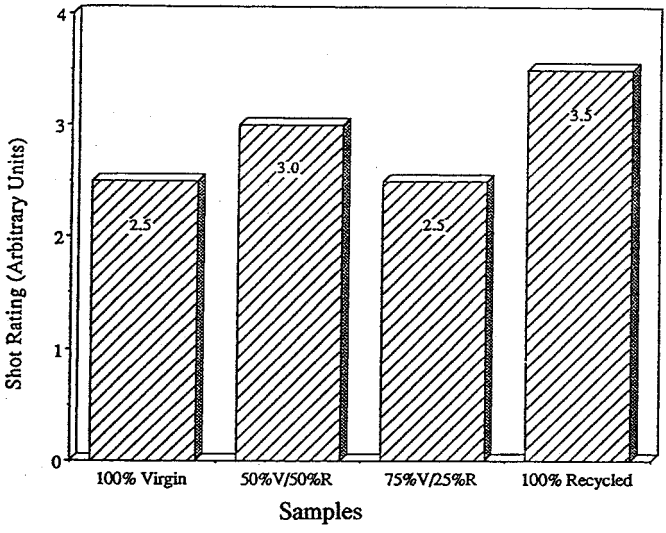

FIG. 5. Shot rating of different melt-blown fabrics.

vantages of higher melt flow rates are in lower processing temperatures and significant reduction in energy consumption, as it has been shown that with increase in processing temperature, energy used goes up, which is the significant portion of the processing cost (12). When using the EG unit, the dwell time is much higher than in an extruder, and as the melting has to take place with no shear, there is an opportunity for an increase in degradation and molecular-weight distribution. This can have some detrimental affect on the properties of the webs.

SUMMARY

Waste from both SB and SMS fabrics, which were reclaimed and then pelletized, could be melt blown successfully to produce quality webs with properties comparable to that from virgin polymers. The results have shown that the extruder gear pump unit can be used to blend recycled materials into the virgin polymer stream. Although slight differences in properties of the web were observed, it should be noted that the amount of recycled content was considerably high. In reality, there is no need to blend more than 10–25% of recycled material. Furthermore, even though the webs with high recycled content were slightly weaker, they were softer and may be better for some products.

ACKNOWLEDGMENT

The authors would like to acknowledge the financial support from the Consortium for Recycled Polymers, consisting of Exxon Chemical Company, Fiber Industries, Far Eastern Textile Ltd., Fiberweb, Inc., and Veratec.

REFERENCES

1. S. R. Malkan and L. C. Wadsworth, *Int. Textiles Bull.: Nonwovens, 37*(2), 46–52 (1991).
2. S. R. Malkan and L. C. Wadsworth, *Int. Textiles Bull.: Nonwovens, 37*(3), 22–28 (1991).
3. L. C. Wadsworth, M. Dever, and S. R. Malkan, in *Proceedings of the TAPPI Nonwovens Conference,* 1990, pp. 1–24.
4. M. Dever, L. C. Wadsworth, and C. Y. Lee, *INDA J. Nonwovens Res., 3*(1), 19–24 (1991).
5. G. S. Bhat, Y. Zhang, M. Dever, and L. C. Wadsworth, *INDA J. Nonwovens Res., 6*(3), 54–61 (1994).
6. Y. Zhang, M. S. thesis, The University of Tennessee, Knoxville, 1992.

7. S. P. Misra and B. L. Deopura, *Rheol. Acta, 23,* 189–194 (1984).
8. E. Bourdeaux, Jr. and J. A. Cuculo, *J. Appl. Polym. Sci., 27,* 301–318 (1982).
9. S. P. Misra and B. L. Deopura, *J. Appl. Polym. Sci., 33,* 759–768 (1987).
10. G. S. Bhat, V. Narayanan, L. C. Wadsworth, and M. Dever, in *Proceedings of the 2nd Annual Conference on Recycling of Fibers, Textile and Carpet Waste,* 1997.
11. P. Tsai and L. C. Wadsworth, in *Proceedings of the Third Annual TANDEC Conference,* 1993.
12. M. W. Milligan, L. C. Wadsworth, and C. Y. Cheng, in *Proceedings of the INDA–TEC 89 Conference,* 1989.

POLYM.–PLAST. TECHNOL. ENG., 38(3), 513–531 (1999)

WOODLIKE PROPERTIES FROM CARPET AND TEXTILE FIBROUS WASTE: MITIGATING THE COMING LANDFILL CRISIS

ABRAHAM M. KOTLIAR

School of Textile and Fiber Engineering
Georgia Institute of Technology
Atlanta, Georgia 30332-0295

Abstract

Large-volume usage of textile and carpet fibrous waste may be achieved with a low-cost material that has woodlike properties. Formulations and properties of composites, laminates, and honeycomb sandwich constructions made from carpet and textile fibrous waste in a high-modulus phenol formaldehyde matrix are described. Using design parameters based on the mechanics of bending beams and the moduli of the fibrous component materials, one can achieve apparent bending moduli of 1 million psi (6.9 GPa) and bending strengths of 10,000 psi (69 MPa). To achieve these woodlike properties, it is best to use waste carpet material in the core and higher-modulus textile materials such as cotton and polyester in the outer layers. About 20 wt.% phenolic resin is suggested for the matrix component.

Key Words: Recycle; Waste carpet; Waste textile; Phenolic resins; Composites; Laminates; Honeycomb.

INTRODUCTION

Limited landfill capacity and an increase in the environmental awareness and government regulations have spurred efforts for the recycling of postcon-

sumer and postindustrial synthetic and natural polymeric materials. These waste polymeric fibrous materials contain about 8 billion pounds of waste (1), primarily cotton, polyester, nylon, and polypropylene. The sources of these postconsumer and postindustrial fibers come from textiles and carpets; for example, in the making of garments, about 10–15% of the fabrics are cutting waste, about 2 billion pounds per year (2). Of these 2 billion pounds, about 1.2 billion pounds are currently being recycled (2). Also, a significant amount of the 2.5 billion pounds of clothing donated to charities are landfill (2). These waste fabrics are primarily composed of cotton, polyester, and cotton–polyester fiber blends. Another large source of waste fibers comes from the carpet industry. About 6 billion pounds of carpet is produced annually in the United States. This material starts showing up as waste in landfills after about 7 years. There is also some 40 million pounds of waste carpet ends (carpet selvage) produced annually in the manufacture of carpets (3), and this constitutes a very serious environmental issue in Dalton, Georgia.

Fabric materials are made of natural fibers (e.g., cotton, wool, and silk) as well as synthetics (e.g., polyester, nylons, acrylics, and polypropylene). These materials are very often composed of blended yarns and fibers (i.e., polyester and cotton). To make these fabrics more attractive, they are almost always dyed in a variety of colors and may contain a variety of surface additives as well as TiO_2 as a delusterant. Because of the variable colors and fiber composition, only a limited use can be found for these waste materials. However this waste is produced at a very limited number of manufacturing sites, making collection a simpler task compared to the collecting from the general public. This material is also clean and can be readily shipped to central processing centers without special handling. Those fabric materials donated to charities are also generally clean and collected from a limited number of sites.

The other very large source of waste fibers is from waste carpets. Typical conventional carpeting includes three primary components:

1. A face yarn that generally consists of nylon 6 or nylon 66 fibers with smaller amounts of polyester, polypropylene, acrylics, wool, and cotton fibers.
2. A carpet packing that is generally made of polypropylene fibers with a much smaller amount of jute fibers.
3. An adhesive material (usually styrene–butadiene rubber) applied as a latex and cured after application. The adhesive is usually filled with an inorganic material such as calcium carbonate.

These typical carpet constructions are well known in the industry and are exemplified in U.S. Patent 4,643,9030.

The diverse chemical structure of waste fibers from textiles and carpets generally precludes the melt processing of the incompatible fiber components.

This makes economical use of this material a particularly difficult technological challenge. Previous efforts for disposing waste textile and home furnishing fiber materials by individuals and corporations have relied on the following:

1. Placing the material in landfills
2. Burning fibrous waste in massive incinerators
3. Separating the components by their density followed by depolymerization to recover the monomers of the polyamides (4–6).
4. The use of supercritical fluids such as CO_2 to dissolve the fibers followed by precipitation (7)
5. Melt extruding the unseparated carpet components into a polyblend composite, which is described in U.S. Patent 5,294,384.

The above processes have not been satisfactory from either environmental or economic points of view, whereas the melt-extruded polyblends have particularly weak interfacial adhesions between the incompatible blend components. This does not produce a very satisfactory product without the use of expensive compatabilizers required to improve the interfacial adhesion. The use of melt-blended carpet materials as the dispersed phase in a virgin nylon or polypropylene matrix does not appear to have been developed. Natural fibers cannot be melt blended with nylon or polyesters because the required high melt temperatures cause extensive degradation.

Our approach to recycling of fibrous waste textiles and carpets is to shred the fabrics to their individual fibers, yarns, and small fiber bundles and coat the mixed but unsegregated fiber components and cured latex particles with a low-viscosity structural adhesive. The precursor structural adhesive can also be present as a low-melting solid that on melting has a low viscosity, about 10 P, which allows the coating of the fine fibers and penetration into fiber bundles. The mixture, which may contain one or more components consisting of coated fibers, yarns, fiber bundles, and fabric bits is then heated under applied pressure to effect a cure of the matrix coating. The polypropylene fibers that may be present in the waste fibrous mixture may be processed in either a melted or unmelted form, depending on the molding temperature selected. Because the polypropylene fiber component does not strongly adhere to structural adhesives, the weight ratio of this fiber component to the strongly adherent fibers, such as nylon, polyester, acrylics, cotton, wool, and silk, will significantly affect the mechanical strength of the composite for a given amount of structural adhesive and curing conditions. The presence of the polypropylene when melted during the curing conditions does provide for viscous flow during the processing step. This fluidity can be particularly important if an extrusion procedure is used in the composite manufacturing. The cured composite can be used as a wood or metal substitute in applications such

as subflooring, roofing materials, house siding, pallets, strand board, supports for outdoor signs, and railings, and in outdoor applications where wood and metal are currently used in transportation and road construction.

MECHANICAL ANALYSIS (8–11)

To act as a wood or metal substitute, we require rigid structures. To a good approximation, the bending modulus of a composite is given by

$$M_{\text{total}} = \sum_i V_i M_i \tag{1}$$

where M_i is the bending modulus of the ith component, V_i is the volume fraction of the ith component, and M_{tot} is the resulting bending modulus.

Table 1 lists the modulus of phenol formaldehyde, carpet fiber components, and textile fibers used in this study. We note that cotton fibers have the highest modulus of about 1.2 million psi (8.3 GPa), followed by oriented polyester fibers. [With synthetic fibers, the modulus is, of course, dependent on the extent of orientation. The values for the moduli for carpet and textile applications are significantly lower than those for industrial applications (e.g., tire cord).] Because our current equipment does not have pressure cycle capabilities, we require some polypropylene to be present to provide the necessary viscous flow during the molding process to transfer the pressure from the composite to spacers. This is necessary to release the steam produced. This high-pressure steam can cause blowouts in the molding if not released. The presence of this high-pressure steam will undoubtedly relax some of the orientation and reduce the effective modulus of the fibers in the composite. Because of the poor bonding of polypropylene to the high-modulus matrix adhe-

TABLE 1
The Bending Modulus (GPa) of Components Used in Study

Component	Molded	Oriented
Cotton		8.3
Wood		6.9
Polyester	2.4	6.9
Polypropylene	1.4	6.9
Nylon	1.6	3.0
Phenol formaldehyde		6.9

Source: Ref. 12.

sive, we consider the polypropylene phase a nonreinforcing filler and assume its contribution to the strength and modulus is small.

For a three-point flexural loading configuration, the flexural modulus (E_B) is given by

$$E_B = \frac{L^3 m}{4bd^3} \tag{2}$$

where L is the support span, b is the width of the beam, d is the depth of the beam, and m is the slope of the tangent to the initial straight-line portion of the load deflection curve.

The flexural rigidity of a rectangular isotropic beam is given by

$$\text{Rigidty} = \frac{Ebd^3}{12} \tag{3}$$

Equation (3) shows that the rigidity of the beam is determined by the modulus of the material for a given set of dimensions.

To improve the rigidity of the composite, a laminate structure can be used, where the core contains the coated waste carpet components, primarily carpet selvage, and the outer layers contain the higher-modulus fibers such as cotton, polyester, and polyester cotton fiber blends (polycotton). This can be seen from the rigidity equations of a sandwich beam with faces of equal thickness:

$$R_{\text{laminate}} = \left(\frac{E_f bt^3}{6}\right) + \left(\frac{E_c bc^3}{12}\right) + \left(\frac{E_f btd^2}{2}\right) \tag{4}$$

where E_f is the modulus of the face layer, E_c is the modulus of the core, b is the width of the beam, c is the core thickness, d is the distance between centriods of the faces, and t is the face thickness. The first and second terms describe the bending stiffness of the faces and core about their centroids. These terms give the stiffness of the beam if the faces were not bonded to the core. The third term is generally the largest because t is usually small for weight reasons and $td^2 \gg t^3$. E_c need not be small with respect to E_f, but because $td^3/2$ is usually much larger than $c^3/12$, again for weight reasons, it makes more sense to put the higher-modulus fibers in the face layer and use the lower-modulus fibers that do not bind strongly to the matrix (e.g., polypropylene) in the core. Equation (4) also points out the importance of interfacial strength between the core and the face because the last term for bonded sandwich beams almost always has, by far, the largest value. With paper honeycombs coated with a phenolic resin, the last term contributes well over 95% of the stiffness (8). This is not always the case with laminates made of waste fibers, where the core can contribute 10–20% to the overall rigidity.

On bending, there is always some contribution to the overall deformation due to the shear deformation of the core, particularly with paper honeycombs. This can give low rigidity values to a test piece compared to that predicted by Eq. (4). This is recognized in the ASTM C393 procedure "Flexural Properties of Sandwich Constructions." Here, both the bending and shear displacements as a function of the applied force are specified. Because the face layers have little shear component, we need only consider the shear component of the core. The stiffness of the sample, P/D, is given by the force (P) versus displacement (D) correlation for three-point bending with thin faces:

$$\frac{D}{P} = \left(\frac{l^3}{24E_f btc^2}\right) + \left(\frac{l}{4bcG_c}\right) \tag{5}$$

Here, G_c is the shear modulus of the core. To make the stiffness large, one makes the width of the beam (b), face thickness (t), and core thickness (c) large while keeping the length of the span (l) short. To minimize the shear component, one makes the length of the span (l) short and the core thickness (c) large. For many applications, one looks for the maximum in the stiffness or strength for a minimum in weight as the selection criteria.

With laboratory testing, one has to be aware that the shear component of the honeycomb core is very significant because of sample size restrictions. This shear displacement reduces the apparent modulus on bending using the force–displacement data. For design work, it is therefore best to measure the bending modulus of the face layers independently using Eq. (1) and then calculate the rigidity of the honeycomb using Eq. (4). Measurement of the force–displacement of the product is always desirable. One can also measure the shear modulus of the honeycomb using ASTM C273 and calculate the force-displacement for the product using Eq. (5). One can also, in principle, evaluate Eq. (5) by measuring the force–displacement of the test sample as a function of length and determine G_c and E_f. Unfortunately, the range of lengths available in the three-point bending apparatus used in this study is quite limited, about 2–5 in. (5–13 cm), and does not permit an accurate evaluation.

EXPERIMENT

Fibrous carpet waste was obtained from shredded carpet selvage or carpet samples. Fibrous textile waste was obtained from shredded cotton socks and polycotton (polyester cotton) fabrics. Wood fibers, about 3 mm long, were obtained from unidentified shredded hardwoods. The fibrous material was then spray-coated with the desired amount of phenol formaldehyde resin, either of the resole or novalac type, and cured in a press under 500 psi (3.4 MPa) and

generally at 195°C. The length of time depended on the plaque thickness. A typical 0.2-in. (0.25-cm) thickness required 20 min. Because our 18-in. × 18-in. (0.46-m × 0.46-m) press did not have the means to control the pressure as a function of time, the use of spacers was found advantageous. As the polypropylene component melted, the pressure was transferred to the spacers, allowing volatile components, primarily water, to be vented. This prevented the occurrence of "blowouts." The hot cured material was then cooled in an adjoining cold press to prevent warpage. Mold release paper was used to prevent sticking to the platens. In joining the cured outer layers to the phenolic-resin-coated paper honeycomb core, it was necessary to sand the surfaces to remove the silicone residue. The same phenolic resin used to coat the fibrous material in the outer layers was used as an adhesive between the core and the outer layers. The sandwich construction was then cured at 190°C for 10 min under a pressure of 50 psi (0.34 MPa).

The flexural properties of the molded samples were determined using ASTM D 790-95a. A 1-in.- (2.5-cm) wide specimen on 4-in. (10.2-cm) supports with a center deflection was generally used in this test. A displacement speed of 0.21 in. (5.3 mm) per minute was used. Flexural testing of honeycomb sandwich laminates used ASTM C 393. Water absorption testing used ASTM D 570 and density measurements used ASTM D 792. The impact strength was evaluated using a falling weight test, ASTM D 3029. A 1.78-kg tub was used.

RESULTS AND DISCUSSION

The primary properties for our targeted applications are flexural properties, water absorption, dimensional changes after soaking in water, impact properties, and creep under load. The flexural properties are dependent on the structure and composition used, particularly the composition of the layers and distance of these layers from the neutral axis of the test piece. In our work, we have used essentially symmetrical structures so that the neutral axis is located near the center of the test specimen. This condition can be relaxed for some applications where one surface may contain more structural adhesive and/or high-modulus fibers. This type of structure will move the neutral axis closer to the higher-modulus fibrous surface and thereby act to lower the contribution of the outer layers to the rigidity of the product.

The structures that we employed are as follows:

1. A composite where the fibrous components are mixed and all the components are coated with the low-viscosity (less than about 30 P) prepolymers of phenol formaldehyde that are usually in a water base. The particular test material is then molded under an initial pressure of 500 psi (3.4 MPa) and at about 195°C for 20 min.

2. Type "A" laminates, where the carpets are laid back to back and only the face yarns are coated with the structural adhesive. Additional layers of coated high-modulus waste fibers and/or wood fibers can be added. To improve the interfacial strength of the backing to face yarn, 3-mm- (1/8-in.) diameter holes on 1/2-in. (1.3-cm) centers or smaller are made in the backing to allow penetration of the uncured resin into the backing. These protrusions of the resin in the backing form strong anchor points with the face yarn layer during curing.
3. Type "B" laminate, where coated shredded fibrous wastes are used as the core with coated higher-modulus fibers (e.g., cotton, flax, and wood) as the outer layers.
4. A honeycomb sandwich structure having a resin-coated (usually a phenolic resin) paper core with outer layers made of a composite, type "A" laminate, or type "B" laminate structure.

The bending moduli of the fibrous waste and whether they adhere to the phenolic resin matrix are very important to their placement. Polypropylene fibers, which are melted in the curing cycle, have a flexural modulus of about 200,000 psi (1.4 GPa). Because these fibers do not adhere well to the matrix, the polypropylene phase contributes little to the rigidity of the sample. It is best placed in the core of a laminate. In a composite, the polypropylene phase near the surface acts at best as a nonreinforcing filler and reduces the bending rigidity of the sample. Carpet selvage with significant polypropylene content, amounting to some 40 million pounds per year in Dalton, GA, is therefore a good choice for the core. The addition of some fibers to the core that bind strongly to the matrix is also desirable. The bending modulus of oriented polyester, nylon 6, and nylon 66 fibers are difficult to characterize because of variable orientation, crystallinity, crystal size, and relaxation of the fiber orientation during curing, which reduces the modulus of the fibers. The moduli for various components are given in Table 1. The phenolic resin bending modulus ranges from 1 to 1.2 million psi (6.9–8.3 GPa). A similar range is found for wood and cotton. It is therefore to be expected and it is found that laminates with waste cotton and wood in the outer layers provide the highest apparent flexural moduli.

The amount of resin used to coat the fibers is also important because it is necessary to ensure complete coverage of the fibers as well as adding stiffness to the material. We found that about 20 wt.% resin solids gave us satisfactory properties. Lower amounts of resin reduce the flexural modulus, whereas larger weight fractions become uneconomical with resin costs of about $1.00 per pound.

Typical values for flexural moduli, strength at break, and center strain at break for selected composite structures are shown in Table 2. Values for the

TABLE 2
Flexural Properties of Selected Composites

Composition	Flexural modulus (GPa)	Flexural strength (MPa)
348: Shred selvage, 27 wt.%; shred cotton, 53 wt.%; phenolic,[a] 20 wt.%	4.4	60
349: Shred selvage, 27 wt.%; shred cotton, 53 wt.%; phenolic,[a] 20 wt.%	4.0	52
350: Shred, selvage, 16 wt.%; shred cotton, 64 wt.%, phenolic,[b] 20 wt.%;	3.3	46
353: Shred selvage, 16 wt.%; shred cotton, 64 wt.%; phenolic,[b] 20 wt.%;	3.2	56
351: Shred selvage, 27 wt.%; shred cotton, 53 wt.%; phenotic,[c] 20 wt.%	2.6	36
352: Shred cotton, 80 wt.%; phenolic,[c] 20 wt.%	5.6	52
468: Shred nylon carpet postconsumer, 80 wt.%; phenolic,[a] 20 wt.%	1.0	15
469: Shred nylon carpet postconsumer, 64 wt.%; wood fiber, 16 wt.%; phenolic,[a] 20 wt.%	2.2	21
470: Shred PET carpet postconsumer, 80 wt.%; phenolic,[a] 20 wt.%	1.9	20
471: Shred PET carpet postconsumer, 64 wt.%; wood fiber, 16 wt.%; phenolic,[a] 20 wt.%	2.4	30
389: Shred selvage, 24 wt.%; shred cotton, 48 wt.%; wood pine, 8 wt.% phenolic,[a] 20 wt.%	2.8	37
390: Shred, selvage, 22 wt.%; shred cotton, 42 wt.%; wood pine, 16 wt.% phenolic,[a] 20 wt.%	3.5	52
391: Shred selvage, 16 wt.%; shred cotton, 32 wt.%; wood pine, 32 wt.% phenolic,[a] 20 wt.%	4.3	50

[a] Oxychem 29353.
[b] Different spacer size.
[c] Ashland DR359.

flexural moduli show about a 20% spread about the mean. This is much larger than encountered with more uniform materials. Compared to cotton fibers in a phenolic matrix, sample 352, the shredded nylon carpet in a phenolic matrix, sample 468, is about one-sixth in its stiffness. This is what one would expect from Eq. (1). Similarly, a comparison made between sample 468 and 470 shows the higher modulus for PET over nylon. Both samples indicate that the presence of polypropylene in the composite acts more like a nonreinforcing

filler or diluent because we would expect a minimum of about 200,000 psi (1.5 GPa) from the phenolic matrix. Similarly, we find the presence of about 16 wt.% polypropylene reduces the modulus by about half in sample 391. This reduction may also imply that there is a preferential migration of the polypropylene volume elements toward the surface of the plaque during molding. The results also show the importance of locating the polypropylene component, which is a significant part of carpet waste, in the core of the product. Increasing the volume fraction of the high-modulus components in all the samples increases the bending modulus even in the presence of polypropylene.

The results for type "A" laminates are shown in Table 3. There is some anomaly between the new 40 oz. carpet, samples 241 and 408, and the post-consumer carpets, samples 245, 246, and 250. Because the results are reasonably reproducible, we believe that the surface finish on this particular 40-oz. carpet made the adhesion of the phenolic resin to the nylon poor. With another new carpet sample from a different carpet company, samples 409, 411, and 412 give very high apparent modulus values. Increasing the wood content so that the outer layer contains 50-wt.% wood fiber gives a product equivalent to plywood in the apparent modulus. These plaques do not show the low values found for plywood when plywood is tested parallel to the fiber direction. In our moldings, the fibrous waste is randomly oriented at least in the length and width directions. The apparent moduli of all samples show an increase as the amount of high-modulus fiber in the outer layers is increased. It is important to note that without the anchoring protrusions, the adhesion between the core would fail and the slippage would limit the contribution of the third term (the largest) of Eq. (4). It should also be pointed out that when the high-modulus fibers are added to type "A" laminate, they are always in the outer layer. This is not necessarily the case in type "B," where the core and the outer layers are shredded and the outer layer contained a mixture of fibers. Although this is not the best arrangement, it reduced the number of parameters to be studied in this initial work.

The results for type "B" laminates are tabulated in Table 4. With this composite configuration, we have the freedom to select and place the fibrous components in the core and outer layers. In particular, we can place the fibrous components that contain polypropylene in the core where it has the least effect on the apparent modulus and strength. When shredded cotton, fabrics containing 60% cotton, and fibrous blends having 40% wood are placed in the outer layers, samples 297, 298, 299, 331, 435, and 458, we get high bending moduli and good strength. These constructions can be optimized to achieve 1 million psi (6.9 GPa) apparent bending moduli and 10,000 psi (69 MPa) strength. The effect of having either too large or too small a spacer selection is shown by comparison of samples 297 and 370, samples 277 and 407, and

TABLE 3
Table of Selected Type "A" Laminates

Composition	Apparent flexural modulus (GPa)	Flexural strength (MPa)	Flexural strain at break (%)
241: New 40-oz. nylon carpet; back to back, holes on ½-in. grid; phenolic,[a] 20 wt.% with respect to face yarn	1.4	31	0.42
408: New 40-oz. nylon carpet; back to back, holes on ½-in. grid; phenolic,[b] 20 wt.% with respect to face yarn	1.4	10	1.1
245: Nylon carpet blue, 28-oz. postconsumer; back to back, holes on ½-in. grid; phenolic,[a] 20 wt.% with respect to face yarn	1.7	30	0.42
246: Nylon carpet orange, 28-oz. postconsumer; back to back, holes on ½-in. grid; phenolic,[a] 20 wt.% with respect to face yarn	2.2	36	0.42
250: Nylon carpet orange, 28-oz. postconsumer; back to back, holes on ½-in. grid; phenolic,[a] 20 wt.% with respect to face yarn	2.4	25	1.6
267: Nylon carpet blue, 28-oz. postconsumer; back to back, holes on ½-in. grid; equal weight of face yarn as 60/40 cotton–PET shred fabric; phenolic,[b] 20 wt.% with respect to face yarn and shred fabric	6.2	77	2.0
275: Nylon carpet blue, 28-oz. postconsumer; back to back, holes on ½-in. grid; equal weight face yarn as waste cotton; phenolic,[b] 20 wt.% with respect to face yarn and cotton	5.4	66	1.6
281: Nylon carpet blue, 28-oz. postconsumer; back to back-holes on ½-in. grid; equal weight of face yarn as 60/40 cotton–PET fabric bits; phenolic,[b] 20 wt.% with respect to face yarn and fabric bits	5.0	54	1.9
409: New 40-oz. nylon carpet; back to back, holes on ½-in. grid; equal weight of face yarn as 60/40 cotton–PET shred fabric; phenolic,[b] 20 wt.% with respect to face yarn and shred fabric	3.2	23	1.8
411: New 40-oz. nylon carpet; back to back, holes on ½-in. grid; equal weight of face yarn as wood; phenolic,[b] 20 wt.% with respect to face yarn and wood (pine)	4.9	27	1.4
412: New 40-oz. nylon carpet; back to back, holes on ½-in. grid; 2 times weight of face yarn as wood; phenolic,[b] 20 wt.% with respect to face yarn and wood (pine)	6.7	60	1.3

[a] Georgia Pacific
[b] OxyChem.

TABLE 4
Table of Selected Type "B" Laminates

Composition	Apparent flexural modulus (GPa)	Flexural strength (MPa)	Flexura strain a break (%
297: Core shred selvage, 50 wt.%, and shred cotton, 50 wt.%; each outer layer of fabric bits (60/40 cotton–PET) contains $\frac{1}{4}$ of total core weight of shred cotton; phenolic,[a] 20 wt.% of total weight; $\frac{1}{4}$–$\frac{1}{2}$–$\frac{1}{4}$ construction	6.7	76	1.7
298: Core shred selvage, 33 wt.% of total; each outer layer of fabric bits, 67 wt.%; phenolic,[a] 20 wt.% of total weight; $\frac{1}{3}$–$\frac{1}{3}$–$\frac{1}{3}$ construction	6.4	62	1.8
299: Core shred selvage, 50 wt.%, and shred cotton, 50 wt.%; each outer layer of fabric bits contains $\frac{1}{8}$ of total core weight of shred cotton; phenolic,[a] 20 wt.% of total weight; $\frac{1}{8}$–$\frac{1}{2}$–$\frac{1}{8}$ construction	4.7	46	1.3
331: Core polypropylene, 50 wt.%, and shred cotton 50 wt.%; each outer layer contains $\frac{1}{4}$ of total core weight of shred cotton; phenolic,[a] 80 wt.% of the outer layers and 20 wt.% for the core; $\frac{1}{4}$–$\frac{1}{2}$–$\frac{1}{4}$ construction	5.9	49	1.3
370: Repeat of 297. Spacers too large	4.2	21	1.3
406: Core polypropylene, 50 wt.%, and shred cotton, 50 wt.%; each outer layer contains $\frac{1}{4}$ of total core weight of shred cotton; phenolic,[a] 80 wt.% of the outer layers and 20 wt.% for the core; $\frac{1}{4}$–$\frac{1}{2}$–$\frac{1}{4}$ construction	5.1	58	2.0
418: Core selvage, 50 wt.%; outer layers shred PET carpet, 50 wt.%, each outer layer contains $\frac{1}{4}$ of total core weight; phenolic,[a] 20 wt.% of total weight $\frac{1}{4}$–$\frac{1}{2}$–$\frac{1}{4}$ construction	1.6	31	3.6
435: Core shred selvage, 50 wt.%, and shred cotton, 50 wt.%; each outer layer contains $\frac{1}{4}$ of total core weight of shred cotton; phenolic,[a] 20 wt.% of total weight; $\frac{1}{4}$–$\frac{1}{2}$–$\frac{1}{4}$ construction	6.9	75	1.4
277: Core shred selvage, 42 wt.%; shred cotton outer layers, 58 wt.%; each outer layer contains $\frac{1}{4}$ of total core weight; phenolic,[a] 20 wt.% of total weight; $\frac{1}{4}$–$\frac{1}{2}$–$\frac{1}{4}$ construction; spacer dif. 0.041	5.7	61	1.5
407: Same as 277; spacer dif. −0.016	1.9	21	2.7
428: Same as 277; spacer dif. 0.007	4.5	61	1.6
420: Core shred selvage and shred PET carpet, each 50 wt.%; each outer layer contains $\frac{1}{4}$ of total core weight; phenolic,[a] 20 wt.% of total weight; $\frac{1}{4}$–$\frac{1}{2}$–$\frac{1}{4}$ construction	1.6	31	3.6
421: Same as 420 with outer layers having 50 wt.% of the PET shred carpet replace with wood; $\frac{1}{4}$–$\frac{1}{2}$–$\frac{1}{4}$ construction	2.0	31	3.0

TABLE 4
Continued

Composition	Apparent flexural modulus (GPa)	Flexural strength (MPa)	Flexural strain at break (%)
445: Core shred selvage, 50 wt.% and shred cotton, 50 wt.%; outer layers nylon fluff, phenolic resin Ga.Pa 442D35, 50 wt.%; 20 wt.% of total weight; $\frac{1}{4}$–$\frac{1}{2}$–$\frac{1}{4}$ construction	1.8	28	3.8
446: Core shred selvage, 50 wt.%, and shred cotton, 50 wt.%; outer layers nylon fluff, phenolic resin Ga.Pa 5236, 50 wt.%; 20 wt.% of total weight; $\frac{1}{4}$–$\frac{1}{2}$–$\frac{1}{4}$ construction	1.8	25	3.7
447: Core shred selvage, 50 wt.%, and shred cotton, 50 wt.%; outer layers nylon fluff, phenolic resin Ga.Pa 582D58, 50 wt.%; 20 wt.% of total weight; $\frac{1}{4}$–$\frac{1}{2}$–$\frac{1}{4}$ construction	2.0	30	3.4
448: Core shred selvage, 50 wt.%, and shred cotton, 50 wt.%; outer layers nylon fluff, phenolic resin OxyChem 29353, 50 wt.%; 20 wt.% of total weight; $\frac{1}{4}$–$\frac{1}{2}$–$\frac{1}{4}$ construction	1.9	28	3.4
450: Core shred selvage, 50 wt.%, and shred cotton, 50 wt.%; outer layers nylon fluff, 20% replaced by wood; phenolic resin,[a] 20 wt.% of total weight $\frac{1}{4}$–$\frac{1}{2}$–$\frac{1}{4}$ construction	2.1	22	2.3
466: Core shred selvage, 50 wt.%, and shred cotton, 50 wt.%; outer layers nylon fluff, 40% replaced by wood; phenolic resin,[a] 20 wt.% of total weight; $\frac{1}{4}$–$\frac{1}{2}$–$\frac{1}{4}$ construction	2.9	34	2.1
457: Core shred selvage; outer layers, PET fluff; phenolic resin,[a] 20 wt.% of total weight; $\frac{1}{4}$–$\frac{1}{2}$–$\frac{1}{4}$ construction	3.2	22	1.3
458: Core shred selvage; outer layers, PET fluff with 40% of PET replaced by wood; phenolic resin,[a] 20 wt.% of total weight; $\frac{1}{4}$–$\frac{1}{2}$–$\frac{1}{4}$ construction	5.6	37	1.2
460: Core shred selvage; outer layers, PET fluff with 20% of PET replaced by wood; phenolic resin,[a] 20 wt.% of total weight; $\frac{1}{4}$–$\frac{1}{2}$–$\frac{1}{4}$ construction	4.4	34	1.1
495: Core shred selvage and cotton, 50/50; outer layers shred fabric 60/40 cotton–PET; phenolic resin,[a] 20 wt.% of total weight; $\frac{1}{4}$–$\frac{1}{2}$–$\frac{1}{4}$ construction	5.7	69	2.1
496: Same as 495 except phenolic resin is 15 wt.%	4.4	52	1.9
496: Same as 495 except phenolic resin is 10 wt.%	2.4	33	3.0

[a] OxyChem 29353.

samples 277 and 428. When the spacer thickness is too large, too early a transfer of the pressure from the molding to the spacers occurs. A too small a set of spacers does not transfer the platen pressure from the molding and allow for the release of steam pressure. When the outer layers are nylon fluff (samples 445–448), we get apparent bending moduli of about 250,000–280,000 psi (1.7–1.9 GPa). This range of flexural modulus encompasses about seven different phenolic resins from Georgia Pacific and OxyChem, indicating that the properties are not sensitive to the particular resole resin used. Using Eq. (1), we would expect about 200,000–240,000 psi (1.4–1.6 GPa) contribution from the phenolic resin and about 350,000 psi (2.4 GPa) for oriented nylon. Unoriented nylon would contribute about 160,000 psi (1.1 GPa). These results suggest that we do not retain most of the modulus due to the orientation of the nylon fibers. Sample 418 shows the results of shredded waste PET carpet in the outer layer. The presence of polypropylene again shows a diluent effect. When PET face yarn is in the outer layer, sample 457, a higher apparent flexural modulus of 466,000 psi (3.2 GPa) is obtained, suggesting that more of the fiber orientation is retained with polyester during the molding. When wood fibers are added to the waste fibers in the outer layers, the apparent flexural moduli show significant increases, samples 450, 458, 460, and 466. Comparison of samples 421 and 458, where the outer layers in sample 421 contain some polypropylene, shows very large differences in the apparent bending modulus, again emphasizing the deleterious effects of polypropylene in the outer layers of laminates. Comparing the values listed for samples 495, 496, and 497, we can see the effect of phenolic resin content on the apparent flexural properties. Increasing the resin level from 10% to 15% to 20% results in an increase in the modulus from 349,000 to 640,000 to 809,000 psi (2.4 to 4.4 to 5.6 GPa). From Eq. (1), this increase primarily reflects the larger value of the phenolic resin compared to the PET content of the shredded fabric. A more complete coating of the fibers is also involved and this factor is better reflected in the increase in the flexural strength.

The effects of a 24-h soak in water on properties are listed for representative samples in Table 5 and 6. There is generally a small decrease in flexural properties on soaking and this decrease can be correlated with the increase in the sample thickness. Because both the initial and water-treated samples were selected from the same plaques, the small increases are all in one direction and appear to be real. The amount of water taken up ranges from 8% to 33%, which is smaller than the 60% found with plywood. We believe most of the water taken up is due to porosity rather than due to the swelling of the coated fibers. The $CaCO_3$ filler present in the adhesive of the waste carpet and in the samples no doubt plays a part in the water uptake. Typical densities for these material are also listed and range from about 1 to 1.2, depending on the components present. Higher amounts of cotton, nylon, and PET fibers as well as

TABLE 5
Effect of a 24-h Soak at Room Temperature on the Flexural Properties; Samples Redried and Conditioned

Composition	Apparent flexural modulus (GPa)	Flexural strength (MPa)	Flexural strain at break (%)	% Water uptake 24-h Soak
450: Core shred selvage, 50 wt.%, and shred cotton, 50 wt.%; outer layers nylon fluff, 20% replaced by wood; phenolic resin,[a] 20 wt.% of total weight $\frac{1}{4}$–$\frac{1}{2}$–$\frac{1}{4}$ construction	1.9	21	2.3	
450: 24-h soak	1.7	23	2.7	21
457: Core shred selvage; outer layers, PET fluff; phenolic resin,[a] 20 wt.% of total weight; $\frac{1}{4}$–$\frac{1}{2}$–$\frac{1}{4}$ construction	3.6	30	1.3	
457: 24-h soak	3.0	32	1.6	19
458: Core shred selvage; outer layers, PET fluff with 40% of PET replaced by wood; phenolic resin,[a] 20 wt.% of total weight $\frac{1}{4}$–$\frac{1}{2}$–$\frac{1}{4}$ construction	5.6	37	1.0	
458: 24-h soak	3.6	25	0.8	14
467: Core shred nylon carpet; outer layers shred cotton weight equal to core; phenolics resin,[a] 20 wt.% of total weight; $\frac{1}{4}$–$\frac{1}{2}$–$\frac{1}{4}$ construction	2.2	15	1.4	
467: 24-h soak	1.4	14	2.5	33
472: Core shred PET carpet; equal weight shred nylon carpet in outer layers; phenolic resin,[a] 20 wt.% of total weight; $\frac{1}{4}$–$\frac{1}{2}$–$\frac{1}{4}$ construction	1.1	36	3.0	
472: 24-h soak	1.1	12	4.0	8
474: Core shred selvage; outer layers, 60 wt.% PET fluff, 40% wood fibers; phenolic resin,[a] 20 wt.% of total weight; $\frac{1}{4}$–$\frac{1}{2}$–$\frac{1}{4}$ construction	5.0	45	1.2	
474: 24-h soak	4.2	40	1.2	7
479: Core shred selvage; outer layers, shred fabric, 60/40 cotton–PET; phenolic resin,[a] 20 wt.% of total weight; $\frac{1}{4}$–$\frac{1}{2}$–$\frac{1}{4}$ construction	4.1	38	1.9	
479: 24-h soak	3.8	34	1.8	28

[a] OxyChem 29353.

TABLE 6
Density and Dimensional Changes for Samples in Table 4 after 24-h Soak at Room Temperature

Sample No.	Density (g/cm^3)	24-h % Water uptake	% Thickness increase
450: Core shred selvage, 50 wt.%, and shred cotton, 50 wt.%; outer layers nylon fluff, 20% replaced by wood; phenolic resin,[a] 20 wt.% of total weight $\frac{1}{4}$–$\frac{1}{2}$–$\frac{1}{4}$ construction	1.09	21	12
457: Core shred selvage; outer layers, PET fluff; phenolic resin,[a] 20 wt.% of total weight; $\frac{1}{4}$–$\frac{1}{2}$–$\frac{1}{4}$ construction	0.99	19	5
458: Core shred selvage; outer layers, PET fluff with 40% of PET replaced by wood; phenolic resin,[a] 20 wt.% of total weight; $\frac{1}{4}$–$\frac{1}{2}$–$\frac{1}{4}$ construction	1.01	13	4
467: Core shred nylon carpet, outer layers shred cotton weight equal to core; phenolic resin,[a] 20 wt.% of total weight; $\frac{1}{4}$–$\frac{1}{2}$–$\frac{1}{4}$ construction.	1.06	33	12
472: Core shred PET carpet; equal weight; shred nylon carpet in outer layers; phenolic resin,[a] 20 wt.% of total weight; $\frac{1}{4}$–$\frac{1}{2}$–$\frac{1}{4}$ construction	1.13	8	1
474: Core shred selvage; outer layers, 60 wt.% PET fluff, 40% wood fibers; phenolic resin,[a] 20 wt.% of total weight; $\frac{1}{4}$–$\frac{1}{2}$–$\frac{1}{4}$ construction	1.04	12	4
479: Core shred selvage; outer layers, shred fabric, 60/40 cotton–PET; phenolic resin,[a] 20 wt.% of total weight; $\frac{1}{4}$–$\frac{1}{2}$–$\frac{1}{4}$ construction.	0.96	25	10

[a] OxyChem 29353.

$CaCO_3$ increase the composite's density above 1, whereas wood and polypropylene will decrease its density.

The typical apparent flexural properties of the honeycomb sandwich construction are listed in Table 7. As pointed out earlier, the shear displacement in samples' short lengths will be considerable and will be much less than the modulus of the outer layers. As the length between supports is increased to about 20 in., as found in typical wood pallets, the effect of the shear displace-

TABLE 7
Flexural Properties of Sandwich Honeycombs

Composition	Depth (cm)	Length (cm)	Modulus of faces (GPa)	Apparent modulus of sandwich honeycomb (GPa)	Breaking stress of sandwich honeycomb (MPa)
377: Core 1.3-cm phenolic-coated paper honeycomb; outer layers shred 60/40 waste fabric; coated with 25 wt.% phenolic resin	1.6	10	5.9	0.83	10
377: Core 1.3-cm phenolic-coated paper honeycomb; outer layers shred 60/40 waste fabric; coated with 25 wt.% phenolic resin	1.6	12.5	5.9	0.98	5.0
377: Core 2.5-cm phenolic-coated paper honeycomb; fabric; outer layers shred 60/40 waste coated with 25 wt.% phenolic resin	3.1	10	5.9 (Nominal)	0.15	1.8
442: Core 2.5-cm phenolic-coated paper honeycomb; outer layers composite 40% wood, 30% waste carpet, 30% cotton; coated with 2 wt.% phenolic resin	3.0	10	5.9 (Nominal)	0.38	7.6
382: Core 1.3-cm paper honeycomb coated by hand; outer layers shred 60/40 waste fabric; coated with 25 wt.% phenolic resin	1.9	10	5.9 (Nominal)	1.00	5.7
438: Core 1.3-cm coated paper honeycomb; outer layers shred fabric 40% replaced by wood; coated with 20 wt.% phenolic resin	1.6	10	5.9 (Nominal)	1.01	7.6

TABLE 8
Typical Impact Properties

Sample type	Sample thickness (cm)	Failure drop height (cm)
Plywood	0.67	91
Composite	0.68	61
Laminate (F–B–B–F) "A"	0.67	61
Laminate "B"	0.59	61
Honeycomb	1.59	46

ment is greatly reduced and the rigidity of the honeycomb will reflect the modulus of the outer layers. This is indicated with sample 377, which was tested with 4- and 5-in. lengths. Increasing the thickness of the core to 1 in. increases the shear displacement with short-length samples and masks the effect of the increase in the rigidity with a larger separation of the outer layers (i.e., a 1-in. honeycomb should be four times more rigid than a 1/2-in. honeycomb. However, one must be aware that the compressive strength of the 1-in. honeycomb is likely to be smaller than the 1/2-in. material.

The drop impact properties of some of the composite materials is shown in Table 8. The fibrous waste materials in a phenolic binder are somewhat less than three-layer plywood.

CONCLUSIONS

Woodlike properties can be achieved using all of the components of textile and carpet fibrous waste in a high-modulus matrix by judicious placement of the fibers in composites. Flexural moduli as high as 1,000,000 psi (6.9 GPa) and strength as high as 10,000 psi (6.9 MPa) were achieved with well-designed laminates. The density of the waste fibers and the amount of matrix resin required are negatives when compared with plywood. The use of these materials in outdoor applications or as outer layers in honeycomb structures is suggested.

ACKNOWLEDGMENTS

The author acknowledges the financial support of DuPont and the State of Georgia through the CCACTI program. The author also acknowledges the help of the score of Georgia Tech undergraduates who carried out the many experiments.

REFERENCES

1. S. Kumar, *in Book of Papers, 1997 International Conference and Exhibition, American Association of Textile Chemists and Colorists,* 1997.
2. C. P. Lehner, in *2nd Annual Conference on Recycling of Fibrous Textile and Carpet Waste,* 1997.
3. Y. Zhang, J. D. Muzzy, and S. Kumar, in *2nd Annual Conference on Recycling of Fibrous Textile and Carpet Waste,* 1997.
4. R. J. Evans, C. C. Clan, and S. Czemik, in *Recycling Division's 3rd Annual Recycling Conference Proceedings,* 1996.
5. E. Duffy, in *Recycling Division's 3rd Annual Recycling Conference Proceedings,* 1996.
6. M. C. Ryan, in *Recycling Division's 3rd Annual Recycling Conference Proceedings,* 1996.
7. A. T. Griffith and C. B. Roberts, in *2nd Annual Conference on Recycling of Fibrous Textile and Carpet Waste,* 1997.
8. J. N. Reddy and A. Miravete, *Practical Analysis of Composite Laminates,* CRC Press, New York, 1995.
9. ASTM D 790, American Society for Testing Materials, Philadelphia, 1995.
10. ASTM C 393, American Society for Testing Materials, Philadelphia, 1994.
11. ASTM D 3029, American Society for Testing Materials, Philadelphia, 1994.
12. W. E. Morton and J. W. S. Hearle, *Physical Properties of Textile Fibers,* John Wiley & Sons, New York, 1975, p. 404.

POLYM.–PLAST. TECHNOL. ENG., 38(3), 533–546 (1999)

UTILIZATION OF RECYCLED CARPET WASTE FIBERS FOR REINFORCEMENT OF CONCRETE AND SOIL

YOUJIANG WANG

School of Textile & Fiber Engineering
Georgia Institute of Technology
Atlanta, Georgia 30332-0295

Abstract

The use of recycled fibers from textile waste for concrete and soil reinforcement is a very attractive approach, with such benefits as performance enhancement, low-cost raw materials, and reduced needs for landfilling. This article discusses the general advantages of fiber reinforcement and reviews some studies on the use of carpet waste fibers for concrete and soil reinforcement. A study on recycled carpet waste fibers for fiber-reinforced concrete (FRC) showed a significant toughness increase and reduced shrinkage. It included two concrete mix designs and a wide range of fiber dosage rates, from 0.07 to 2.0 vol.%. A research program on fiber-reinforced soil is underway for fiber characterization, analysis of the engineering properties of the fiber–soil systems, and field trials. A significant improvement in soil behavior under the triaxial loading condition was observed.

Key Words: Concrete; Fiber-reinforced soil; Textile waste; Recycling.

INTRODUCTION

The carpet waste generated each year and accumulated in landfills represents an abundance of useful resources, as it may be converted into various useful

products (1,2). The amount of carpet waste, including production waste and postconsumer carpet, is estimated at over 2 million tons per year. Because of the high cost of developing and managing landfills, waste disposal in landfills has become increasingly difficult.

A carpet typically consists of two layers of backing (usually fabrics from polypropylene tape yarns), joined by $CaCO_3$-filled styrene–butadiene latex rubber (SBR), and face fibers (majority being nylon 6 and nylon 66 textured yarns) tufted into the primary backing. The SBR adhesive is a thermoset material, which cannot be remelted or reshaped. Some waste is generated before the application of SBR. Such waste is termed *soft waste*, and most of it is reused as a filling material or as nonwoven mats. The waste containing the SBR (termed *hard waste*) has not found significant uses and it forms the major part of the waste going into the landfills.

Concrete and soil are used in great quantities in construction. Studies have shown that the properties of these materials can be enhanced by fiber reinforcement. In this article, a literature review is provided on the advantages of fiber reinforcement of concrete and soil. The article also reviews the results of laboratory and field studies using carpet waste fibers for concrete and soil reinforcement.

FIBER-REINFORCED CONCRETE

Background

Concrete is the most heavily used construction material in the world. However, it has low tensile strength, low ductility, and low energy absorption. An intrinsic cause of the poor tensile behavior of concrete is its low toughness and the presence of defects. Therefore, improving concrete toughness and reducing the size and amount of defects in concrete would lead to better concrete performance. An effective way of improving the toughness of concrete is by adding a small fraction (usually 0.5–2% by volume) of short fibers to the concrete mix during mixing. In the fracture process of fiber-reinforced concrete (FRC), fibers bridging the cracks in the matrix can provide resistance to crack propagation and crack opening before being pulled out or stressed to rupture. After extensive studies, it is widely accepted that such fiber reinforcement can significantly improve the tensile properties of concrete. Orders-of-magnitude increases in toughness (energy absorption) over plain concrete is commonly observed (3–6). Another advantage of fiber reinforcement is the reduction of the shrinkage and shrinkage cracking of concrete associated with hardening and curing. Reduced shrinkage cracking has been observed even with fiber volume fractions as low as 0.1% of polypropylene fibers (7).

Other benefits of fiber-reinforced concrete include improved fatigue strength, wear resistance, and durability (3). By using FRC instead of con-

ventional concrete, section thickness can be reduced and cracking can be effectively controlled, resulting in a lighter structure with a longer expected life (4). Fiber-reinforced concrete is currently being used in many applications, including buildings, highway overlays, bridges, and airport runways (3–5). In load-bearing applications, it is generally used along with traditional steel reinforcement (8). In building constructions, it has become a more common practice to use low-dosage synthetic fiber reinforcement for floor slabs.

One type of waste material suitable for concrete reinforcement is carpet production trims and postconsumer waste. They consist of mainly crimped nylon face fibers and polypropylene tape yarns, both proven durable and effective in FRC. Studies on recycled carpet waste fibers for FRC showed a significant toughness increase and reduced shrinkage, and a full-scale construction project using carpet waste FRC has demonstrated the feasibility of using such a material in construction (9–11).

Laboratory Studies

Two laboratory studies on concrete reinforcement with carpet waste fibers were carried out at the Georgia Institute of Technology (9,11). The carpet waste fibers used were shredded from carpet trims, a waste generated in carpet manufacturing. The fiber length was not uniform and typically ranged from 12 to 25 mm. A quantitative analysis of the shredded edge trim was conducted, and the relative amounts of the primary components were as follows: polypropylene (36%), nylon (18%), and SBR+$CaCO_3$ (46%).

In the first study (9), the following concrete mix weight ratios were used: Type I Portland cement (1.0), river sand (0.85), crushed granite (0.61), water (0.35), and a small amount of superplasticizer (a water-reducing agent). Fiber volume fractions for the waste fibers were 1% and 2%. Only the actual fiber portion (excluding SBR+$CaCO_3$) was included for calculating the fiber volume fraction for the waste fiber-reinforced concrete. FiberMesh® (Fibermesh Company, Chattanooga, TN, U.S.A.), a virgin polypropylene fiber (19 mm long), at 0.5% and 1% volume fractions was also included in this study for comparison purposes.

A four-point flexural test and a cylinder compressive test were conducted on a hydraulic testing machine. In the compressive test, the plain concrete specimens failed in a brittle manner and shattered into pieces. In contrast, all the FRC samples could still remain as an integral piece after reaching the peak load, with fibers holding the concrete matrices tightly together. In the flexural test, it was observed that the plain concrete samples broke into two pieces once the peak load was reached, with very little energy absorption. The FRC specimens, on the other hand, exhibited a pseudoductile behavior and fibers bridging the beam crack can be seen. Because of the fiber bridging mechanism, the energy absorption during flexural failure was found to be much higher than that for plain concrete.

In commercial applications, low-dosage reinforcement with synthetic fibers, mostly polypropylene at about 0.1 vol.%, is widely used for controlling shrinkage cracking. For structural applications, however, a higher dosage (1–2 vol.%) may be desirable. To evaluate the effect of fiber dosage rate on FRC properties, a second test program was carried out on the flexural and compressive properties of concrete containing various dosages of fibers (11). The dosage ranged from 0.89 to 17.85 kg/m^3 for the recycled carpet material (Mixes 2–8 in Table 1), based on the total weight of the shredded material including SBR and $CaCO_3$. Specimens with FiberMesh virgin polypropylene at 0.89 kg/m^3 were also tested (Mix 1). Because the carpet waste contains components in addition to fibers and because nylon has a higher density than polypropylene, the estimated fiber volume fraction in Table 1 for the recycled fiber is lower than that with virgin polypropylene, even at the same dosage rate based on fiber mass. The concrete mix used was in the following proportions: cement (1.00), water (0.44), sand (1.71), crushed rock (2.63), and an appropriate amount of fiber. No chemical admixtures were added.

Table 1 summarizes the test results of the second laboratory study (11), in which each data point represents the average from about 10 specimens. The workability of the fresh concrete was measured by a slump test in accordance with ASTM C143-90a. Good workability (180–230 mm slump) was observed for mixes with up to 1.8 kg/m^3 of waste fibers. The slump decreases to 70 mm for 5.95 kg/m^3, 51 mm for 8.93 kg/m^3, 48 mm for 11.9 kg/m^3, and to near zero for 17.85 kg/m^3. Thus, the workability for dosages from 5.95 to 11.9 kg/m^3 is low but manageable. In actual construction, a small amount of superplasticizer can be added to increase the workability to an acceptable level.

The compressive test was conducted on 76-mm (diameter) × 152-mm (height) cylinders according to ASTM C39-86 at an age of 28 days. As seen from Table 1, the compressive strengths varied from mix to mix, most likely due to normal variation. However, it appears that the compressive strength for Mix 8 with 1.4 vol.% waste fibers was lower due to the fiber addition. In all the tests, good shatter resistance was observed because of the fiber reinforcement, especially in those with relatively high fiber dosage rates (Mixes 5–8).

The flexural test was performed on 102×102×356-mm beams in adherence to ASTM C1010 at a span length of 305 mm. Typical flexural test curves for selected mixes are shown in Fig. 1. From Table 1, it is seen that the flexural strength, corresponding to the maximum flexural load in the test, was similar for all the mixes, suggesting that the addition of fibers to concrete had little effect on the flexural strength of the concrete beams. The variability, as represented by the coefficient of variation, was generally low.

Fiber reinforcement provides significant improvement of concrete toughness. ASTM C1010 is a standard test method to characterize the toughness of fiber-reinforced concrete. Toughness indices indicate the energy absorption

TABLE 1
Test Results for Concrete Reinforced with Carpet Waste Fiber

Mix	Dosage (kg/m^3)	Approx. V_F (%)	Slump (mm)	Comp. strength		Flex. strength		Toughness		
				MPa	CV[a]	MPa	CV	I_5	I_{10}	I_{20}
1[b]	0.89[b]	0.15	178	22.8	0.11	3.74	0.09	3.22	4.69	6.33
2	0.89	0.07	229	20.0	0.12	3.64	0.07	3.64	3.07	4.21
3	1.34	0.11	184	24.3	0.13	4.20	0.07	4.20	2.98	4.01
4	1.79	0.14	191	25.6	0.08	4.06	0.08	2.96	4.06	5.03
5	5.95	0.47	70	27.6	0.07	3.79	0.07	2.71	3.64	4.76
6	8.93	0.70	51	23.7	0.02	4.11	0.08	2.95	4.17	5.77
7	11.90	0.93	48	23.1	0.14	3.77	0.07	3.06	4.41	6.41
8	17.85	1.40	0	17.4	0.20	3.73	0.10	3.29	5.17	7.91

[a] CV = coefficient of variation.
[b] With FiberMesh polypropylene fibers.
Source: Ref. 11.

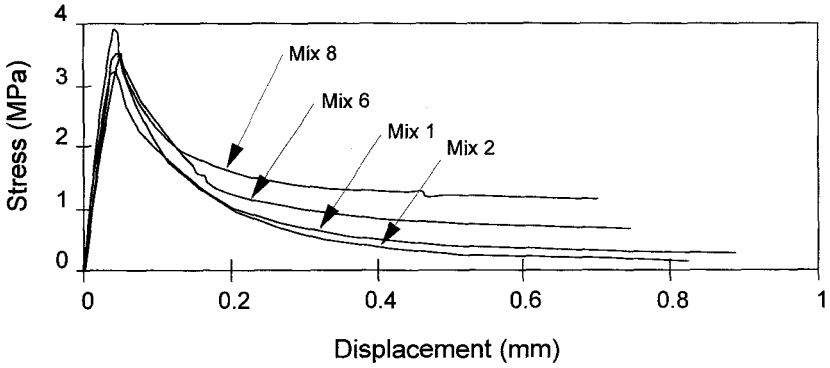

FIG. 1. Typical flexural test curves of fiber-reinforced concrete. (From Ref. 11.)

ratio compared with a perfectly brittle material. I_5, I_{10}, and I_{20} are the three indices calculated from the flexural load–deflection curve for three different deflection ranges. These quantities are explained and discussed in ASTM C1018 and C1116.

It can be observed from the data in Table 1 that the I_5 index was insensitive to the fiber dosage rate. I_{10} and I_{20}, corresponding to larger deflection ranges, showed an increase with the dosage rate. The mixes with high fiber content exhibited very good toughness properties. These mixes could be used for structural applications and highway pavements. After the peak load corresponding to matrix cracking, fiber-reinforced concrete can still carry a significant level of load over a wide range of continued deflection. Thus, the fibers are very effective in keeping the cracked concrete pieces together and preventing spalling and pothole formation. For applications where the goal of reinforcement is to provide integrity to concrete rather than to carry tensile load, discontinuous fibers may be used to replace steel rebars. One such example might be a pavement on a relatively stiff foundation.

Field Study

The laboratory study has indicated that the carpet waste fiber was very effective in improving the toughness and shrinkage properties of concrete. In 1994, Shaw Industries, Inc. completed a 11,000-m^2 R&D Center in Dalton, Georgia that used concrete reinforced with carpet waste fibers in the construction project. About 20 tons of carpet production waste was consumed in the project, which would otherwise have been sent to a landfill. The concrete mix followed a typical design for concrete with a 28-MPa (4000-psi) compressive strength, consisting of cement, sand, and rock. The water-to-ce-

ment ratio was 0.5 and the cement content was about 260 kg/m^3. Superplasticizer was added to maintain the desired workability. The amount of waste fiber included was 5.95 kg/m^3. Mixing was done by adding fibers to the mixing truck directly, after which the fibers were found to be uniformly dispersed in the concrete without balling or clumping. Mixing, pouring, and finishing followed standard procedures, used conventional equipment, and went smoothly. The compressive and flexural strengths met specifications, and reduced shrinkage cracking was observed. Such concrete containing waste fibers was used for floor slabs, driveways, and walls of the building. The project demonstrated the feasibility of using a large amount of carpet waste for concrete reinforcement in a full-scale construction project. Besides reducing the need for landfilling, the use of low-cost waste fiber for concrete reinforcement could lead to improved infrastructure with better durability and reliability.

FIBER-REINFORCED SOIL

Background

A soil can often be regarded as a combination of four basic types: gravel, sand, clay, and silt. They generally have low tensile and shear strength and their characteristics may depend strongly on the environmental conditions (e.g., dry versus wet). Soil reinforcement with geotextile fabrics is a well-established technology and is widely used in road construction for soil reinforcement, stabilization, drainage, and separation (12). Soil reinforcement with randomly distributed fibers is another approach that may increase the internal cohesion of soil. In a simple process, fibers, typically at a dosage rate of 0.2–2% by weight, are added and mixed into silt, clay, sand, or lime and cement-stabilized soil. Studied have shown that such fiber reinforcement can improve the properties of soil, including the shear strength, compressive strength, bearing capacity, postpeak-load strength retention, and the elastic modulus (13–18).

Fibers in the soil generally act as tensile reinforcing members. Even when the soil deforms in shear or compression, the normal strains in certain other directions may be a tensile extension. Because the fibers are generally stronger and stiffer than the soil, the deformation is resisted by fibers in the direction of the tensile strains through fiber–soil frictional interactions. The overall failure surface is larger and nonplanar due to the presence of fibers, and the failure load and energy are increased. Fibers being stretched still provide resistance; thus, the postpeak strength retention is also increased, making the soil more ductile or tougher.

The increase of the load-carrying capability of soil due to fiber reinforcement could result in significant savings in construction cost and time. An increase in allowable slope angle would reduce the space and the amount of soil

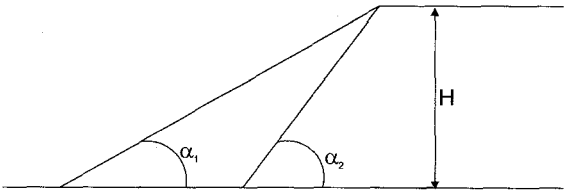

FIG. 2. Illustration of the cross section of a slope versus the slope angle.

needed for a slope. As illustrated in Fig. 2, the reduction of soil volume (V) can be calculated from

$$V = \frac{1}{2} LH^2 \left(\frac{1}{\tan \alpha_1} - \frac{1}{\tan \alpha_2} \right)$$

where L is the length, H is the height, and α_1 and α_2 are the allowable slope angles for the unreinforced and reinforced soil, respectively. For example, for a 1-km-long, 10-m-high slope, the increase of the slope angle from 20° to 30° would save over 50,000 m^3 of soil and reduce the width of the slope by 10 m. This could directly translate into cost and time savings and reduced environmental impact.

One distinguishing feature of fiber reinforcement in comparison with geotextile fabric reinforcement is its maintenance of property isotropy and the absence of weak planes parallel to oriented reinforcement (19). Successful uses of various fibers, including virgin polypropylene and glass, to reinforce soil and sand in field studies have been reported (20–22). Up to a 95% increase in pavement durability has been observed due to soil reinforcement with polypropylene fibers (18). Additional property enhancement may be achieved by using fiber-reinforced soil along with geotextile fabrics.

Chemicals are also used to stabilize soil for certain applications. Lime-stabilized clay and Portland-cement-stabilized sand are two of the examples. The chemical stabilizers, normally added at a 2–10% rate, increase soil internal cohesion via chemical bonding. Chemically stabilized soils, which are stiffer and stronger than the unreinforced soils, also exhibit tensile cracking as a major mode of failure. The addition of fibers in such instances can effectively control the opening and propagation of cracks through the bridging actions of the fibers. Enhanced performance of chemically stabilized materials due to fiber reinforcement has been reported (22), and the use of fibers may allow for a reduction in chemical stabilizer content. Alternatively, the use of fibers may allow reduction in the thickness of the layer in which they are used. Sangineni

(23) computed thickness reductions on the order of 5–16% using data for chemically stabilized materials incorporating fibers.

Laboratory Studies

A laboratory test program was carried out to evaluate the properties of carpet waste fiber-reinforced soil (24). The soil used in the laboratory studies was obtained from Wilkes County, Georgia. It is a silty clayey sand with a maximum dry density of 1724 kg/m^3 at an optimum moisture content of 16.5%.

Tests have been conducted on soil specimens reinforced with the same carpet waste fibers as that used in the concrete studies (about 19 mm long). The California Bearing Ratio (CBR) test (ASTM D1883–92) was performed; it measures the compressive stress for given soil deformation resulting from the penetration of the loading rod into the cylindrical soil specimen in a metal mold. The specimens were prepared with the same moisture content (16.5%) and compacted with standard effort as described in test method ASTM D698. The strength of unsoaked specimens decreased slightly (1% and 8%, respectively) with the inclusion of 1% and 2% by weight of fibers at 2.54 mm (0.1 in.) penetration, and the strength increased slightly (6% and 5%, respectively) with 1% and 2% fibers at 5.08 mm (0.2 in.) penetration. A similar trend was also observed in the test of soaked specimens. Examination of the test curves suggested that the initial slope of the load–displacement curve is lowered with fiber inclusion, possibly due to the interference with soil compaction by the fibers. It appears that at low deformation levels, the fibers have not been stressed high enough to show their reinforcement effect. The finding is similar to that reported by Hoare (25), who studied fiber reinforcement of sandy gravel. Others, on the other hand (e.g., Ref. 16), have observed a significant increase in CBR values with fiber reinforcement.

The same fiber soil systems have also been tested under triaxial compression with and without a 34.5-kPa (5-psi) confinement pressure. All samples were compacted to the maximum dry density of 1724 kg/m^3 at optimum moisture of 16.5%, and tested in the as-compacted condition. The resistance to deformation is measured by the principal stress difference (i.e., the compressive stress minus the confining pressure). The peak stress difference increased for all the fiber contents when confinement was changed from 0 to 34.5 kPa. The test curves are shown in Fig. 3. The confining pressure provides lateral resistance on the side of the samples, simulating the *in situ* lateral earth pressure. This resistance results in higher vertical loads and therefore higher stresses necessary to fail the sample.

Several improvements in the stress–strain properties of the soil can be seen in the test curves. As the fiber content increases, the peak stress

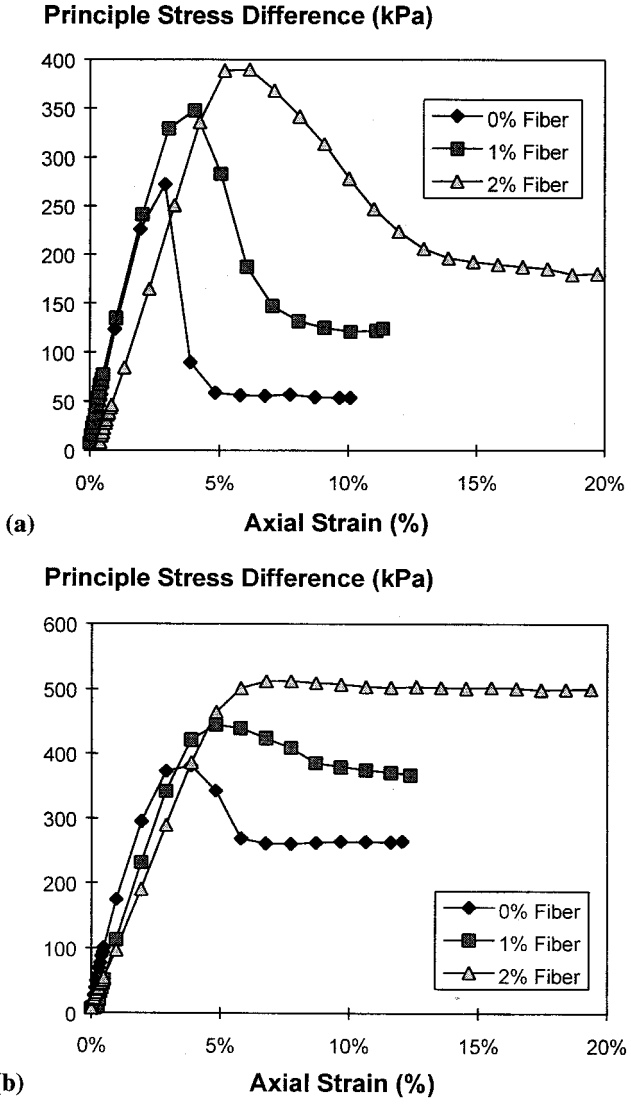

FIG. 3. Test curves for the triaxial compression test: (a) unconfined and (b) with a 34.5-kPa confinement pressure. (From Ref. 24.)

difference at failure also increases. For unconfined tests, the peak principle stress difference increased from 272 to 389 kPa when the fiber content was increased from 0.0% to 2.0%, a 43% increase. Similar results were observed for the test performed at 34.5 kPa confinement. The increase in stress went from 381 kPa for 0.0% fiber up to 512 kPa for 2.0% fiber, a 34% increase.

For both test conditions the samples show signs of strain softening. The strength of the samples decreased dramatically after peak stress at failure was obtained. However, there is a definite trend indicating less strain softening with increased fiber content. In both the confined and unconfined samples, the residual strength of the soil is at least 100% higher for the 2% fiber samples. When confined, the 2.0% fiber sample showed almost no signs of strain softening once a peak stress was obtained, and the failure mode changed from shear to bulging (Fig. 4). However, it is noted from the triaxial test that the initial stiffness of specimens reinforced with fibers appears to be lower than that of the control soil specimens. This may indicate that fiber reinforcement of soil is especially advantageous for applications where the load-bearing capability of the soil at large deformation is needed, and that fiber reinforcement may not fully show its benefits if load bearing at small deformation is critical.

Additional laboratory tests are carried out to study the effect of specimen moisture content and compaction on the triaxial compressive behavior of the fiber–soil system and on the use of other types of carpet and textile waste fibers at the Georgia Institute of Technology (26). Studies are also underway to conduct specially designed tests to isolate the effect of fiber reinforcement from other factors such as specimen compaction.

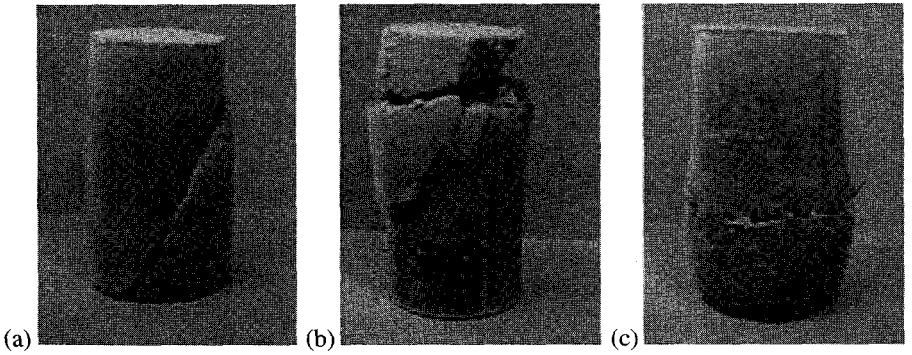

FIG. 4. Specimens after the triaxial compression test with a 34.5-kPa confinement pressure. Fiber content: (a) 0%, (b) 1%, (c) 2%.

Field Studies

In a joint effort involving the carpet and fiber industry, several Georgia counties, the Georgia Department of Transportation, and the Georgia Institute of Technology, among others, a preliminary field study was carried out to demonstrate the feasibility of incorporating carpet waste fibers in road construction. The field trial sites for unpaved county roads were selected to represent typical types of soil found in the state of Georgia. Trial sections with carpet waste fibers and virgin fibers were installed in several Georgia counties (27,28). The installation involves ripping the soil to a 150-mm depth, spreading the shredded carpet fibers, blending the fibers into the soil, and smoothing and compacting the soil. The fibers used were shredded into a length up to 70 mm long, and about 0.33% by weight of fibers were added. It was very encouraging to observe that the fibers could be mixed into soil with reasonable consistency in the field. Assessment of the unpaved roads by visual inspections confirmed that fibers in soil could improve the durability for certain types of soil, thus reducing the need for frequent regrading. However, it appears that the fibers were less effective for sandy types of soil, as the fibers might eventually migrate to the surface of the road. The study also points to the need for a more systematic and quantitative assessment of the effectiveness of waste fiber for soil stabilization. A better understanding of the fundamental mechanisms is necessary for predicting the performance of the fiber–soil system for potential applications based on the fiber and soil characteristics.

CONCLUSION

The carpet waste disposed in landfills each year in the United States amounts to about 40,000 tons of production waste and 2 million tons of postconsumer waste. Reinforcements of concrete and soil with discrete fibers are proven technologies to enhance the performance of these construction materials. The benefits of using carpet waste fibers for such reinforcements have been discussed in this article.

A study on the properties of FRC with carpet waste fibers has been conducted with different fiber dosage rates, from 0.07 to 2.0 vol.%. Tests were performed to evaluate their compressive strength, flexural toughness, and flexural strength. The study showed that waste fiber reinforcement can effectively improve the shatter resistance, toughness, and ductility of concrete. The use of low-cost waste fiber for concrete reinforcement could lead to improved infrastructure with better durability and reliability. Other applications could include pavements, columns, bridge decks, and barriers, and for airport construction as runways and taxiways.

The use of carpet waste for soil reinforcement was shown to increase the triaxial compressive strength and residual strength of soil. Field trials showed that shredded carpet waste fibers (to 70 mm long) can be blended into soil with conventional equipment, and they confirmed other advantages such as improved durability for certain types of soil. Studies are still underway to achieve a better understanding of the reinforcement mechanisms.

REFERENCES

1. H. C. Gardner, *Int. Fiber J., 10*(4), 36 (1995).
2. Y. Wang, in *Proceedings of the Second International Textile Environmental Conference (Ecotextile '98),* 1998.
3. ACI Committee 544, State-of-the-art report on fiber reinforced concrete. 544.1R-82 (reapproved 1986), American Concrete Institute, Detroit, 1982.
4. J. G. Keer, in *New Reinforced Concretes: Concrete Technology and Design* (R. N. Swamy, ed.), Surrey University Press, Surrey, U.K., 1984, Vol. 2, pp. 2–105.
5. A. Bentur, and S. Mindess, *Fiber Reinforced Cementitious Composites,* Elsevier, London, 1990.
6. Y. Wang, S. Backer, and V. C. Li, *J. Mater. Sci., 22,* 4281 (1987).
7. *Fibermesh Company Product Literature,* Fibermesh Co., Chattanooga, TN, 1989.
8. ACI Committee 544, Design consideration for steel fiber reinforced concrete. ACI 544.4R-88, American Concrete Institute, Detroit, 1988.
9. Y. Wang, A. H. Zureick, B. S. Cho, and D. E. Scott, *J. Mater. Sci., 29*(16), 4191 (1994).
10. Y. Wang, in *Disposal & Recycling of Organic and Polymeric Construction Materials* (Y. Ohama, ed.), E & FN Spon, London, 1995, pp. 247–305.
11. Y. Wang, in Brittle Matrix Composites 5 (A. M. Brandt, V. C. Li, and I. H. Marshall, eds.), Woodhead Publishing, Cambridge, 1997, pp. 179–186.
12. T. S. Ingold, *The Geotextiles and Geomembranes Manual,* Elsevier Advanced Technology, New York, 1994.
13. D. R. Freitag, *J. Geotech. Eng., 112*(8), 823 (1986).
14. D. H. Gray and T. Al-Refeai, *J. Geotech. Eng., 112*(8), 804 (1986).
15. S. A. Ola, *Eng. Geol., 26* (2), 125 (1989).
16. W. W. Freed, U.S. Patent 4,790,691 (December 13, 1988); U.S. Patent 4,867,614 (September 19, 1989).
17. T. Al-Refeai, *Geotextiles Geomembr., 10,* 319 (1991).
18. R. C. Ahlrich and L. E. Tidwell, Report No. WES/TR-GL-94-2, Army Engineer Waterways Experiment Station, Vicksburg, MS, 1994.
19. M. H. Maher, and D. H. Gray, *J. Geotech. Eng., 116*(11), 1661 (1990).
20. D. A. Charleson and R. A. Widger, in *Proceedings of the Canadian Geotechnical Conference,* 1989, p. 111.
21. W. P. Grogan and W. G. Johnson, Report No. WES/TR/CPAR-GL-94-2, Army Engineer Waterways Experiment Station, Vicksburg, MS, 1994.
22. W. W. Crockford, W. P. Grogan, and D. S. Chill, in *72nd Annual Meeting of the Transportation Research Board,* 1993, Paper 930888.

23. S. M. Sangineni, M. S. Thesis, Texas A&M University, 1992.
24. D. Causby, Special Project Report, School of Textile & Fiber Engineering, Georgia Institute of Technology, May 1996.
25. D. J. Hoare, *Proc. Int. Conf. Soil Reinforcement, 1,* 47–52 (1977).
26. Y. Wang and J. D. Frost, Report to Consortium on Competitiveness for the Apparel, Carpet, and Textile Industry (CCACTI), 1997.
27. Fibers for Soil Stabilization, *Georgia County Government,* 10–13 (January 1997).
28. D. Boyd, *Georgia Milepost* 6 (Spring 1997).

POLYM.–PLAST. TECHNOL. ENG., 38(3), 547–567 (1999)

CARPET RECYCLING: DETERMINING THE REVERSE PRODUCTION SYSTEM DESIGN

MATTHEW J. REALFF,*,[1] JANE C. AMMONS,[2] and DAVID NEWTON[2]

[1]*School of Chemical Engineering*
[2]*School of Industrial and Systems Engineering*
Georgia Institute of Technology
Atlanta, Georgia 30322-0100

Abstract

Roughly 4 billion pounds of carpet are disposed of in the United States each year. This carpet is composed of a significant fraction of nylon, polypropylene, and polyester fiber. A key limiting factor to recycling is effective design and development of the reverse production system to collect and reprocess this large volume of valuable material. A reverse production system is composed of material and chemical recycling functional elements interconnected by transportation steps. In this article, we develop a mixed-integer programming model to support decision-making in reverse production system design. To illustrate its use and applicability, we apply the model to a representative U.S. carpet recycling industrial case study. The overall economic feasibility of recycling is strongly dependent on the volumes that can be expected from investments in collection infrastructure. The geographic location of processing centers influences the network economics, and the subdivision of recycling tasks to avoid the shipment of low value material is proposed as an effective strategy for carpet recycling.

* To whom correspondence should be sent.

Key Words: Nylon recycling; Reverse logistics; Environment; Carpet reuse; Mathematical programming.

INTRODUCTION

The recycling of thermoplastics has been technically feasible from the first conception and synthesis of this broad class of materials. It has been the economic viability, societal inertia, and costs of establishing the necessary systems to recycle them that have been the highest barriers to widespread adoption of "closed-loop" production systems. The main technical challenges center on processes to extract materials from the products in which they have been embodied. This must be done with minimum effort and cost, with the resulting material in forms pure enough to guarantee physical properties. The combination of material and chemical recycling tasks, suffixed by a set of distribution tasks that connect to the final end use, constitutes a *reverse production system* (RPS). Figure 1 depicts the general structure of the RPS and its associated forward production system.

The central theme of this article is the development of models to support the construction of efficient reverse production systems. This means simultaneously considering the end uses to which the recycled material should be directed, the tasks that will regenerate the material from products, and the appropriate scale and location of those tasks. In addition, the structure of the RPS will not be static over time, because recycling technologies, economic incentives, and volumes of material are in flux. We will present a model

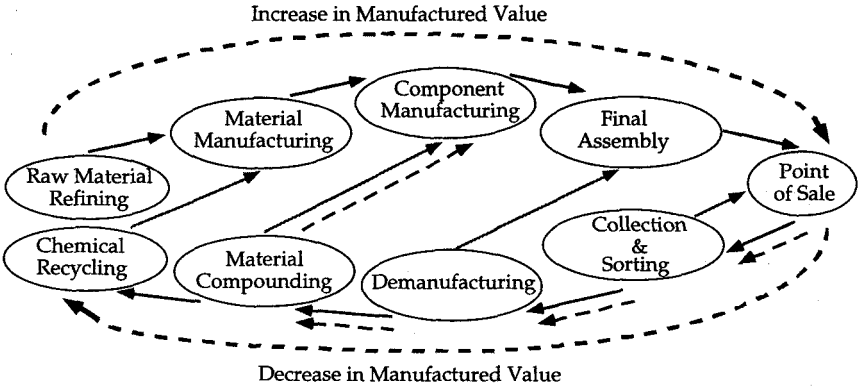

FIG. 1. Material flows in forward and reverse production systems.

that supports a decision-maker in addressing these questions at a strategic level.

To illustrate the application of the model to polymer recycling, we will use carpet, as this is the focus of significant industrial effort to establish reverse production systems and has many of the features of any product containing significant fractions of thermoplastic materials. A useful starting point is to estimate the overall magnitude of the problem, both in terms of material volumes and overall value. Some important statistics related to carpet production which are relevant to recycling are given in Table 1 (1).

The most striking feature of the waste produced by replacing existing carpet is not the landfill volume it generates, about 1% of the total, or the cost of disposal, about $100 million, based on a landfill cost of $50/ton, but the lost opportunity of the material value. This material is valued at $750 million, based on nylon staple and BCF shipments and a price of $0.50/lb. Thus, if diverted from landfill, nylon carpet represents a vast untapped source of raw material. However, the question remains: How to capture this value?

PREVIOUS WORK

Today, much of the published research in reverse productions systems is product- or system-specific and generally features a scope of the problem definition

TABLE 1
U.S. Statistics Relevant to Carpet Recycling Figures for 1995

Overall Carpet Statistics	
Total carpet sales	1.57 billion sq. yards
Total carpet weight	6.8 billion lbs.
Total value of sales	9.5 billion
Replacement market	2/3 of total
Residential market	2/3 of total
Commercial market	1/3 of total
Broadloom Carpet Market	
Homeowner purchase	62%
Specifier purchase	13%
Nylon Fiber	
% of face fiber market	63%
Nylon staple & BCF shipments	1.8 billion lbs.

Source: Ref. 1.

that varies among authors. A large proportion of the current research is being conducted in Europe because of a greater awareness for the need to recycle and a generally more proactive stance by governmental agencies. Examples of current research on recycling and resource recovery for specific materials such as aluminum, building materials, paper, plastics, iron, and sand include Refs. 2–6. Materials recycling models are complemented by models for packaging recycling (7–10) and durable-product recycling (11). Previous work in carpet recycling studies include Ref. 12, which presents an analysis of the economics and engineering issues associated with carpet recycling. This article builds on the initial work in carpet recycling infrastructure design described in Ref. 13. We are unaware of any other analytic approaches for carpet reverse production system design. Perhaps closest to the work described here are the preliminary models proposed in Ref. 14 and the model given in Ref. 6.

In the next section, we present a description of our model, its assumptions, and the mathematical form of the reverse production system problem; the details of the formulation are given in the Appendix. In the section Model Application to Strategic Infrastructure Design, an example of the model is presented to address a specific strategic question for a recycling network based loosely on an existing network developed by DuPont. In the final section, we provide conclusions and directions for future work.

REVERSE PRODUCTION SYSTEM MODEL

The mathematical description given in this section is an abstract and reasonably general model to describe reverse production system allocation/location problems of both design and operational types. The primary purpose of the model is to aid in decision-making at the strategic level of recycling infrastructure design. We do not envision the model being used to actually coordinate the operation of such a system once the basic design has been established, because the logistics component is not detailed enough. At the level of operation, the problem should be capable of being cast into a standard logistics formulation.

Basic Model Elements

The framework of our model is a general network of reverse production tasks located across a set of sites and connected by transportation links. The model has a basic similarity to the resource task network framework used in chemical engineering scheduling formulations (15).

- *Sites.* These are geographic locations at which various tasks can be performed. The important information describing a site, for our purposes,

is the means to compute distances and available travel modes between it and other sites, the reverse production tasks that either can or are being performed there, and any capacity restrictions on tasks or storage of material.

- *Recycling Tasks.* These are the processes that constitute the reverse production chain. In most cases, the task chain will begin with collection and then go through a series of sorting, separation, and material recycling tasks. The important information about a task is the material types that are consumed and produced by the task, and its cost. The task is assumed to produce given fractions of prespecified material from input materials; for example, a sorting task might produce "nylon carpet" and "other carpet" from "unsorted carpet." The task would have a maximum extent given in terms of pounds of material per time unit. The fractions of material entering the task from the input states must sum to 1, similarly for the output state fractions.
- *Transportation Tasks.* These tasks link the various sites together by transferring material between them. The tasks are specified by the two sites that they connect and by the mode of the transportation that is employed. The shipping costs are assumed to be a linear function of the amount of material shipped by that route. This is obviously an oversimplification, but it is a reasonable approximation for this level of operational analysis.

An illustration of the base case network of tasks is shown in Fig. 2. The carpet is collected at various points, of which only one is shown, and then moved by truck to a central facility where the carpet is sorted and separated into nylon and other types of carpet. The other types of carpet are then moved by truck to another nearby reprocessing facility to be turned into a shoddy material and dirt/latex. As examples, shoddy can be used for furniture stuffing, and the stream of dirt, calcium carbonate, and latex can be used as a soil enhancer (the details of this are not shown). The nylon carpet is further processed through a task that separates the material into three states: nylon, polypropylene, and the dirt/latex backing. The nylon and polypropylene are then subject to transportation tasks so as to transform them into states in which they can be compounded with virgin material in final products. The fate of the dirt and latex materials is the same as that for the other carpet.

To study modifications to this base case, additional model elements can be added. For example, alternative transportation tasks can be added from some of the collection points to a facility that sorts carpet and sends the nylon on to the existing facility but which generates shoddy that can be sold locally. The addition of this structure does not force the material to be routed through these tasks but generates the necessary superstructure such that the optimal network can be selected by the optimization algorithm in its search for the

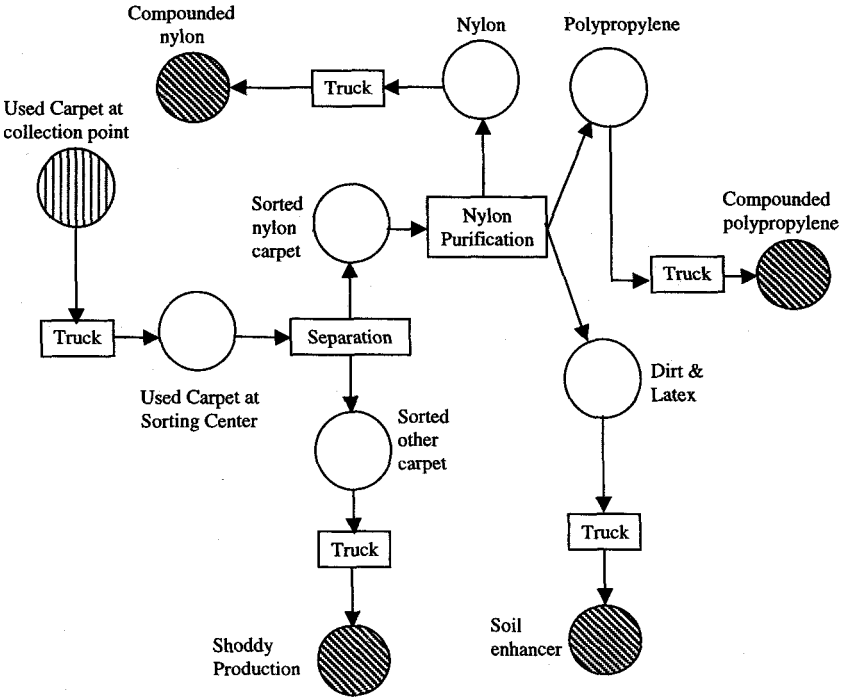

FIG. 2. Task network for carpet recycling.

highest revenue solution. The revenue is determined by the value of the final end materials minus the various costs of operating the network. These costs are both the fixed costs of establishing the capital equipment for the facilities and the variable costs based on the volume of material processed. The model can be configured in a variety of ways, either with the infrastructure fixed to evaluate network operation or variable to assess which sites to open and where to locate recycling tasks.

A verbal description of the model can now be given as follows:

Maximize: *Net Profit* (Revenues − Operating and fixed costs)

Subject to: *Flow balances between sites* (based on material consumed and produced by the tasks located at those sites)

Upper and lower bounds (based on storage, transportation, and processing of material at sites)

Logical constraints on sites (such as the need to open a site before allowing tasks to be located there)

The full mathematical statement of the model can be found in the Appendix. The model was validated using data from an industrial partner's operation and obtained a solution that matched the actual operational values. After validation, we used the model to investigate a number of questions related to the design and operation of the carpet reverse production system design and operations.

To obtain the results described in the following section, the problem required the solution of a formulation of the model presented in the Appendix with 1476 integer variables, 10,117 continuous variables, and 13,447 constraints. This problem was solved on a Windows-based 200 MHz Pentium II personal computer with 48 MB of memory using AIMMS commercial mixed-integer programming software (16). Computational solution time varied from less than 81 s to 130 min.

MODEL APPLICATION TO STRATEGIC INFRASTRUCTURE DESIGN

To examine strategic design issues for carpet recycling, we have worked with a representative industrial system to explore the following:

- The *overall scale* of the network—What is the appropriate volume to be recycling now, and in the future?
- The *morphology* of the network—What is the appropriate distribution and aggregation of recycling tasks?
- The *growth pattern* of the network—How should we evolve the network over time?
- The *end uses* of the materials circulating in the network—Into what products should the materials be recycled?

For our case studies, the used carpet collection points are located throughout the United States. Figure 3 gives the rough geographical location of these points. Currently, there is a single reprocessing site, located in Chattanooga, TN, to which all collected material is shipped by either truck or rail. All case studies are run for a period of 1 year, so collection volumes are considered annual volumes.

In the case studies, various hypothetical alternatives to this arrangement are considered. The first is the default strategy of simply landfilling the material. Other alternative processing networks and growth strategies are considered. Finally, a number of recycled materials are generated from the carpet that are put to specific end uses or, in the case of nylon, can be directed to different end uses. There are three different processes for generating final materials. The first is grinding and separation, which is assumed to generate a stream of nylon pure enough for use as a molding compound. The second is *depoly1*,

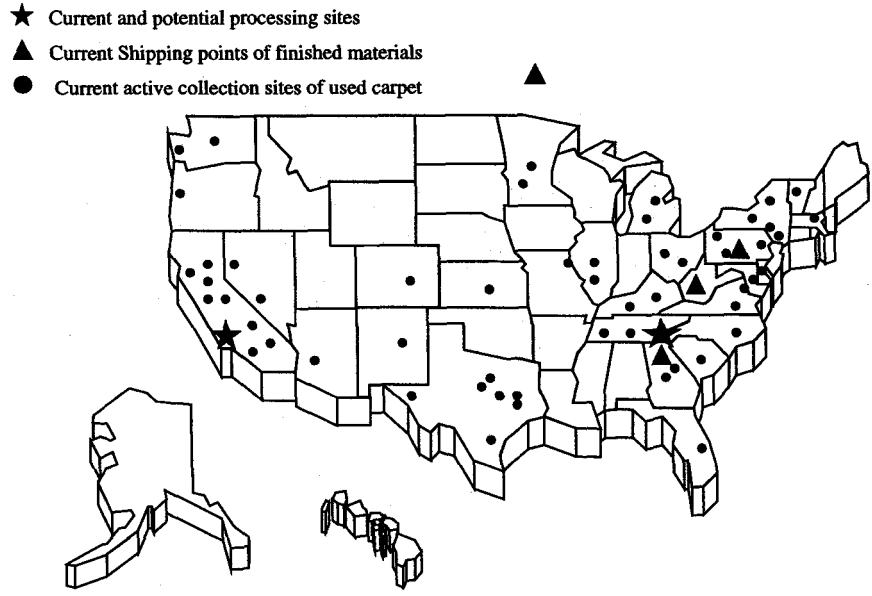

FIG. 3. Geographical distribution of initial carpet collection and reprocessing network.

which converts the nylon 6 back to caprolactam; processes for carrying this out are given in Refs. 17 and 18. The third is ammonolysis, which converts the nylon 6 or 66, back into hexamethylene diamene (HMD), this will be referred to as *depoly2* (19). The various investment and operating costs for these two processes are our estimates and do not represent actual data on the processes from the patents or commercialized processes.

There are several assumptions made in the case studies concerning prices that influence the outcomes. *The case studies do not replicate any existing industrial system*; instead, where possible, prices and carpet composition numbers were obtained from Refs. 12 and 20. The specific numbers used in the study, apart from distances, are given in Table 2. It is assumed that the equipment for shredding can be chosen for any of the sites. The case studies assume that depoly2 can only be located at Kingston, and depoly1 can only be located at the Birmingham site, with the assumption that the depoly1 process cost is estimated to be approximately 1.25 times the cost of the depoly2 process. It is also assumed that either type of depolymerization process can triple its capacity by doubling the equipment cost. This is done to incorporate a notion of "economy of scale" for the processing capability. An additional processing assumption is that sorting can be done at collection sites or at the processing sites, but it is assumed that the setup costs for the collection sites would be

TABLE 2
Data Used in Case Studies

Description	Value
Selling price of caprolactam, from Ref. 20	\$0.90 per pound
Selling price of HMD, from Ref. 20	\$0.72 per pound
Selling price of HMD pellets	\$0.25 per pound
Selling price of compost	0
Selling price of shoddy per pound	\$0.20 per pound
Disposal of waste to incinerator	−\$0.05 per pound
Dumping other types of carpet, from Ref. 12	−\$0.025 per pound
Charge for collection in scenarios	\$0.025 per pound
Cost to sort used carpet	\$0.01 per pound
Cost to set up to sort at a processing site with 60,000,000-lb. capacity	\$1,714 per annum[a]
Cost to set up to sort at a nonprocessing site with 60,000,000-lb. capacity	\$51,714 per annum
Cost to set up for grinding; 60,000,000-lb. capacity	\$1,534,000 per annum
Cost of grinding	\$0.01 per pound
Cost to set up for depoly2; 100,000,000-lb. capacity	\$6,010,000 per annum
Cost to set up for depoly2; 200,000,000-lb. capacity	\$9,080,000 per annum
Cost to set up for depoly2; 400,000,000-lb. capacity	\$13,760,000 per annum
Cost to set up for depoly1; 100,000,000-lb. capacity	\$7,570,000 per annum
Cost to set up for depoly1; 200,000,000-lb. capacity	\$11,430,000 per annum
Cost to set up for depoly1; 400,000,000-lb. capacity	\$17,320,000 per annum
Cost to pelletize, nylon or polypropylene, from Ref. 13	\$0.09 per pound
Cost of shipment	\$0.078 per ton per mile
Cost for opening processing site (Kingston or Birmingham)	\$1,000,000 per annum
Carpet makeup used, from Ref. 12	Nylon 66: 40% Nylon 6: 27.5% Polypropylene: 21% Polyester: 10.5% Waste: 1%

[a] Annualized costs are based on taking the total capital costs and depreciating them over 7 years to generate an annualized equivalent cost.

more expensive due to the necessity of having to rent or own additional warehouse space.

Information on U.S. population density obtained from the United States Census Bureau was used to allocate collection distribution among the various sites so that carpet volume collection is distributed according to population in the collecting areas. As volume is increased, it is done uniformly throughout the network; for example, it is assumed that if carpet collection volume is doubled overall, collection is simply doubled at each collection location.

Case Study 1. Overall Scale of the Network

The first case study is a simple exercise to demonstrate the capabilities and operation of the model. For this case study, we investigate the impact of volume—how much used carpet is collected for reprocessing—on the optimal processing and shipping configuration of the network. For this study, we consider adding a potential West Coast collection center to the existing system shown in Fig. 3 and assume that unsorted, used carpet is shipped to one of two collection centers: Los Angeles, California or Chattanooga, Tennessee. After processing, the recycled nylon fiber is then sent to Kingston, Ontario or Birmingham, Alabama, as shown in Fig. 4. Because this process has only two cen-

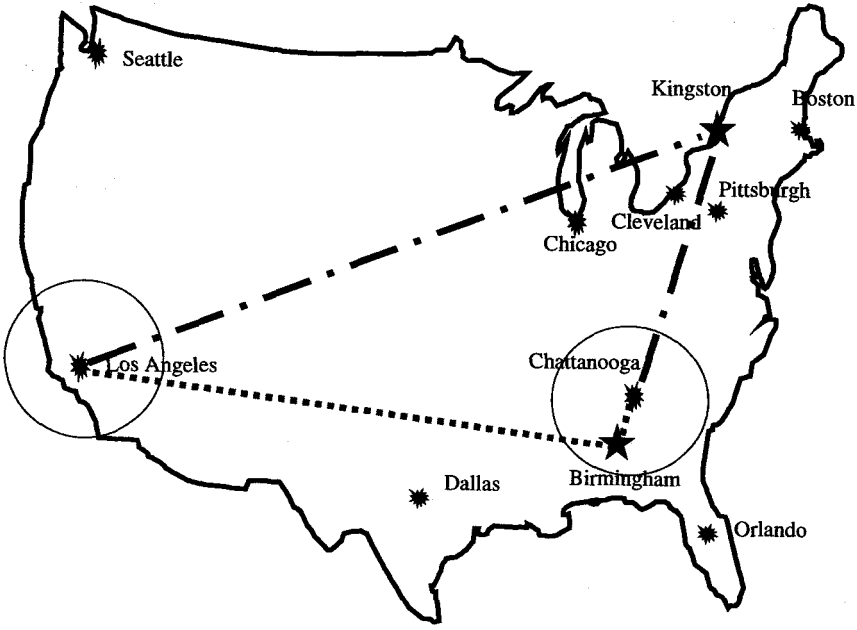

FIG. 4. Aggregated processing and reuse network for case study 1.

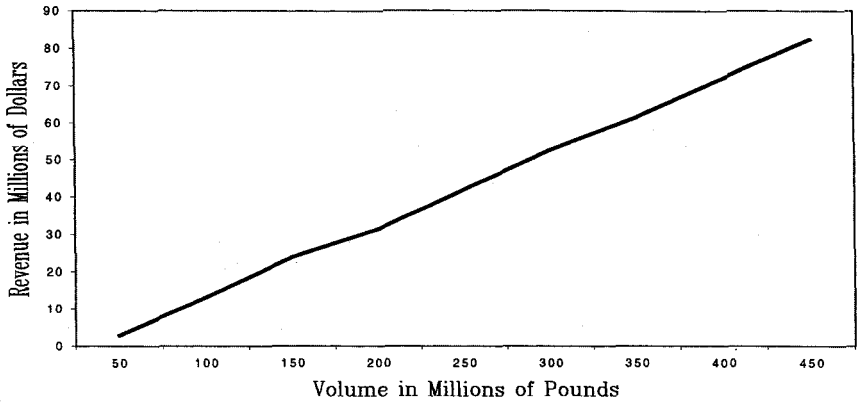

FIG. 5. Net revenue as a function of carpet collection volume for case study 1.

tralized collection sites, this will be referred to as the *aggregate* case scenario. To determine the best network configuration at different volumes, the model was run at collection volumes that were parametrically varied from 50 million pounds to 450 million pounds in increments of 50 million pounds.

The optimal configuration and resulting net revenue were determined for each level of carpet collection volume. Because depoly1 can only process nylon 6, depoly2 tends to dominate the solutions, despite the closer proximity of Birmingham to the majority of the collection sites and lower value of HMD; this shows that volume is a strong driver of infrastructure investment. This is due to the fact that in the case study data, nylon 6 only makes up 27.5% of carpet collections, whereas nylon 66 combined with nylon 6 makes up 67.5% of all carpet collections. The net revenue associated with the optimal solution obtained for each level of collection volume is given in Fig. 5. The revenue curve is strictly monotonic, increasing over the covered interval. This would indicate that volume is a powerful driver of the derived revenue with the values used in this case study. This is similar to the result found in Ref. 13.

Case Study 2. Morphology of the Network

Here, we wish to investigate how the optimal structure of the reverse production system is influenced by the problem parameters. For this case study, the task of separating the carpet into nylon and other types was allowed to be allocated to different geographic sites and the shoddy generation task treated as a separate investment. This generates different possible network structures, as carpet can be processed in a separate location, near collection centers with reasonable geographic density, such as California, rather than at one facility lo-

cated in the eastern half of the United States. This allows a more diffuse collection network, which we designate as the *disaggregate* scenario. Nine different U.S. population centers were chosen, as shown in Fig. 6. Using the same data values except for network structure as in the first (aggregate) case study, again the collection volumes were varied from 50 million to 450 million pounds; depoly1 can be located at Birmingham, whereas depoly2 can be located at Kingston.

As in the first case study, the optimal configuration and resulting net revenue were determined for each level of carpet collection volume. For these comparable data sets, a disaggregated network structure seems to dominate the aggregate one because the profits are consistently higher for the disaggregate scenario compared to those found for the aggregate scenario, as shown in Fig. 7. However, note that the shapes of the two curves are similar.

The relatively higher profits for the disaggregate scenario are believed to be due to a lower average transportation cost, as a large percentage of the U.S. population is to be found on the East Coast. The similar shape of the curves result from similar decisions being made about which processes should be

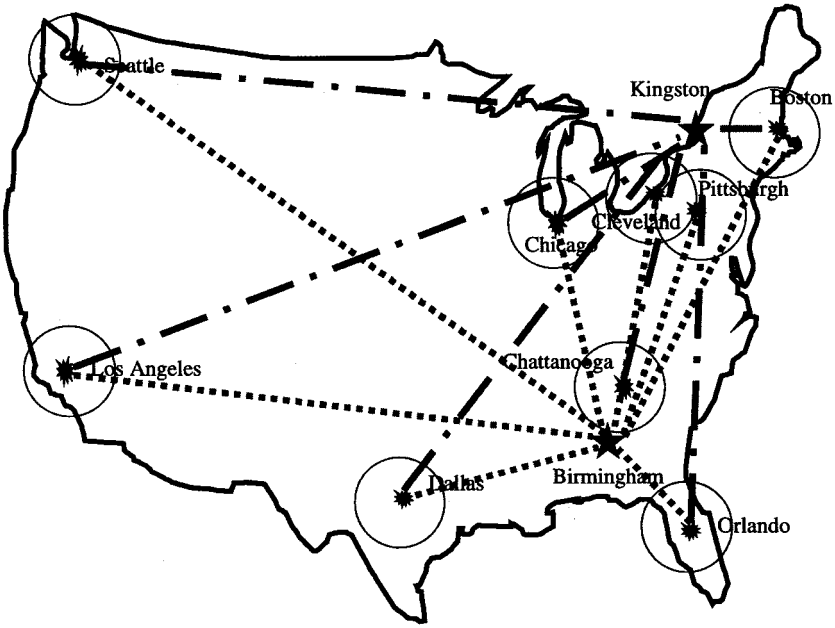

FIG. 6. Disaggregated reverse production network used in case study 2.

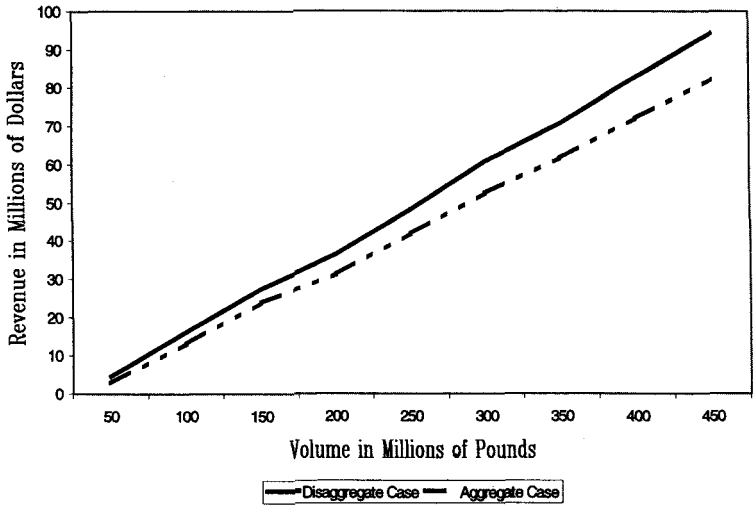

FIG. 7. Net revenue at various collection volumes for two alternative scenarios.

used at each collection level. These would seem to indicate that decisions are based more on collection volume than morphology of the network. Kingston once again dominated the solution because of the greater versatility of the depoly2 process.

Case Study 3. Growth Pattern of the Network

In this case study, we examine the utility of the model for determining the growth pattern of the network. One way to demonstrate this is by examining the way the production capacity evolves in the optimal solutions for growing collection volumes in the previous case studies. At every level where production occurs, shoddy production is chosen for the optimal solution because its production equipment is relatively less expensive than the depolymerization equipment and there are certain carpet types that would have to be landfilled if this option was not chosen.

Depoly2 is also chosen at some level for each collection volume except at the lowest collection levels of the aggregate scenario, as it can impart a higher value to the nylon 66 carpet waste, which makes up most of the used nylon carpet. For the first two case studies, the solution was selecting from among three levels of the depoly1 and depoly2 production capabilities: 100, 200, and 400 million pounds of nylon carpet. The 400 million pound level was never

TABLE 3
Level of Depoly1 Production Capacity in the Optimal Solutions

	Aggregate case		Disaggregate case	
Millions of pounds	Depoly1 100-mmlb capacity	Depoly1 200-mmlb capacity	Depoly1 100-mmlb capacity	Depoly1 200-mmlb capacity
50–300	No	No	No	No
350–450	Yes	No	Yes	No

TABLE 4
Level of Depoly2 Production Capacity in the Optimal Solutions

	Aggregate case		Disaggregate case	
Millions of pounds	Depoly2 100-mmlb capacity	Depoly2 200-mmlb capacity	Depoly2 100-mmlb capacity	Depoly2 200-mmlb capacity
50	No	No	Yes	No
100–150	Yes	No	Yes	No
200–450	No	Yes	No	Yes

chosen in these scenarios, and so will not be referred to again. Tables 3 and 4 show the level of depoly1 and depoly2 production capacities included in the optimal solution for the different collection volumes in the aggregate and disaggregate scenarios.

The optimal solutions for the aggregate and disaggregate cases are the same except at the 50 million pound level. For the aggregate case, neither depolymerization process is viable at 50 million pounds (mmlb) and grinding and pelletizing was done in Chattanooga. For the disaggregate case, the lower collection and shipping costs allow the investment in the relatively expensive depoly2 process to be profitable even at 50% of its capacity. This is particularly important if we are unable to accurately predict the volumes that will be returned since there is a wide scope for making profit even if volumes are substantially less than predicted capacity. This couples the morphology, aggregate or disaggregate, with the collection volume: The optimal decision at the same volume level is different for the two morphologies.

TABLE 5
Production Amount of Nylon Pellets at Different Collection Levels for Both Aggregate and Disaggregate Cases

Million of pounds of collection volume	Millions of pounds of nylon pellets produced and sold
50, 100	0.0
150	3.8
200, 250	0.0
300	27.7
350, 400	0.0
450	11.5

Case Study 4. End Uses of Materials

For this final case study, we wish to explore the *end uses* of the materials circulating in the network—how to obtain the highest value for the materials circulating through the network. Nylon 6 carpet is generally of higher intrinsic value for the processes used in this study, as it can be robustly used for both depolymerization processes and can be converted into the higher-value caprolactam. Yet, we found that in most of the optimal solutions, nylon 6 was instead used as a lower-valued material due to processing limitations.

There were also several times when nylon pellets were sold without going through depolymerization despite the possibility of adding value to the material. This is shown in Table 5. At the levels which nylon pellets were produced, capacity on the current set of equipment had been reached, but it was not profitable to open a larger depolymerization process at the given collection volume. These are also the breakpoints found in Tables 3 and 4 as well as the concavities experienced in the curves of Fig. 7. Consequently, nylon 6 was used for HMD or for pelletizing. At these collection volumes, the resulting production network is not getting the highest value from the carpet due to capacity limitations.

CONCLUSIONS

The model results show several qualitative trends about systems for carpet recycling. First, the volume of carpet recycled significantly impacts the feasi-

bility of certain processing options and the overall economics of recycling. Different capital-intensive processes become feasible at various levels of volume and tend to crowd out small processes because of their ability to generate high-value, high-purity commodity chemicals that can be sold as virgin material on the spot market. Between the jumps in capacity that are natural with these large-scale investments, other less capital-intensive, lower-volume processes can usefully consume the carpet material. The difficulty is in predicting the elasticity of the volume with respect to either the price charged to take the carpet or the price paid to the carpet owner. Second, the ability to consume all the collected carpet is advantageous. The disposal of a significant fraction of the carpet, either whole because of the inability to recycle the particular face fiber, or the material generated by separation or removal of the high value fiber, can lower the overall network profit significantly. This suggests that collaborations between companies engaged in carpet recycling will profit all parties, as the costs of running the collection and sorting parts of the network will be shared over a broader material base. Third, the more distributed the sorting task can become, the better the network performs; this is driven by the fact that the heavy carpet is not shipped only to be discarded. This can result in the ability to have higher capital investment in the chemical recycling and thus generate higher-value materials at lower volumes. The enabler of distributed sorting is low-cost identification technology, which has recently been developed for carpet (21).

Overall, we believe that this type of strategic model can be a useful tool to help scope the development of a recycling network for a variety of products over time. It can demonstrate the sensitivity of revenues to volume assumptions and provides the basis for doing a robust design to account for the uncertainties in price and volume that are frequently encountered in recycling operations.

APPENDIX: MATHEMATICAL MODEL

The mathematical model for reverse production system design and operation is developed using the following notation for indices, decision variables, and parameters. Because some of the decision variables are integer in definition, the formulation is developed as a mixed-integer programming problem. First, we define indices used to distinguish model elements in Table A1.

For ease of notation, we have distinguished between different groups of parameters and variables using superscripts, as given in Table A2. In Table A3, the notation for the decision variables used in the model is defined and Table A4 presents the notation used to define parameters for the model. Using this notation, the mixed-integer programming model for reverse production systems strategic infrastructure determination is stated in Table A5.

TABLE A1
Model Indices

i	Sites
j	Material type
m	Transportation mode
p	Process type
q	Replication of recycling task
t	Time period

TABLE A2
Model Superscripts

c	Collection
r	Storage
s	Site
h	Transportation
d	Material sales

TABLE A3
Model Decision Variables

M_{ijt}	Amount of material collected of type j at site i at time period t
S_{ijt}	Amount of material stored of type j at site i at time period t
$H_{iji'mt}$	Amount of material shipped from site i to site i' of type j using transportation mode m at time period t
D_{ijt}	Amount of material sold at site i of type j at time period t
ξ_{ipt}	Extent of process p performed at site i during time period t
$y_i^{(c)}$	1 if collection is to be performed at site i, 0 otherwise
$y_{ii'm}^{(h)}$	1 if shipment is to be allowed between sites i and i' by transportation mode m, 0 otherwise
y_{ipq}	1 if replication q of process p is to be allowed at site i, 0 otherwise
$y_i^{(r)}$	1 if storage is to be allowed at site i, 0 otherwise
$y_{ij}^{(d)}$	1 if material j is allowed to be sold at site i, 0 otherwise
$y_i^{(s)}$	1 if site i is to opened, 0 otherwise

TABLE A4
Model Parameters

P_{ijt}	Price of selling material j at site i at time t
$K_i^{(r)}$	Charge per unit per time period for storage at site i
$K_i^{(c)}$	Charge per unit per time period for collection at site i
K_{ip}	Charge per unit flow per time period for process p at site i
$K_{ii'm}^{(b)}$	Transportation cost in unit flow per distance from site i to i' for transportation mode m
$b_{ii'm}$	Distance from site i to i' by transportation mode m
$f_i^{(s)}$	Fixed cost of opening site i
$f_i^{(r)}$	Fixed cost of storage capability at site i
$f_i^{(c)}$	Fixed cost of collecting material at site i
f_{ip}	Fixed cost of process p at site i
$f_{ii'm}^{(h)}$	Fixed cost for transportation from site i to site i' by transportation mode m
$e_{ijt}^{(c)}$	Maximum capacity for collection of material type j at site i at time period t
$e_{ij}^{(d)}$	Maximum amount of material type j that can be sold at site i in any time period
$e_i^{(r)}$	Maximum amount of material that can be stored at site i in any time period
$e_{ii'm}^{(h)}$	Maximum amount of material that can be shipped for site i to i' by transportation mode m
e_{ipt}	Maximum amount of material that process p can produce at site i at time period t
$\alpha_i^{(r)}$	1 if storage is allowed at site i, 0 otherwise
$\alpha_{ij}^{(d)}$	1 if material j can be sold at site i, 0 otherwise
$\alpha_{ii'm}^{(h)}$	1 if shipment by transportation mode m is allowed between sites i and i', 0 otherwise
α_{ip}	1 if process p is allowed at site i, 0 otherwise
$\alpha_i^{(c)}$	1 if collection is allowed at site i, 0 otherwise
ρ_{jp}	Proportion of material type j consumed by process p
ρ'_{jp}	Proportion of material type j produced by process p

TABLE A5
Mixed-Integer Programming Model for Reverse Production Systems

		Net revenue
Maximize:		
$\sum_t \sum_i \sum_j P_{ijt} D_{ijt}$	=	Sales revenue
$-\sum_i (f_i^{(c)} y_i^{(c)} + f_i^{(s)} y_i^{(s)} + f_i^{(r)} y_i^{(r)})$		
$-\sum_i \sum_p \sum_q f_{ip} y_{ipq} - \sum_i \sum_{i' \neq i} \sum_m f_{ii'm}^{(h)} y_{ii'm}^{(h)}$		− Fixed costs
$-\sum_t \sum_i \sum_j K_i^{(r)} S_{ijt}$		− Storage costs
$-\sum_t \sum_i \sum_j K_i^{(c)} M_{ijt} - \sum_t \sum_i \sum_p K_{ip} \xi_{pit}$		− Collection and processing costs
$-\sum_t \sum_i \sum_j \sum_{i' \neq i} \sum_m K_{ii'm}^{(h)} b_{ii'm} H_{iji'mt}$		− Shipping costs
Subject to:		
$S_{ijt} = M_{ijt} + S_{ijt-1} - \sum_p \rho_{jp} \xi_{ipt} + \sum_p \rho'_{jp} \xi_{ipt}$		Net conservation of flow
$+ \sum_{i' \neq i} \sum_m H_{i'jimt} - \sum_{i' \neq i} \sum_m H_{iji'mt} - D_{ijt}$	$\forall\, i, j, t$	
$y_i^{(c)} \leq y_i^{(s)}$	$\forall\, i$	Logical variable requirements
$y_{ipq} \leq y_i^{(s)}$	$\forall\, i, p, q$	
$y_i^{(r)} \leq y_i^{(s)}$	$\forall\, i$	
$y_{ij}^{(d)} \leq y_i^{(s)}$	$\forall\, i, j$	
$y_i^{(c)} \leq \alpha_i^{(c)}$	$\forall\, i$	
$y_{ipq} \leq \alpha_{ip}$	$\forall\, i, p, q$	Capacity constraints
$y_i^{(r)} \leq \alpha_i^{(r)}$	$\forall\, i$	
$y_{ij}^{(d)} \leq \alpha_{ij}^{(d)}$	$\forall\, i, j$	
$y_{ii'm}^{(h)} \leq \alpha_{ii'm}^{(h)}$	$\forall\, i, i' \mid i \neq i', m$	
$y_{ipq+1} \leq y_{ipq}$	$\forall\, i, p, q$	
$M_{ijt} \leq e_{ijt}^{(c)} y_i^{(c)}$	$\forall\, i, j, t$	
$H_{iji'mt} \leq e_{ii'm}^{(h)} y_{ii'm}^{(h)}$	$\forall\, i, j, i' \mid i \neq i', m, t$	
$S_{ijt} \leq e_{ij}^{(r)} y_{ij}^{(r)}$	$\forall\, i, j, t$	
$D_{ijt} \leq e_{ij}^{(d)} y_{ij}^{(d)}$	$\forall\, i, j, t$	
$\xi_{ipt} \leq \sum_q e_{ipt} y_{ipq}$	$\forall\, i, p, t$	
$M_{ijt}, S_{ijt}, H_{iji'mt}, D_{ijt}, \xi_{ipt} \geq 0$	$\forall\, i, j, i' \neq i, p, m, t$	Variable restrictions
$y_i^{(c)}, y_{ii'm}^{(h)}, y_{ipq}, y_i^{(r)}, y_{ij}^{(d)}, y_i^{(s)} \in \{0, 1\}$	$\forall\, i, j, i' \neq i, p, m, q$	

ACKNOWLEDGMENTS

This research has been partially supported by the Consortium for Competitiveness in Carpet, Apparel and Textile Industries (CCACTI) of the state of Georgia and by the United States National Science Foundation under grant DMI-9800198. The authors are grateful for the generous interaction and guidance provided from many industry experts, and particularly acknowledge the contributions of many helpful people from Interface Inc., Rob Glass of Global-GIX Canada Inc., Howard Janco of Global Industrial Technologies Inc., and especially those from Mark Ryan of DuPont. We would like to thank the editor and the reviewers for their help in improving the clarity of the article. It should not be assumed that the results in the article's case studies can be used to judge the economics of current carpet recycling efforts. Although the data are representative of general trends and qualitative differences, none of the numbers or networks described can be interpreted as the operational reality of any existing company or system.

REFERENCES

1. Carpet and Rug Institute (CRI), *Carpet and Rug Institute Industry Review,* CRI Dalton, GA, 1996.
2. R. Holmes, *Refuse Recycling and Recovery,* John Wiley & Sons, New York, 1981.
3. A. Huttunen, in *Proceedings of the First International Seminar on Reuse* (S. D. Flapper and A. J. De Ron, eds.), Eindhoven University of Technology, Eindhoven, 1996, pp. 177–187.
4. T. L. Pohlen and M. Farris II, *Int. J. Phys. Distrib. Logist. Manag., 22*(7), 35–47 (1992).
5. A. I. Barros, R. Dekker, and V. Scholten, in *Proceedings of the First International Seminar on Reuse* (S. D. Flapper and A. J. De Ron, eds.), Eindhoven University of Technology, Eindhoven, 1996, pp. 23–33.
6. Th. Spengler, H. Püchert, T. Penkuhn, and O. Rentz *Eur. J. Oper. Res., 97*(2), 308–326 (1997).
7. P. Kelle and E. A. Silver, *Oper. Manag., 8*(1), 17–35 (1989).
8. P. Kelle and E. A. Silver, *IIE Trans., 21*(3), 349–354 (1989).
9. L. Kroon and G. Vrijens, *Int. J. Phys. Distrib. Logist. Manag., 25*(2), 56–68 (1995).
10. A. J. D. Lambert and M. A. M. Splinter, in *Proceedings of the First International Seminar on Reuse* (S. D. Flapper and A. J. De Ron, eds.), Eindhoven University of Technology, Eindhoven, 1996, pp. 213–222.
11. H. R. Krikke, A. Van Harten, and P. C. Schuur, *Int. J. Product. Res., 36*(1), 111–139 (1998).
12. L. Lave, N. Conway-Schempf, J. Harvey, D. Hart, T. Bee, and C. MacCraken, *J. Ind. Ecol., 2*(1), 117–126 (1998).

13. J. C. Ammons, M. J. Realff, and D. Newton, *Eur. J. Oper. Res.*, submitted.
14. L. Villaneuva, *The Design of Strategic Collection Systems for Recyclable Materials,* Georgia Institute of Technology, Atlanta, 1992.
15. C. C. Pantelides, in *Proceedings Second Conference on Foundations of Computer Aided Operations (FOCAPO)* (D. Rippin and J. Hale, eds.), CACHE Publications, Austin, TX, 1994, pp. 253–274.
16. J. Bisschop and R. Entriken, *AIMMS, the Modeling System,* Paragon Decision Technology, Haarlem, The Netherlands, 1993.
17. S. Sifniades, A. B. Levy, and J. O. Hendrix, U.S. Patent 5,681,952 (to Allied Chemical Corporation) (1997).
18. T. F. Corbin, E. A. Davis, and J. A. Dellinger, U.S. Patent 5,169,870 (to BASF Corporation) (1992).
19. R. J. McKinney, U.S. Patent 5,302,756 (to E. I. Du Pont de Nemours and Company) (1994).
20. *Chemical Market Reporter, 253*(24) (June 15, 1998).
21. M. R. Costello, in *Third Annual Conference on Recycling of Fibrous Textile and Carpet Waste,* 1998.

POLYM.–PLAST. TECHNOL. ENG., 38(3), 569–579 (1999)

ADVANCED PROCESS RESEARCH AND DEVELOPMENT TO ENHANCE MATERIALS RECYCLING*

E. J. DANIELS

Energy Systems Division
Argonne National Laboratory
9700 S. Cass Ave., Bldg. 362
Argonne, Illinois 60439-4815

Abstract

Innovative, cost-effective technologies that have a positive life-cycle environmental impact and yield marketable products are needed to meet the challenges of the recycling industry. Two polymeric materials-recovery technologies that are being developed at Argonne National Laboratory in cooperation with industrial partners are described in this article.

INTRODUCTION

The materials recovery and recycling industries have historically and will continue to be important to a sustainable society. The value-added services of these industrial sectors conserve material and energy resources, reduce environmental burdens associated with energy use and solid-waste disposal, provide employment, and internationally disseminate wealth. Materials recycling

Published by Marcel Dekker, Inc. www.dekker.com

in the United States is estimated to conserve 2.1×10^{15} kJ/year of energy and reduce CO_2 emissions by 136 million tons/year by recycling about 110 million tons/year of material.

In 1997, the U.S. recycling industry recovered and processed almost 55 million tons of scrap iron and steel from diverse sources, including industrial scrap, obsolete cars and appliances, and municipal waste. The industry also recovered and processed 8 million tons of nonferrous metals, 34 million tons of paper, and 13 million tons of other materials, including scrap tires, automotive fluids and industrial solvents, fibers and cloth, and plastics (1).

As new products are developed, existing products evolve, and environmental constraints on the recycling industry intensify, the recycling industry faces new challenges:

- Substitution of other materials such as plastics for metals, and the consequent reduction of metal content in obsolete products, especially in such consumer durables as cars and household appliances, reduces the economic incentive for collection of these products and recovery of the metals.
- The increasing complexity of materials such as polymer matrix composites and metal matrix composites to meet high-performance applications will require new recycling technology.
- Improved purity and performance specifications for virgin materials engender demand for higher-quality recycled materials.
- Increased expense, unbounded risks, and decreased availability of and/or bans on landfills compel that alternatives be found for disposal of wastes and by-products from recovery processes.

To meet these challenges, innovative cost-effective technologies, particularly novel separation processes, that have a positive life-cycle environmental impact and yield marketable products need to be developed and commercially demonstrated. Argonne National Laboratory, in cooperation with industrial partners, is developing technologies to respond to specific obstacles identified by the recycling industries. Among these are (1) dezincing of galvanized steel scrap, (2) material recovery from auto-shredder residue, (3) high-value plastics recovery from obsolete appliances, and (4) aluminum salt cake recycling. Materials recovery from shredder residue and plastics recovery from appliances are discussed in this article.

MATERIAL RECOVERY FROM AUTO-SHREDDER RESIDUE

Discarded vehicles, which contain as much as 75 wt.% iron and steel, are a primary source of ferrous scrap to the steelmaking industry. After dismantling at the "junk yard" to remove reusable and remanufacturable parts and certain recycled

materials such as batteries, radiators, and catalytic converters, the remaining auto hulks are flattened for transportation to scrap processors. There, the auto hulks with other source materials are fed to hammermill shredders, which shred the hulk into fist-sized pieces of material at the rate of about one hulk per minute. The ferrous and nonferrous metals are recovered from the shredded material, leaving a residual known as automobile shredder residue (ASR), which amounts to 20–25% of the original weight of the vehicle. The generation of ASR in North America is estimated at 3–5 million tons/year. Equivalent quantities are estimated to be generated in Europe and the Pacific Rim.

Automobile shredder residue is a complex, diverse-sized mixture of dirt, glass, wires, wood, tar, rocks, sand, rust, rubber, fibers, fabrics, paper, automotive fluids, moisture, and plastics [polyurethane foams, reinforced polyesters, bulk molding compounds, sheet molding compounds, polyethylene (PE), polypropylene (PP), polyvinyl chloride (PVC), acrylonitrile–butadiene–styrene (ABS), nylons, acrylics, and phenolics]. The composition and density of ASR may change from day to day and site to site as different types of source materials are shredded. The approximate composition for ASR is presented in Fig. 1.

Historically, ASR has been landfilled. As the trend of light-weighting vehicles continues by replacing metals with plastics and other complex materials, the amount of ASR generated per ton of metal recovered from obsolete vehicles will increase, thereby decreasing the economic incentive of the scrap processor to use obsolete cars as a source of recycled metal. New technology is required to recover the recyclable materials from shredder residue to sustain the economic viability of obsolete car recycling.

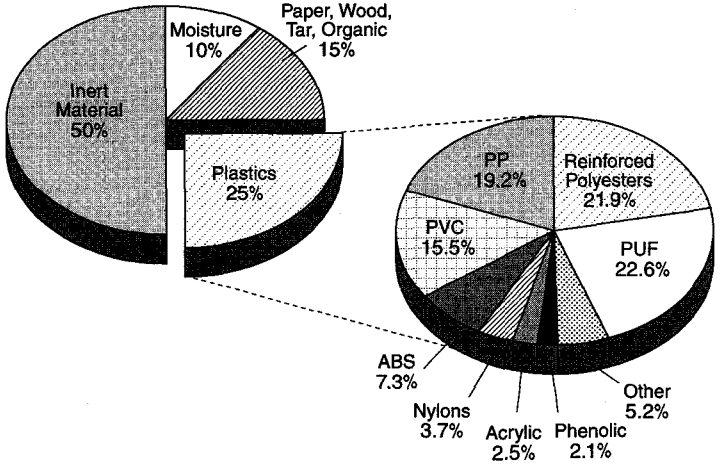

FIG. 1. Approximate composition of ASR. (From Ref. 2.)

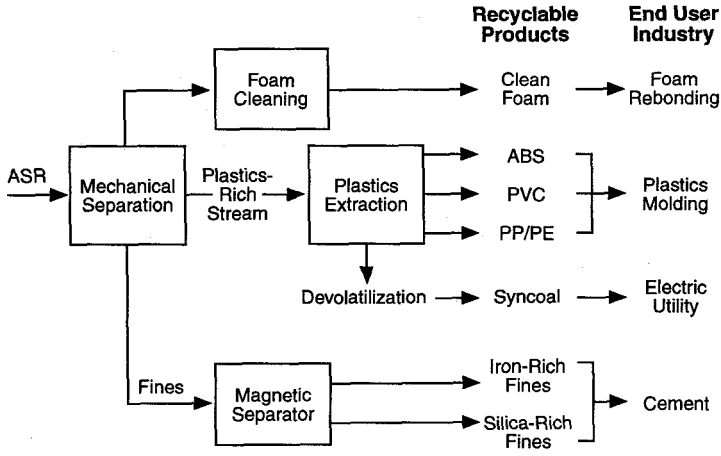

FIG. 2. Argonne strategy for processing shredder residue.

Because of the heterogeneous character of ASR, recovery of recyclable materials is difficult. We approached the problem of materials recovery from ASR by identifying potentially marketable, high-value materials, and then developing separation and purification processes to recover them. The recycling strategy that has evolved is represented by the material flow diagram in Fig. 2. The potentially marketable materials targeted for recovery are polyurethane foam (PUF), inorganic fines for use by the cement industry, and certain thermoplastics, such as ABS, PVC, nylons, PE, and PP, that are compatible with virgin plastics.

Technology Description

The Argonne ASR recycling technology involves several steps (3–6): (1) mechanical separation of the foam, plastics, and fines; (2) polyurethane foam cleaning; (3) upgrading of the fines to meet requirements of the cement industry; (4) recovery of thermoplastics; (5) recovery of energy from the residual material. Our development efforts on the first three of these steps are the most advanced.

Mechanical separation equipment must ultimately be adapted to the equipment existing at individual shredder facilities. Commonly, shredded materials that have had their ferrous components removed by magnetic separation are fed to a trommel to remove fines and then to an eddy-current separator to recover nonferrous metals. In such an arrangement, the fines can be subjected to additional size segregation to recover fines <0.6 cm, followed by magnetic separation to generate an iron-rich fines fraction suitable as an alternative iron unit for the cement industry.

The nonmetallic fraction from the eddy-current separator, combined with an air-classified light fraction if generated in the shredder facility, is the feedstock to the foam recovery unit. A schematic diagram of the foam recovery and cleaning process is given in Fig. 3. A patent is pending on this process (7).

The mixed feed material is routed to a trommel of unique design to separate the foam from a plastics-rich stream containing residual dirt and fines. The dirty foam separated in the trommel is conveyed to a foam shredder, where it is reduced to a consistent size of about 4 × 7 cm. Size reduction is necessary for effective cleaning and subsequent drying of the foam, and it also assists in liberating entrained dirt and metals. The sized foam is processed further to ensure that no entrained metals or rigid noncompressible objects are fed to the downstream cleaning operations.

The sized metal-free foam is washed in a linear washing machine that automatically conveys the foam. The washing solution is water containing a surfactant for liberation of entrained oils and dirt. Wash water is maintained between 50°C and 80°C, depending on the surfactant. The dirty wash water cycles through hydrocyclones, an ultrafilter, and a settling tank prior to recycling it to the wash tank. Oils are skimmed from the top, and entrained solids are screw-conveyed from the bottom of the settling tank for disposal. Effluents from processing 100 tons of dirty foam are about 83 tons clean foam, 13 tons dirt, and 4 tons oily water.

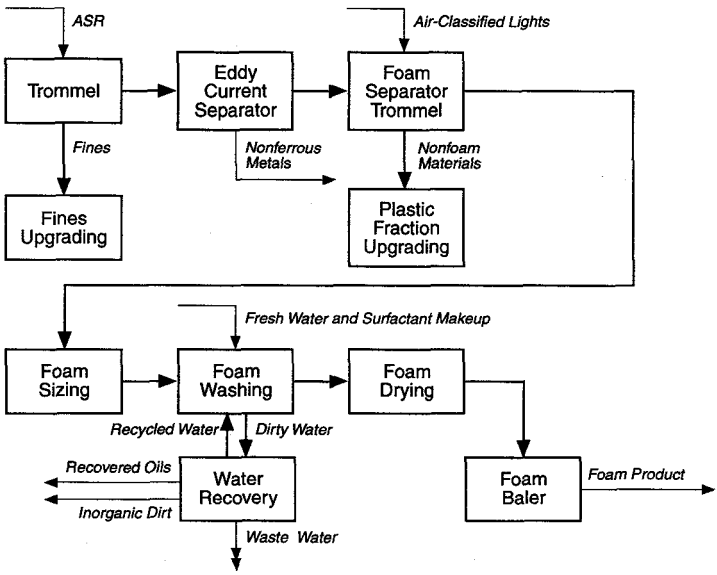

FIG. 3. Schematic diagram of the polyurethane foam recovery process.

The washed foam is rinsed with water at 70°C in another linear washing machine of similar design to the first one. The clean foam is then dried in a linear conveyor dryer with hot air. Residence time in the dryer is less than 10 min to achieve a retained moisture content of less than 1 wt.% in the foam. The clean dry foam is then conveyed to a horizontal baler to densify it for shipment to the customer.

The plastics-rich stream separated in the foam recovery trommel may be processed further to recover and purify target polymers. The specific chemical treatment processes applied depend on the physical and chemical properties of the target product and waste stream. In the laboratory, we have evaluated froth flotation and selective solvent dissolution processes to recover high-purity ABS, PVC, and polyolefins. Process economics favor froth floatation technology, which is discussed in the next section for a specific plastics separation system.

Process Economics

In this article, we present only the economics for the PUF processing/cleaning section, as displayed in Table 1. The cost of equipment for separating the foam and other materials from the shredder residue is site-specific.

The raw materials consumed in virgin PUF applications are valued at $1900–$2200/ton. Our market research suggests that the recovered clean foam could be sold in the scrap foam market at $660/ton.

TABLE 1
Process Economics (Annual Basis) for Polyurethane Foam Recovery and Cleaning

Revenues, $thousand/year	
Polyurethane foam ($660/ton PUF)	300.0
Total revenues	300.0
Operating Costs, $thousand/year	
Chemicals	6.3
Waste disposal	24.0
Utilities	32.3
Labor (one operator/shift)	30.0
Maintenance	25.0
Total operating costs	117.6
Net Income, $thousand/year	182.4
Capital Cost, $thousand	525.0

Note: Capacity of 450 tons/year clean foam (11,000 tons/year ASR feed); single-shift operation.

The annual operating costs for a 450-ton/year facility are estimated at $118,000/year relative to revenues of $300,000/year. Equipment capital cost is estimated at $525,000, yielding a payback in about 3 years.

Status/Future Research

The mechanical separation of foam, plastics, and fines in ASR has been demonstrated in our pilot plant, which has a 2-ton/h feed capacity. This pilot plant includes a shredder, a specially designed four-stage trommel, magnetic separators, an eddy-current separator, and material transport conveyors. This pilot plant can also process other solid-waste streams. To date, we have used this equipment to concentrate plastics from ASR, obsolete appliance fluff, and electronics waste.

The foam separation and purification process has been demonstrated in a batch-operation pilot plant (producing more than 2 tons of clean foam) and in a continuous foam-processing system (0.05 tons/h capacity) installed at an auto-shredder site. The foam recovered from the batch tests was found to meet both the specifications of the market for scrap foam and the performance criteria for new material carpet padding for automotive applications. Operations of the continuous pilot facility have been completed. From these operations, which yielded nearly 3 tons of clean foam product, engineering data for the design of a commercial-scale plant and for confirmation of process economics have been generated.

HIGH-VALUE PLASTICS RECOVERY FROM OBSOLETE APPLIANCES

Appliances are manufactured from a variety of materials, including metals, polymers, foam, and fiberglass. Metals compose more than 75% of the total weight. Appliance recycling has been driven by the value of the steel, with obsolete appliances processed in auto-shredders to recover their metallic content. In the past 15 years, the use of polymers in appliance manufacturing has increased substantially at the expense of metals. As a consequence, a greater volume of nonmetallic fraction (shredder residue or fluff), containing higher-value polymers, is being generated and landfilled by the traditional recycling method.

Landfilling of the fluff represents a significant cost to the metal recovery process and wastes valuable resources. Argonne National Laboratory has developed and patented (8) a process to recover acrylonitrile-styrene-butadiene (ABS) and high-impact polystyrene (HIPS), at high purity, from appliance shredder fluff. Process development and commercial demonstration are being conducted by Argonne in cooperation with Appliance Recycling Center of America.

Technology Description

A schematic of the appliance recycling concept appears in Fig. 4. Obsolete appliances that cannot be reconditioned for resale are partially disassembled in a production-line operation. Hazardous materials, such as polychlorinated biphenals (PCBs) (from old electronic equipment), mercury switches, and refrigerants, are removed. The refrigerants are redistilled to meet original specifications and sold for reuse. Mercury switches and PCBs are disposed of as hazardous waste.

The appliance hulks are then shredded in a hammermill. Ferrous metals are recovered by magnetic separation, and nonferrous metals are recovered by eddy-current separation. Fines and foam (fluff) are removed by air classification. The remaining fraction, constituting about 9% of the original total appliance weight, is fed to the plastics-separation process.

The mixed-plastic feedstock, containing approximately 73 wt.% ABS, 12 wt.% HIPS, 6 wt.% light materials, and 9 wt.% heavies, is granulated to a consistent particle size of about 0.6 cm. The grinding process facilitates the complete liberation of rigid foam from refrigerator plastic-liner materials. The material exiting the granulator is slurried with water and surfactant and pumped to the first-stage density separation tank. In this tank, maintained at a specific

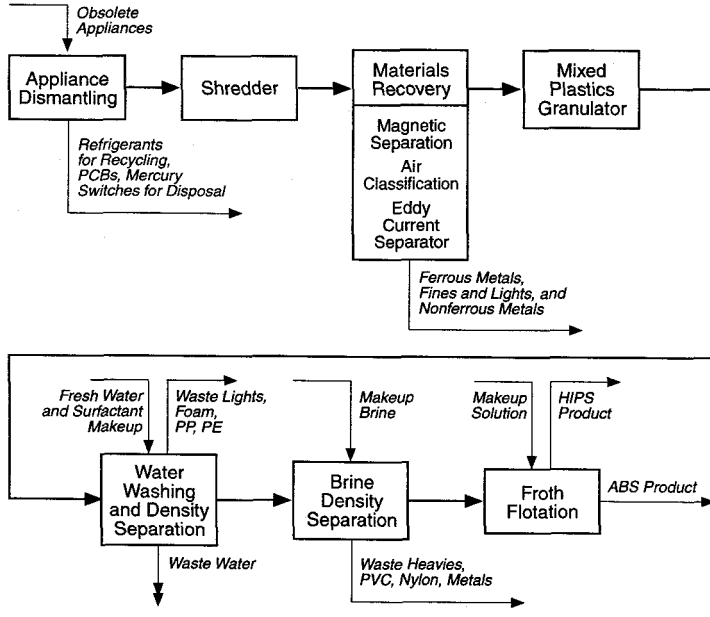

FIG. 4. Schematic diagram of the obsolete appliance recycling process.

gravity of 1.0, the light components (including PP, PE, and rigid foams) float to the top and are separated for disposal. The heavier plastics, including ABS and HIPS, which sink in the separation tank, are also washed in the process. Water and surfactant, with a small purge for quality control, are filtered to remove dirt and recycled.

The bottom slurry from the first-stage separator is dewatered and reslurried with a brine solution at a specific gravity of 1.11. The effluent slurry is pumped to the second-stage density-separation tank, where the heavies sink and the ABS and HIPS particles float. The heavies are dewatered for solid-waste disposal. The mixed ABS/HIPS fraction is washed, dewatered, and fed to the final stage of separation. The brine solution is recovered for internal recycle.

Because ABS and HIPS have essentially the same density (specific gravities of 1.045–1.15), they cannot be separated by traditional sink–float technology. Effective separation requires a froth flotation process, which can separate the two materials on the basis of their respective hydrophilic/phobic characteristics. In the froth flotation separation tank, the HIPS surface is modified by a proprietary solution that causes the HIPS to float and separate from the ABS, which sinks. High-purity ABS is recovered by a single froth flotation separation followed by washing and drying. The recovery of a high-purity HIPS product requires a second froth flotation stage. The product polymers are dewatered, washed, and dried. The proprietary solutions and rinse waters are internally recycled.

Process Economics

The ABS/HIPS recovery process is expected to be highly profitable, as shown by the economics summarized in Table 2. These figures were derived for a plant capacity of 450 kg/h mixed-plastics feed, operating for 8 h/day and 300 days/year. Given appliances with an average weight of 68 kg, of which 9 wt.% is mixed plastics, the annual plant capacity for obsolete appliances would equate to 180,000 units/year. The production capacity of the plant would be 760 tons/year of ABS and 110 tons/year of HIPS.

The market price for virgin ABS is \$1500–\$2200/ton, and for virgin HIPS, it is \$900–\$1100/ton. Our economics are based on recovered ABS and HIPS prices of \$880/ton and \$440/ton, respectively. However, our market research suggests that the quality of the recovered ABS and HIPS could potentially command a higher price if they are marketed for refrigerator/freezer liner, electronic housing, or small-appliance applications. The key to attaining a high price for the ABS and HIPS products is recovering them at greater than 99% purity. ABS and HIPS are not compatible, and the presence of small quantities of one in the other can result in a significant degradation of properties.

TABLE 2
Process Economics (Annual Basis) for ABS and HIPS Recovery from Obsolete Appliances

Revenues, $thousand/year	
ABS ($880/ton ABS)	672.0
HIPS ($440/ton HIPS)	48.0
Total revenues	720.0
Operating Costs, $thousand/year	
Feedstock (credit for avoided disposal)	−24.0
Chemicals	133.4
Waste disposal	4.8
Utilities	39.6
Labor	115.2
Maintenance	17.5
Total operating costs	286.5
Net Income, $thousand/year	433.5
Capital Cost, $thousand	500.0

Note: 1900 tons/year mixed-plastics feed (approximately 180,000 appliances/year); operation 300 days/year, 8 h/day.

Labor and chemicals (makeup for losses of separation solutions) are the major operating-cost components for the process. The process contains no unique or highly expensive equipment; hence, cost and manpower requirements for operations and maintenance should not be exceptional.

Status/Future Research

The density and froth flotation processes have been demonstrated in batch-scale tests, producing nearly 300 kg of product with a greater than 99.5 wt.% ABS content. The recovered material met the specifications of the ABS recycle market. A pilot-scale demonstration unit with a design capacity of 0.5 tons/h mixed-plastics feed has been built and is being operated at the Appliance Recycling Center of America's plant in Minneapolis, MN.

Research activities will focus on improving the efficiency of the separation processes and identifying cost-effective methods to improve the quality and, consequently, market value, of the ABS and HIPS recovered from obsolete appliances.

Research is ongoing to apply this technology to other plastics wastes streams.

CONCLUDING REMARKS

Almost all materials are recyclable. They are not recycled because either a market for the material is not well defined and/or a cost-effective process for recovering the material in a form that meets the needs of the market is not available. To be sustainable, the overall mechanism of collecting, sorting, recovering, processing, and use of scrap materials in the production of new products must provide a sufficient economic incentive to those firms involved in the recovery and supply of the material and to those firms that will use the material.

At Argonne, we are working with industry to develop processes involving novel separation technologies that will conserve energy, reduce wastes, and promote sustainable development. We have focused our efforts on developing cost-effective processes for recovery of high-quality scrap materials from a variety of waste streams.

ACKNOWLEDGMENT

This work was supported by the U.S. Department of Energy, Assistant Secretary for Energy Efficiency and Renewable Energy, under contract W-31-109-Eng-38.

REFERENCES

1. R. J. Garino, *Scrap 13* ,75–89 (1997).
2. B. J. Jody, E. J. Daniels, and A. P. Teotia, in *Conversion and Utilization of Waste Materials* (Taylor and Francis, eds.), American Chemical Society, Washington, DC, pp. 77–104.
3. P. V. Bonsignore, B. J. Jody, and E. J. Daniels, SAE Techn. Paper 910854 (1991), pp. 59–63.
4. B. J. Jody and E. J. Daniels, *Hazardous Waste Hazard Mater. J. 8*, 219–230 (1992).
5. E. J. Daniels, B. J. Jody, and P. V. Bonsignore, *J. Res. Manag. Technol., 20*, 14–26 (1992).
6. B. J. Jody, E. J. Daniels, P. V. Bonsignore, and F. B. Brockmeier, *J. Metals* (February 1994).
7. B. J. Jody, E. J. Daniels, and J. Libera, U.S. Patent Application S.N.08/692.801.
8. B. J. Jody et al., Patent 5,653,867 (to The University of Chicago, Chicago, II) (August 5, 1997).

POLYMER–PLASTICS TECHNOLOGY AND ENGINEERING

INSTRUCTIONS TO AUTHORS

Aims and Scope. The journal *Polymer–Plastics Technology and Engineering* will provide a forum for the prompt publication of peer-reviewed, English language articles such as state-of-the-art reviews, full research papers, reports, notes/communications, and letters on all aspects of polymer and plastics technology that are industrial, semi-commercial, and/or research oriented. Some examples of the topics covered are specialty polymers (functional polymers, liquid crystalline polymers, conducting polymers, thermally stable polymers, and photoactive polymers), engineering polymers (polymer composites, polymer blends, fiber forming polymers, polymer membranes, pre-ceramics, and reactive processing), biomaterials (bio-polymers, biodegradable polymers, biomedical plastics), applications of polymers (construction plastics materials, electronics and communications, leather and allied areas, surface coatings, packaging, and automobile), and other areas (non-solution based polymerization processes, biodegradable plastics, environmentally friendly polymers, recycling of plastics, advanced materials, polymer plastics degradation and stabilization, natural, synthetic and graft polymers/copolymers, macromolecular metal complexes, catalysts for producing ultra-narrow molecular weight distribution polymers, structure property relations, reactor design and catalyst technology for compositional control of polymers, advanced manufacturing techniques and equipment, plastics processing, testing and characterization, analytical tools for characterizing molecular properties and other timely subjects).

Submission. Manuscripts in triplicate (please provide your fax number and e-mail address) should be submitted to the Editor at the following address:

Dr. Munmaya K. Mishra
P.O. Box 5806
Glen Allen, VA 23058-5806, USA
Fax: 1-804-364-2810
E-mail: 751-5990@mcimail.com

If you plan to send your manuscript via any courier service, please use the following address: Dr. Munmaya K. Mishra, Ethyl Corporation, R & D, 500 Spring Street, Richmond, VA 23218-2158, USA; Tel.: 1-804-788-5323.

Please note that if your contribution is acceptable for publication, you will be requested to submit an electronic copy (diskette) of your manuscript. This allows a substantial decrease in production time and ensures that there are no re-keying errors in the article. Please note that once you submit the final copy on diskette, after all revisions, you will not receive proofs since manuscripts will be printed di-

rectly from the electronic copy (after appropriate formatting) and no further editing will be done.

All contributions will be evaluated by at least two independent referees. Submission of a manuscript implies that the work therein has not been published previously and is not under consideration for publication elsewhere in any medium. Authors are solely responsible for the factual accuracy of their papers.

Typing of Manuscript. Manuscripts (including captions, footnotes, and references) must be in English and should be typed double-spaced throughout on only one side of 8.5″ × 11″ or A4 sheets leaving at least 1″ margins on all sides. The first page should contain only (1) the title, the name(s), and address(es) of the author(s), (2) a short title, (3) name, address, fax number, and e-mail of the author to whom correspondence should be sent. An ABSTRACT (up to 250 words) typed double-spaced on a separate page, defining the scope and major conclusions of the work, should precede the main text. The manuscript must also contain a CONCLUSION section.

Key Words. Two lines below the abstract, list four to eight key words that will help in computer searches and indexing.

Units of Measure. Units of measurement, abbreviations, and symbols should follow the International System of Units (SI).

Tables and Illustrations. Tables should be given short informative titles and should be numbered consecutively in Arabic numerals. Tables may be reproduced by photo-offset, i.e., directly from the typed manuscript. Figures in a form suitable for reproduction should be submitted separately from the text as original drawings or as high contrast, unmounted photographs on glossy paper. Lettering on figures should be proportional to the size of the figure to ensure legibility after reduction. Use scale bars on micrographs. Please write the illustration number and author's name in pencil on the reverse of each illustration. All chemical structures should be supplied as artwork suitable for direct reproduction. All figures and tables should be cited consecutively in the text and a list of captions should be provided at the end of the paper.

References. The references should be cited in the text in a sequential manner and the reference numbers should be in parentheses "(1)" [no superscripts or subscripts]. A list of references should be attached on a separate page at the end of the text in the numerical order. Please model your references according to the style of the samples below. References to journals should be given in this order: Initials and last name(s) of author(s), standard abbreviated title of periodical (italicized), volume number (underlined), issue number, only if applicable, in parentheses, first relevant page, year of publication in parentheses, e.g.:

1. M. K. Mishra, *Macromolecules*, 29, 5228 (1996).

References to an authored book, an edited book, and a paper in an edited book should be listed according to the following style, respectively:

2. J. M. Dealy and K. F. Wissbrun, *Melt Rheology and Its Role in Plastics Processing*, Chapman & Hall, London, p. 84–89 (1995).
3. M. K. Mishra, O. Nuyken, S. Kobayashi, Y. Yagci, and B. Sar (eds.), *Macromolecular Engineering: Recent Advances*, Plenum Press, New York (1995).
4. H. Ritter, in *Functional Polymers*, R. Arshady (ed.), pp. 103–113. American Chemical Society, Washington, DC (1996).

If a publication is in press, the reference should be made as complete as possible, e.g., by stating the name of the journal and adding "in press."

Copyrighted Material. Each figure or table taken from a copyrighted source requires a letter from the copyright holder (generally the publisher) granting permission to reproduce it. A credit line acknowledging the source must accompany each table and figure being reproduced. Credit lines should also be used for published material which has not been copyrighted, such as US government publications.

Reprints. The corresponding author of each article will receive 20 free reprints of their article. Additional reprints are available in quantities of 50 or 100 and multiples thereof. Prices apply to orders received before the journal goes to press. An order form *must* be filled out with complete "ship to" instructions and received prior to publication in order to receive your gratis reprints.

Electronic Submission. Authors are requested to also submit the final manuscript in the form of a $3^1/_2''$ disk (PC-compatible preferred) containing the complete manuscript in Microsoft Word for Windows or WordPerfect. Text (including tables) and figures (if in electronic format) should be saved in separate files on the disk. Label the disk with the authors' last names, title of article, abbreviated Journal name, and date. Original figures should be submitted with the final, revised manuscript even if art is submitted electronically. Please provide a list of the software programs used for the art and the text and the file names on the disk. Package the disk in a disk mailer or protective cardboard.

*Develop **stronger, more reliable** ceramic structures for a wide variety of industrial applications for use up to very high temperatures with...*

FINE CERAMIC FIBERS

edited by **ANTHONY R. BUNSELL** and **MARIE-HÉLÈNE BERGER**,
École Nationale Supérieure des Mines de Paris, Evry, France

March, 1999 / 320 pages, illustrated / ISBN: 0-8247-1951-4 / $150.00

This unique reference presents the **most recent techniques** for the manufacture —and the **most recent research** on the behavior—of high performance flexible ceramic fibers used to develop structural materials for applications up to very high temperatures, allowing the optimization of ceramic composites in **jet engine components, heat exchangers, refractory insulators,** and other components.

Demonstrating the physicochemical processes that govern behavior up to high temperatures of ceramic reinforcements under stress, and detailing both apparent limitations and the exciting possibilities for further research, ***Fine Ceramic Fibers***

- describes fibers based on aluminosilicates, α-alumina, mullite, and silicon carbide, as well as filaments such as continuous monocrystals and extremely fine "whiskers"
- reveals the properties of the filaments at high temperatures and analyzes the intimate relationships between the mechanical behavior and the microstructure down to the atomic level
- shows how the scatter of fiber properties can be treated statistically
- illustrates sol-gel processes for manufacturing high-temperature ceramics, including spinning, drying, and ceramization
- reviews production processes of polycrystalline, alumina-based fibers such as Saffil, Altex, Fiber FP, PRD-166, and the Nextel series of fibers
- details the chemistry of the polymer precursors such as polycarbosilane, polytitanocarbosilane, and polysilazane used for the manufacture of silicon carbide and silicon nitride fibers
- explains cross-linking processes used with organosilicon precursors
- describes the production, microstructures, and properties of all commercially available fine SiC fibers, such as the Nicalon and Tyranno fiber series and the latest stoichiometric fibers
- proposes avenues of research to further improve the high temperature performance of the fibers and how an ideal fiber may be developed
- and much more!

Containing over 600 references, tables, and drawings, and photographs—**including almost 90 state-of-the-art micrographs**—this useful compendium is indispensable for materials scientists; polymer, plastics, manufacturing, composite, and ceramics engineers; physical, surface, and colloid chemists; engineers in the aerospace and energy conversion industries; and upper-level undergraduate and graduate students in these disciplines.

CONTENTS

This book is printed on acid-free paper.

Explores complex ceramic microstructures down to the atomic level!

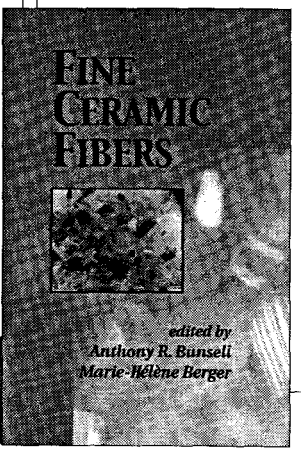

MARCEL DEKKER, INC.
270 MADISON AVENUE, NEW YORK, NY 10016
212-696-9000
HUTGASSE 4, POSTFACH 812, CH-4001 BASEL, SWITZERLAND
061-261-8482
Visit our website at www.dekker.com

Of related interest...

ANDBOOK OF IBER CHEMISTRY

ond Edition, Revised and Expanded

national Fiber Science and Technology Series/15)

ed by

NACHEM LEWIN, *Hebrew University of Jerusalem, Israel.*
Polytechnic University, Brooklyn, New York

M. PEARCE, *Polytechnic University, Brooklyn, New York*

pages, illustrated / ISBN: 0-8247-9471-0 / $275.00

n old and trusty friend, winning its place in the handiest shelf on sheer merit....

his hefty volume **offers a world of surprises** in its compass, s well worth the money to mill labs." *—Textile Asia*

vould make **a very good addition** to the reference section of r or polymer library." *—Polymer News*

ONTENTS

ester Fibers
E. McIntyre
amide Fibers
Robert K. Reimschuessel
propylene Fibers
Irvin Wishman and Gerald E. Hagler
Fibers
Hiro Sakurada and Takuji Okaya
and Related Mammalian Fibers
Julie N. Jones, Donald E. Rivett, and Cyril J. Tucker
Composition, Structure, and Properties
Ruth M. Robson
and Kenaf
Roger M. Rowell and Harry P. Stout
Long Vegetable Fibers: Abaca, Banana, Sisal, Henequen, Ramie, Hemp, Sunn, and Coir
Subhash K. Batra
n Fibers
T. Wakelyn, N. R. Bertoniere, A. D. French, S. H. Zeronian, J. J. Nevell, D. P. Thibodeaux, E. J. Blanchard, T. A. Calamari, A. Triplett, C. K. Bragg, C. M. Welch, J. D. Timpa, W. R. Goynes, H. W. E. Franklin, R. M. Reinhardt, and T. L. Vigo
n Fibers
John Dyer and George C. Daul
lose Acetate and Triacetate Fibers
Harry W. Steinmann
lic Fibers
Vance G. Frushour and Raymond S. Knorr

r Credit Card and
rchase Orders, *and* Customer Service
ALL TOLL-FREE 1-800-228-1160
on.-Fri., 8:30 a.m. to 5:45 p.m. (EST)
FAX your order to 914-796-1772

CORROSION OF CERAMICS

(Corrosion Technology Series/7)

RONALD A. McCAULEY, *Rutgers University, Piscataway, New Jersey*

320 pages, illustrated / ISBN: 0-8247-9448-6 / $145.00

Discusses a wide range of ceramic materials and corrosive environments. Provides engineers and scientists working with ceramics with the information necessary to **explain existing ceramic corrosion problems and create the most corrosion-resistant systems possible.**

CONTENTS

Introduction
Fundamentals
Methods of Corrosion Analysis
Test Corrosion Procedures
Corrosion of Specific Crystalline Materials
Corrosion of Specific Glassy Materials
Properties and Corrosion
Methods to Minimize Corrosion
Glossary of Terms
Epilogue

Mail today! ORDER FORM

Send your order to your regular book supplier or directly to your nearest ***Marcel Dekker, Inc.*** *office:*

USA / Canada / South America
MARCEL DEKKER INC., Cimarron Road, P.O. Box 5005, Monticello, NY 12701-5185
Toll-Free 1-800-228-1160 / Fax: 1-914-796-1772 / E-Mail: bookorders@dekker.com

Europe / Africa / Middle East / Far East / Australia / India / China
MARCEL DEKKER AG, Hutgasse 4, Postfach 812, CH-4001 Basel, Switzerland
Tel.: +41-61-261-8482 / Fax: +41-61-261-8896 / E-Mail: intlorders@dekker.com

❑ Please send me _____ copy(ies) of ***Fine Ceramic Fibers*** (ISBN: 0-8247-1951-4) edited by Anthony R. Bunsell and Marie-Hélène Berger at $150.00 per volume.

❑ Please send me _____ copy(ies) of the ***Handbook of Fiber Chemistry, Second Edition*** (ISBN: 0-8247-9471-0) edited by Menachem Lewin and Eli M. Pearce at $275.00 per volume.

❑ Please send me _____ copy(ies) of ***Corrosion of Ceramics*** (ISBN: 0-8247-9448-6) by Ronald A. McCauley at $145.00 per volume.

For USA & Canada: Please add $3.50 for postage and handling per volume; on prepaid orders, add only $2.00 per volume. *For other countries:* Add $5.00 for postage and handling per volume (orders must be prepaid).

I enclose payment in the amount of $ _____ by: ❑ check ❑ money order

❑ Visa ❑ MasterCard, EuroCard, Access ❑ Am.Exp. ❑ Diner's Club

Card No. _____ Exp. Date _____

Signature _____
(must be signed for credit card payment)

Please bill my company: P.O. No. _____

❑ Please send me a pro forma invoice, including shipping and handling charges.

Name _____

Address _____

_____

City/State/Zip/Country _____

E-Mail: _____

N. Y. residents must add appropriate sales tax. Canadian customers add 7% GST. Prices are subject to change without notice.

Form No. 039904 **Printed in U.S.A.**

Tailor interphase design in thermoplastic engineering with...

HANDBOOK OF POLYPROPYLENE AND POLYPROPYLENE COMPOSITES

(Plastics Engineering Series/51)

Replace metals with polypropylene thermoplastics in high- and low-temperature, high-burst strength, and high-ductility applications!

edited by
HARUTUN G. KARIAN,
Technical Product Manager—Polypropylene Products, Thermofil, Inc., Brighton, Michigan

March, 1999 / 576 pages, illustrated / ISBN: 0-8247-1949-2 / $195.00

Keying on up-to-the-minute developments in interphase technology, the ***Handbook of Polypropylene and Polypropylene Composites*** presents the exciting possibilities of **new catalyst systems** for manufacturing more durable thermoplastics, and details the use of additives that promote **impact resistance, controlled rheology, thermal stability,** and other desirable characteristics of the polymer matrix.

A superb collection of contributions from internationally esteemed experts in plastics engineering, the ***Handbook of Polypropylene and Polypropylene Composites***

- illustrates the behavior of **the interphase region**—the polymeric coating of any type of dispersed particulate incorporated in the polymer matrix—composed of materials such as mineral filler particles and glass fibers
- reviews the **current technology** of polypropylene resin manufacture and **new methods** of modifying its microstructure with various additives
- describes materials that contribute best to suitable thermal and mechanical behavior in polypropylene-based composites
- demonstrates how **chemical coupling** can make polypropylene composites capable of withstanding heat to 150°C and cold to -40°C
- discusses **promising applications of interphase design** such as glass fiber-reinforced polypropylene (GFRP) and mega-coupled type chemical coupling
- explores the characterization of long-term creep-fatigue behavior as a means of estimating service lifetime of thermoplastic components
- and more!

Employing the novel strategy of mirroring its content in its format—by arranging chapters as metaphorical ingredients of the formulation of a polypropylene composite—this cutting-edge reference contains information and analysis vital to breakthroughs in plastics technology. The ***Handbook of Polypropylene and Polypropylene Composites*** is an invaluable resource for plastics, chemical, design, process, manufacturing, and technical service engineers; materials scientists; polymer chemists; and upper-level undergraduate and graduate students in these disciplines.

CONTENTS

This book is printed on acid-free paper.

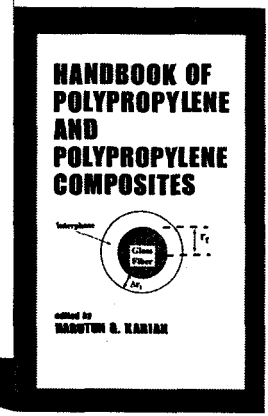

MARCEL DEKKER

MARCEL DEKKER, INC.
270 MADISON AVENUE, NEW YORK, NY 10016
212-696-9000
HUTGASSE 4, POSTFACH 812, CH-4001 BASEL, SWITZERLAND
061-261-8482
Visit our website at www.dekker.com

Also in the ***Plastics Engineering Series...***

PLASTICS TECHNOLOGY HANDBOOK

Third Edition, Revised and Expanded

"well written ....recommended"

MANAS CHANDA,
Indian Institute of Science, Bangalore, India
SALIL K. ROY,
National University of Singapore, Singapore

1214 pages, illustrated /
ISBN: 0-8247-0066-X / $250.00

Praise for the third edition...

"...useful as an introductory text for polymers—synthesis, characterization, and processing....**well written** and easily understandable....**recommend[ed].**" —*Polymer News*

And for the second...

"...**excellent** updating and expansion."
—*IEEE Electrical Insulation Magazine*

"...provides a broad overview of plastic materials, methods of manufacturing and testing, and applications....

"...ambitious...covers this wide subject well. The material...is cohesive....a **state-of-the-art** summary in the plastics field." —*Medical Device Technology*

"...**a fine general encyclopedia of polymeric materials**, their technology and environment... extremely useful." —*Cep-Inform*

CONTENTS

For Credit Card and Purchase Orders, *and* Customer Service

CALL TOLL-FREE 1-800-228-1160

Mon.-Fri., 8:30 a.m. to 5:45 p.m. (EST) or FAX your order to 914-796-1772

www.dekker.com

Mail today! ✂ **ORDER FORM**

Send your order to your regular book supplier or directly to your nearest ***Marcel Dekker, Inc.*** *office:*

USA / Canada / South America
MARCEL DEKKER INC., Cimarron Road, P.O. Box 5005, Monticello, NY 12701-5185 • Toll-Free 1-800-228-1160 / Fax: 1-914-796-1772 / E-Mail: bookorders@dekker.com

Europe / Africa / Middle East / Far East / Australia / India / China
MARCEL DEKKER AG, Hutgasse 4, Postfach 812, CH-4001 Basel, Switzerland • Tel.: +41-61-261-8482 / Fax: +41-61-261-8896 / E-Mail: intlorders@dekker.com

Please send me _____ copy(ies) of the ***Handbook of Polypropylene and Polypropylene Composites*** (ISBN: 0-8247-1949-2) edited by Harutun G. Karian at $195.00 per volume.

Please send me _____ copy(ies) of ***Plastics Technology Handbook, Third Edition*** (ISBN: 0-8247-0066-X) by Manas Chanda and Salil K. Roy at $250.00 per volume.

For USA & Canada: Please add $3.50 for postage and handling per volume; for prepaid orders, add only $2.00 per volume. *For other countries:* Add $5.00 for postage and handling per volume (orders must be prepaid).

I enclose payment in the amount of $ _____ by: ❑ check ❑ money order
❑ Visa ❑ MasterCard, EuroCard, Access ❑ Am.Exp. ❑ Diner's Club

Card No. _____ Exp. Date _____

Signature _____
(must be signed for credit card payment)

Please bill my company: P.O. No. _____

❑ Please send me a pro forma invoice, including shipping and handling charges.

Name _____

Address _____

_____

City/State/Zip/Country _____

E-Mail: _____

N. Y. residents must add appropriate sales tax. Canadian customers add 7% GST. Prices are subject to change without notice.

Form No. 039910 **Printed in U.S.A.**

Choose the best up-to-date methods for evaluating a vast range of polymeric materials with...

Handbook of Polymer Testing

Physical Methods

(Plastics Engineering Series/50)

edited by

ROGER BROWN,
Rapra Technology, Ltd., Shrewsbury, England

December, 1998
880 pages, illustrated
ISBN: 0-8247-0171-2
$225.00

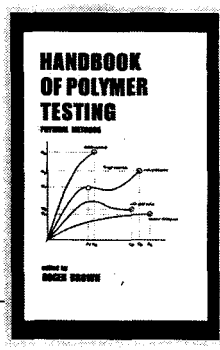

This comprehensive handbook provides—*in a single volume*—virtually all currently used techniques for measuring and testing the physical properties of polymers.

Features complete coverage of ***mechanical, optical, electrical,*** *and* ***thermal*** *properties!*

Analyzing a wide array of physical parameters, the ***Handbook of Polymer Testing***

- highlights all the **main polymer classes**—including rubber, plastics, foams, textiles, coated fabrics, *and* composites
- includes **standardized adhesion tests** for solid polymers adhered to rigid and flexible substrates
- covers resistance to degradation, nondestructive testing, *and* tests for processability
- presents the fundamental principles regulating each property
- clarifies **international *and* English-language standards** for different polymer classes
- compares approaches to testing in different branches of the polymer industry
- and more!

Complete with over 2350 references, tables, equations, drawings, and photographs, the ***Handbook of Polymer Testing*** is an indispensable reference for plastics, polymer, chemical, and design engineers; polymer and materials scientists; polymer physicists; polymer technologists; and upper-level undergraduate and graduate students in these disciplines.

Contents

This book is printed on acid-free paper.

MARCEL DEKKER, INC.
270 MADISON AVENUE, NEW YORK, NY 10016 • 212-696-9000
HUTGASSE 4, POSTFACH 812, CH-4001 BASEL, SWITZERLAND • 061-261-8482
Visit our website at www.dekker.com

POLYM.–PLAST. TECHNOL. ENG., 38(3), (1999)

CONTENTS (*continued*)

POLYMER–PLASTICS TECHNOLOGY AND ENGINEERING

Volume 38 Number 3 1999

Special Issue on Polymer and Fiber Recycling

CONTENTS OF THIS ISSUE

(*continued on inside back cover*)

MARCEL

MARCEL DEKKER, INC. NEW YORK • BASEL

Contributions to this journal are published free of charge